

**ROLE OF ULTRASOUND ACOUSTIC RADIATION
FORCE IMPULSE IN DIFFERENTIATING BENIGN
FROM MALIGNANT PALPABLE LYMPH NODES**

A dissertation submitted in partial fulfilment of M.D. Radiodiagnosis (Branch VIII)
examination of the Tamil Nadu Dr M.G.R Medical University, Chennai to be held in

April, 2017

CERTIFICATE

This is to certify that the dissertation entitled 'Role of Ultrasound Acoustic Radiation Force Impulse in Differentiating Benign from Malignant Palpable Lymph Nodes' is a bonafide original work of Dr Reettika Chanda, submitted in partial fulfilment of the requirement for MD Radiodiagnosis (Branch VIII) Degree Examination of the Tamil Nadu Dr. M.G.R Medical University, Chennai to be held in April 2017.

Guide:



Dr Vinu Moses, MD, DNB

Professor

Department of Radiodiagnosis

Christian Medical College, Vellore


Tamil Nadu



CERTIFICATE

This is to certify that the dissertation entitled 'Role of Ultrasound Acoustic Radiation Force Impulse in Differentiating Benign from Malignant Palpable Lymph Nodes' is a bonafide original work of Dr Reettika Chanda, submitted in partial fulfilment of the requirement for MD Radiodiagnosis (Branch VIII) Degree Examination of the Tamil Nadu Dr. M.G.R Medical University, Chennai to be held in April 2017.

Head of Department:



Dr Shyamkumar N K, DMRD, DNB, FRCR, FRANZCR

Professor & Head

Department of Radiodiagnosis

Christian Medical College, Vellore

Tamil Nadu

*HEAD OF THE DEPARTMENT,
DEPARTMENT OF RADIODIAGNOSIS,
C.M.C. HOSPITAL, VELLORE - 4.*

CERTIFICATE

This is to certify that the dissertation entitled 'Role of Ultrasound Acoustic Radiation Force Impulse in Differentiating Benign from Malignant Palpable Lymph Nodes' is a bonafide original work of Dr Reetika Chanda, submitted in partial fulfilment of the requirement for MD Radiodiagnosis (Branch VIII) Degree Examination of the Tamil Nadu Dr. M.G.R Medical University, Chennai to be held in April 2017.

Principal:

Dr Anna B Pulimood, MD, (Path), Ph.D

Principal

Christian Medical College, Vellore

Tamil Nadu

DECLARATION

I, Dr Reettika Chanda, hereby declare that this dissertation 'Role of Ultrasound Acoustic Radiation Force Impulse in Differentiating Benign from Malignant Palpable Lymph Nodes' is an original work done by me in partial fulfilment of the requirement for MD Radio Diagnosis (Branch- VIII) Degree Examination of The Tamil Nadu Dr M.G.R Medical University, Chennai to be conducted in April, 2017.

Candidate:



Dr Reettika Chanda

Post Graduate Resident

Department of Radiodiagnosis

Christian Medical College, Vellore

Tamil Nadu



ORIGINALITY REPORT



Digital Receipt

This receipt acknowledges that Turnitin received your paper. Below you will find the receipt information regarding your submission.

The first page of your submissions is displayed below.

Submission author: 201518055 Md Rad Diag REETIKA..
Assignment title: 2015-2015 plagiarism
Submission title: ROLE OF ULTRASOUND ACOUST...
File name: Draft_2_Turnitin.docx
File size: 8.31M
Page count: 89
Word count: 13,318
Character count: 72,782
Submission date: 19-Sep-2016 11:44 PM
Submission ID: 707614508

**ROLE OF ULTRASOUND ACOUSTIC RADIATION
FORCE IMPULSE IN DIFFERENTIATING BENIGN
FROM MALIGNANT PALPABLE LYMPH NODES**

A dissertation submitted in partial fulfillment of M.D. - Radiodiagnosis (Branch VEE)
examination of the Tamil Nadu Dr. MGR Medical University, Chennai, to be held in:
April, 2017

Turnitin logo and navigation tabs: Class Portfolio, Peer Review, My Grades, Discussion, Calendar.

NOW VIEWING: HOME > THE TAMIL NADU DR.M.G.R.MEDICAL UTY 2015-16 EXAMINATIONS

Welcome to your new class homepage! From the class homepage you can see all your assignments for your class, view additional assignment information, submit your work, and access feedback for your papers.

Class Homepage

This is your class homepage. To submit to an assignment click on the "Submit" button to the right of the assignment name. If the Submit button is grayed out, no submissions can be made to the assignment. If resubmissions are allowed the submit button will read "Resubmit" after you make your first submission to the assignment. To view the paper you have submitted, click the "View" button. Once the assignment's post date has passed, you will also be able to view the feedback left on your paper by clicking the "View" button.

Info	Dates	Similarity	
2015-2015 plagiarism	Start 23-Nov-2015 2:27PM Due 07-Nov-2016 11:59PM Post 01-Dec-2015 12:00AM	20% ■	Resubmit View

Turnitin Document Viewer - Google Chrome

https://turnitin.com/dv?o=707614508&u=1055594891&s=&student_user=1&lang=en_us

The Tamil Nadu Dr.M.G.R.Medical ... 2015-2015 plagiarism - DUE 07-Nov-20...

Originality GradeMark PeerMark

ROLE OF ULTRASOUND ACOUSTIC RADIATION FORCE IMPULSE IN
BY 201518055 MD RAD DIAG REETIKA CHANDA

turnitin 20% SIMILAR OUT OF 0

Match Overview

1	e-sciencecentral.org Internet source	2%
2	Ahuja, A. "Sonograph... Publication	2%
3	www.jultrasoundmed.org Internet source	1%
4	radiology.rsna.org Internet source	1%
5	www.biomeddefine.com Internet source	1%
6	Dudea, Sorin M.; Leng... Publication	1%
7	"ECR 2015 Book of Ab... Publication	1%
8	www.biomedcentral.com Internet source	1%
9	F. Alam. "Accuracy of ... Publication	1%

ROLE OF ULTRASOUND ACOUSTIC RADIATION
FORCE IMPULSE IN DIFFERENTIATING BENIGN
FROM MALIGNANT PALPABLE LYMPH NODES

A dissertation submitted in partial fulfillment of M.D. Radiodiagnosis (Branch VIII)

PAGE: 1 OF 88

INSTITUTIONAL REVIEW BOARD CLEARANCE LETTER



OFFICE OF RESEARCH INSTITUTIONAL REVIEW BOARD (IRB) CHRISTIAN MEDICAL COLLEGE, VELLORE, INDIA

Dr. B.J. Prashantham, M.A., M.A., Dr. Min (Clinical)
Director, Christian Counseling Center,
Chairperson, Ethics Committee.

Dr. Alfred Job Daniel, D Ortho MS Ortho DNB Ortho.
Chairperson, Research Committee & Principal

Dr. Nihal Thomas,
MD, MNAMS, DNB (Endo), FRACP (Endo), FRCP (Edin), FRCP (Glasg)
Deputy Chairperson,
Secretary, Ethics Committee, IRB
Additional Vice-Principal (Research)

December 21, 2015

Dr. Reetika Chanda
PG Registrar,
Department of Radiodiagnosis,
Christian Medical College,
Vellore 632 004.

Sub: Fluid Research grant project NEW PROPOSAL:

Role of Ultrasound Acoustic Radiation force impulse in differentiating benign from malignant palpable lymph nodes.

Dr. Reetika Chanda, Emp. No. 29271, PG Registrar, Radiodiagnosis, Dr. Vinu Moses, Emp. No. 28371, Professor, Radiodiagnosis, Dr. Madhavi K, Emp. No. 33314, Asst. Professor, Radiology, Dr. Shyam Kumar N.K. Emp. No. 20030, Radiodiagnosis, Dr. Rajnikanth K, Emp. No. 31352, Assoc. Professor, Dr. Elanthenral Sigamani, Emp. No. 33230, Asst. Professor, General Pathology.

Ref: IRB Min No: 9675 [DIAGNO] dated 20.10.2015

Dear Dr. Reetika Chanda

The Institutional Review Board (Blue, Research and Ethics Committee) of the Christian Medical College, Vellore, reviewed and discussed your project titled "Role of Ultrasound Acoustic Radiation force impulse in differentiating benign from malignant palpable lymph nodes" on October 20th 2015.

I enclose the following documents:-

1. Institutional Review Board approval
2. Agreement

Could you please sign the agreement and send it to Dr. Nihal Thomas, Addl. Vice Principal (Research), so that the grant money can be released.

With best wishes,

Dr. Nihal Thomas
Secretary (Ethics Committee)
Institutional Review Board

Dr. NIHAL THOMAS
MD, MNAMS, DNB (Endo), FRACP (Endo), FRCP (Edin), FRCP (Glasg)
SECRETARY - (ETHICS COMMITTEE)
Institutional Review Board,
Christian Medical College, Vellore - 632 002.

Cc: Dr. Vinu Moses, Dept. of Radio diagnosis, CMC

1 of 4



**OFFICE OF RESEARCH
INSTITUTIONAL REVIEW BOARD (IRB)
CHRISTIAN MEDICAL COLLEGE, VELLORE, INDIA**

Dr. B.J. Prashantham, M.A., M.A., Dr. Min (Clinical)
Director, Christian Counseling Center,
Chairperson, Ethics Committee.

Dr. Alfred Job Daniel, D Ortho MS Ortho DNB Ortho.
Chairperson, Research Committee & Principal

Dr. Nihal Thomas,
MD, MNAMS, DNB (Endo), FRACP (Endo), FRCP (Edin), FRCP (Glasg)
Deputy Chairperson,
Secretary, Ethics Committee, IRB
Additional Vice-Principal (Research)

December 21, 2015

Dr. Reettika Chanda
PG Registrar,
Department of Radiodiagnosis,
Christian Medical College,
Vellore 632 004.

Sub: Fluid Research grant project NEW PROPOSAL:

Role of Ultrasound Acoustic Radiation force impulse in differentiating benign from malignant palpable lymph nodes.

Dr. Reettika Chanda, Emp. No. 29271, PG Registrar, Radiodiagnosis, Dr. Vinu Moses, Emp. No. 28371, Professor, Radiodiagnosis, Dr. Madhavi K, Emp. No. 33314, Asst. Professor, Radiology, Dr. Shyam Kumar N.K. Emp. No. 20030, Radiodiagnosis, Dr. Rajnikanth K, Emp. No. 31352, Assoc. Professor, Dr. Elanthenral Sigamani, Emp. No. 33230, Asst. Professor, General Pathology.

Ref: IRB Min No: 9675 [DIAGNO] dated 20.10.2015

Dear Dr. Reettika Chanda ,
The Institutional Review Board (Blue, Research and Ethics Committee) of the Christian Medical College, Vellore, reviewed and discussed your project titled "Role of Ultrasound Acoustic Radiation force impulse in differentiating benign from malignant palpable lymph nodes" on October 20th 2015.

The Committee reviewed the following documents:

1. IRB Application format
2. Patient Information Sheet and Informed Consent Form (English, Tamil, Hindi, Bengali)
3. Proforma
4. Cvs of Drs. Vinu Moses, Madhavi K , Shyam Kumar N.K, Rajnikanth K, Elanthenral Sigamani
5. No. of documents 1 - 4

The following Institutional Review Board (Blue, Research & Ethics Committee) members were present at the meeting held on October 20th 2015 in the CREST/SACN Conference Room, Christian Medical College, Bagayam, Vellore 632002.

2 of 4



**OFFICE OF RESEARCH
INSTITUTIONAL REVIEW BOARD (IRB)
CHRISTIAN MEDICAL COLLEGE, VELLORE, INDIA**

Dr. B.J. Prashantham, M.A., M.A., Dr. Min (Clinical)
Director, Christian Counseling Center,
Chairperson, Ethics Committee.

Dr. Alfred Job Daniel, D Ortho MS Ortho DNB Ortho.
Chairperson, Research Committee & Principal

Dr. Nihal Thomas,
MD, MNAMS, DNB (Endo), FRACP (Endo), FRCP (Edin), FRCP (Glasg)
Deputy Chairperson,
Secretary, Ethics Committee, IRB
Additional Vice-Principal (Research)

Name	Qualification	Designation	Affiliation
Dr. B. J. Prashantham	MA(Counseling Psychology), MA(Theology), Dr. Min(Clinical Counselling)	Chairperson, Ethics Committee, IRB. Director, Christian Counseling Centre, Vellore	External, Social Scientist
Dr. Nihal Thomas	MD, MNAMS, DNB(Endo), FRACP (Endo) FRCP(Edin) FRCP (Glasg)	Professor & Head, Endocrinology. Additional Vice Principal (Research), Deputy Chairperson (Research Committee), Member Secretary (Ethics Committee), IRB, CMC, Vellore	Internal, Clinician
Mrs. Pattabiraman	BSc, DSSA	Social Worker, Vellore	External, Lay Person
Dr. Rajesh Kannangai	MD, PhD.	Professor, Clinical Virology, CMC, Vellore	Internal, Clinician
Dr. Jayaprakash Muliyl	BSc, MBBS, MD, MPH, Dr PH (Epid), DMHC	Retired Professor, CMC, Vellore	External, Scientist & Epidemiologist
Mrs. Emily Daniel	MSc Nursing	Professor, Medical Surgical Nursing, CMC, Vellore	Internal, Nurse
Mrs. Sheela Durai	MSc Nursing	Professor, Medical Surgical Nursing, CMC, Vellore	Internal, Nurse
Mr. C. Sampath	BSc, BL	Advocate, Vellore	External, Legal Expert
Dr. Anuradha Rose	MBBS, MD, MHSC (Bioethics)	Associate Professor, Community Health, CMC, Vellore	Internal, Clinician
Dr. Vivek Mathew	MD (Gen. Med.) DM (Neuro) Dip. NB (Neuro)	Professor, Neurology, CMC, Vellore	Internal, Clinician
Dr. Chandrasingh	MS, MCH, DMB	Professor, Urology, CMC, Vellore	Internal, Clinician

IRB Min No: 9675 [DIAGNO] dated 20.10.2015

3 of 4



**OFFICE OF RESEARCH
INSTITUTIONAL REVIEW BOARD (IRB)
CHRISTIAN MEDICAL COLLEGE, VELLORE, INDIA**

Dr. B.J. Prashantham, M.A., M.A., Dr. Min (Clinical)
Director, Christian Counseling Center,
Chairperson, Ethics Committee.

Dr. Alfred Job Daniel, D Ortho MS Ortho DNB Ortho.
Chairperson, Research Committee & Principal

Dr. Nihal Thomas,
MD, MNAMS, DNB (Endo), FRACP (Endo), FRCP (Edin), FRCP (Glasg)
Deputy Chairperson,
Secretary, Ethics Committee, IRB
Additional Vice-Principal (Research)

Ms. Grace Rebecca	M.sc (Biostatistics)	Lecturer, Biostatistics, CMC, Vellore	Internal, Statistician
Dr. Simon Pavamani	MBBS, MD	Professor, Radiotherapy, CMC, Vellore	Internal, Clinician
Dr. Inian Samarasam	MS, FRCS, FRACS	Professor, Surgery, CMC, Vellore	Internal, Clinician
Dr. Balamugesh	MBBS, MD(Int Med), DM, FCCP (USA)	Professor, Pulmonary Medicine, CMC, Vellore	Internal, Clinician
Dr. Niranjana Thomas	DCH, MD, DNB (Paediatrics)	Professor, Neonatology, CMC, Vellore	Internal, Clinician
Dr. Mathew Joseph	MBBS, MCH	Professor, Neurosurgery, CMC, Vellore	Internal, Clinician
Dr. RatnaPrabha	MBBS, MD	Associate Professor, Clinical Pharmacology, CMC, Vellore.	Internal, Pharmacologist

We approve the project to be conducted as presented.

Kindly provide the total number of patients enrolled in your study and the total number of withdrawals for the study entitled: "Role of Ultrasound Acoustic Radiation force impulse in differentiating benign from malignant palpable lymph nodes" on a monthly basis. Please send copies of this to the Research Office (research@cmcvellore.ac.in)

Fluid Grant Allocation:

A sum of Rs.50,000/- INR (Rupees Fifty Thousand Only) will be granted for 12 months and out of which a maximum of Rs.5,000/- can be spent for stationery, printing, Xeroxing and computer charges (if computer used are within the institution).

Yours sincerely

Dr. Nihal Thomas
Secretary (Ethics Committee)
Institutional Review Board
Dr. NIHAL THOMAS
MD, MNAMS, DNB (Endo), FRACP (Endo), FRCP (Edin), FRCP (Glasg)
SECRETARY - (ETHICS COMMITTEE)
Institutional Review Board,
Christian Medical College, Vellore - 632 002.

IRB Min No: 9675 [DIAGNO] dated 20.10.2015

4 of 4

ACKNOWLEDGEMENT

First and foremost, I thank Almighty God for being with me all the way.

I take immense pleasure to express my deep sense of gratitude to my thesis guide Dr Vinu Moses for his motivation and exemplary guidance throughout the course of my research.

I would also like to thank the rest of my thesis committee for their insightful comments, which incited me to widen my research from various perspectives.

I am grateful to Dr Visali Jayaseelan for her passionate participation in data analysis.

A special word of thanks also goes to my office staff and the staff of Clean Minor Theatre for their continuous help.

I would like to extend my sincerest thanks and appreciation to all my patients who graciously agreed to participate in my study.

I sincerely acknowledge my alma maters and all my teachers for making this study and course a reality.

Finally, I must express my profound gratitude to my parents, family and friends for providing me with continuous encouragement and unfailing support throughout my years of study and through the process of researching and writing this dissertation.

This accomplishment would not have been possible without them.

Thank you.

LIST OF COMMON ABBREVIATIONS

AR	Area ratio
ARFI	Acoustic radiation force impulse
AUC	Area under curve
CD	Colour Doppler
CEUS	Contrast-enhanced ultrasound
CI	Confidence interval
CT	Computed tomography
FNAB	Fine needle aspiration biopsy
FNAC	Fine needle aspiration for cytology
GAR	Grey scale area
HIV	Human immunodeficiency virus
HPE	Histopathological examination
LN	Lymph node
LS	Long axis – short axis ratio
LR	Likelihood ratio
MRI	Magnetic resonance imaging
NPV	Negative predictive value
PACS	Picture archiving and communication system
PET	Positron emitting tomography
PPV	Positive predictive value
PI	Pulsatility index
RI	Resistive index

ROI	Region of interest
ROC	Receiver operating characteristic
SAD	Short axis diameter
SD	Standard deviation
SE	Standard error
SI	Système international
SR	Strain ratio
SWV	Shear wave velocity
US	Ultrasound, Ultrasonography
VAR	VTI area
VTI	Virtual touch imaging
VTQ	Virtual touch quantification

CONTENTS

Abstract.....	2
Introduction	4
Aim	5
Objectives	6
Literature Review	7
Anatomy Of Lymph Node	7
Causes Of Lymphadenopathy	11
Assessment Of Lymphadenopathy.....	15
Imaging Assessment Of Lymphadenopathy	19
Ultrasound.....	19
Colour Doppler	27
Elastography	31
Acoustic Radiation Force Impulse Imaging	42
Other Imaging Modalities.....	52
Methodology.....	55
Statistical Analysis	61
Case Based Imaging Findings & HPE Correlation	77
Discussion.....	85
Limitations.....	87
Conclusion	88
Bibliography	89
Annexure 1. Data Collection Sheet	97
Annexure 2A-D. Patient Information Sheets.....	101
Annexure 3A-D. Consent Forms	110
Annexure 4. Study Data.....	116

ABSTRACT

TITLE: Role of Ultrasound Acoustic Radiation Force Impulse in Differentiating Benign from Malignant Palpable Lymph Nodes

OBJECTIVE:

The purpose of this study was to evaluate the diagnostic performance of acoustic radiation force impulse imaging in differentiating benign from malignant peripheral lymphadenopathy.

METHODS:

This was a prospective study approved by the Institutional Review Board with financial grant for the same. Ultrasound and ARFI imaging of peripheral lymph nodes were performed and correlated with pathological results, which were used as the reference standard. The virtual touch tissue imaging and virtual touch tissue quantification parameters of ARFI were analysed in 86 lymph nodes of which 78 were included in the study. Using receiver operating characteristic curve analysis, the diagnostic usefulness of ARFI values were evaluated with respect to their sensitivity, specificity, and area under the curve.

RESULTS:

The mean area ratio of benign lymph nodes was 0.88 (± 0.2) and that of malignant lymph nodes was 1.17 (± 0.14). The mean shear wave velocities (SWV) of benign and malignant lymph nodes were 2.02 m/s (± 0.94) and 3.7 m/s (± 2.27) respectively. The

sensitivity, specificity, PPV, NPV & AUC of VTI area ratio was 97%, 77%, 77% 97% & 0.86, of SWV lymph node was 71%, 70%, 66%, 75% & 0.78, and of SWV ratio was 68%, 79%, 72%, 75% and 0.82, respectively.

CONCLUSION:

ARFI has a superior diagnostic performance over conventional ultrasound and colour Doppler in differentiating malignant from benign lymph nodes.

INTRODUCTION

The presence of a palpable lymph node is a commonly picked up finding during clinical examination. The aetiology behind this enlargement can range from mere reactive changes to inflammatory or infective conditions to more sinister causes such as malignancy or metastasis.

With the assumption that malignant tissue is harder than normal tissue, clinical examination uses palpation as a tool to discern how firm a node is.

Sonographic examination of lymph nodes is more sensitive than clinical palpation. Ultrasound elastography is yet another technique that works on similar principles of clinical palpation to determine the stiffness of a tissue. However, the amount of manual compression applied on the tissue becomes a reducible but not removable factor that can cause erroneous measurements.

Here comes the role of Acoustic Radiation Force Impulse (ARFI) elastography in measuring tissue stiffness. ARFI can perform both qualitative and quantitative measurements of tissue stiffness and is independent of the amount of manual compression.

AIM

This study is aimed at assessing the diagnostic accuracy of ARFI elastography in differentiating benign and malignant palpable lymph nodes in patients by means of 'Area Ratio' of lesions on conventional ultrasound and virtual touch imaging, calculation of shear wave velocity ratios between the lymph node and surrounding normal tissue, and also to compare the performance of ARFI to that of conventional ultrasound in the characterization of palpable lymph nodes, using histopathologic diagnosis as the gold standard.

OBJECTIVES

To assess the diagnostic values of virtual touch quantification and virtual touch imaging of ARFI elastography and ultrasound imaging in differentiating benign from malignant palpable lymph node enlargement, using histopathological diagnosis as the reference standard.

The variables studied will include:

1. Ultrasound characteristics of lymph node
2. Area ratio and brightness pattern of lymph node on virtual touch imaging
3. Shear wave velocity of lymph nodes using virtual touch quantification
4. Ratio of the shear-wave velocity between lesion and surrounding normal tissue

LITERATURE REVIEW

The lymphatic system is a part of the circulatory pathway that provides an accessory route for fluid to circulate from the interstitium into blood (1).

The first full description of the human lymphatic system was given by Thomas Bartholin, a Danish physician, in December 1652. The word 'lymph' is derived from the Latin word *lymphā* meaning water.

Lymph nodes are small, oval organs that are widely distributed throughout the body, lying along the course of lymphatic vessels. They contain B and T lymphocytes and other cells of the immune system.

As lymph circulates through the lymph nodes, the resident immune system gets activated and filters foreign antigens and cancer cells, attempting to destroy or almost entirely remove these particles.

Activation of this resident immune system causes morphological changes within the lymph nodes causing them to get enlarged due to a tumor or inflamed due to infection (2).

ANATOMY OF LYMPH NODE

Lymph nodes are encapsulated structures that lie along the course of lymphatic vessels.

They are small, measuring ~ 0.1 – 2.5 cm in length, oval or reniform in shape with a small indentation on the hilum.

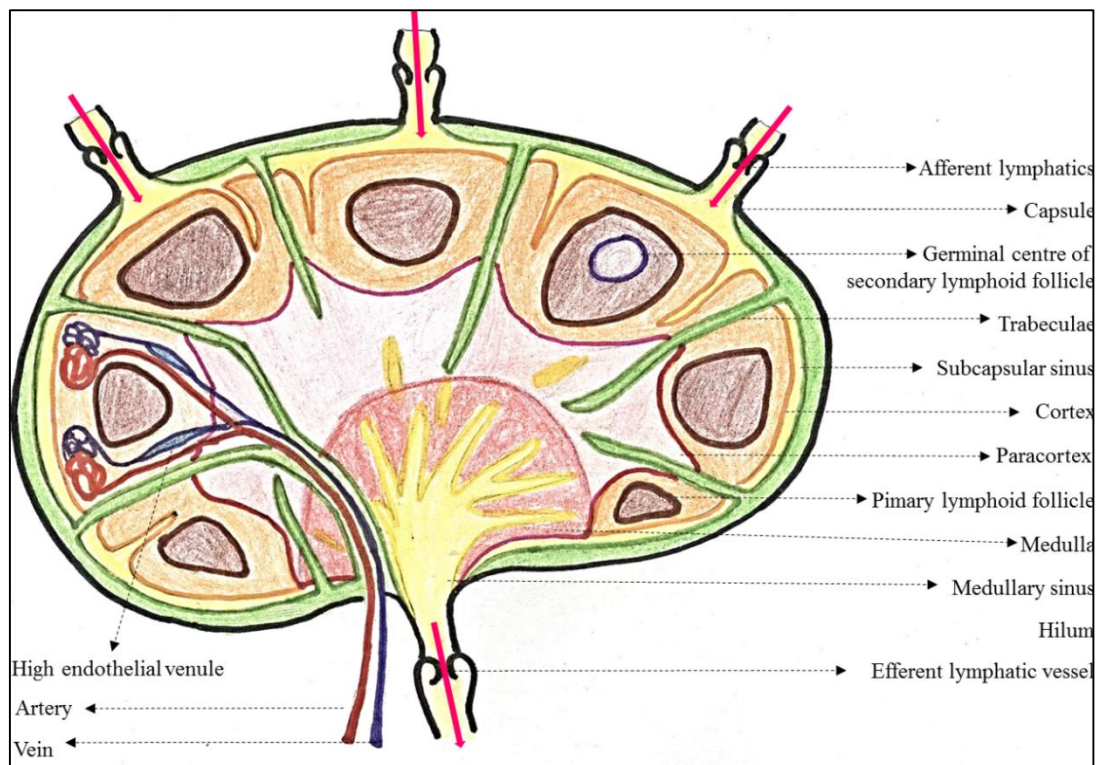


Fig. 1. Structure of a lymph node. Adapted from (3).

A lymph node consists of two parts, a cortex that is highly cellular and a medulla which contains a network of minute sinuses. At the hilar region, the cortex is absent and the medulla reaches the surface.

The capsule is made of collagen, elastin and few fibroblasts. Dense connective tissue extend radially from the capsule interiorly into the node. Reticulin fibrils are fine type III collagen which are continuous with the dense connective tissue. Reticulin forms a fine network that interconnects and supports the lymphoid tissue (3).

LYMPH NODE MICROSTRUCTURE

In the cortex, cells are densely packed, forming lymphoid follicles in the outer cortical area. B cells and specialized follicular dendritic cells populate these follicles.

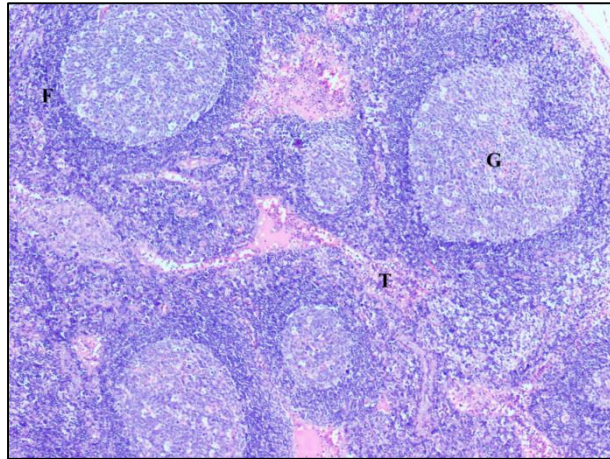


Fig. 2. Lymph node section showing lymphoid follicles (F), with germinal centres (G), and connective tissue trabeculae (T). 40x, H&E stain.

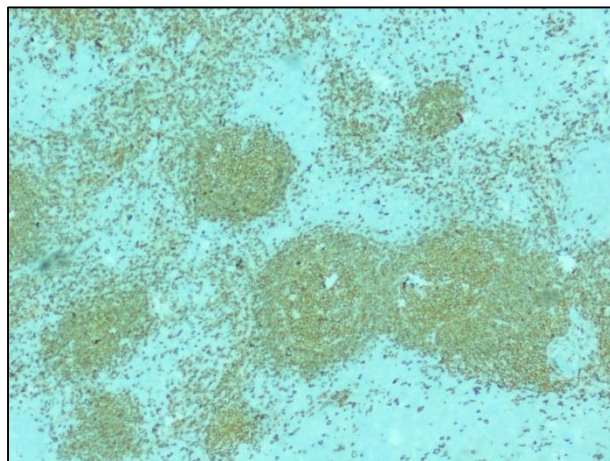


Fig. 3. Lymph node section showing CD-20 staining the follicles.

A primary follicle is one which is uniformly populated by quiescent lymphocytes, whereas a follicle containing a germinal centre is termed as a secondary follicle. Germinal centres provide a microenvironment for B cell maturation.

The paracortex or deep cortex lies in between the cortical follicles and the medulla. It contains mainly T cells which are in a non-follicular arrangement. Interdigitating dendritic cells are also present in the paracortex.

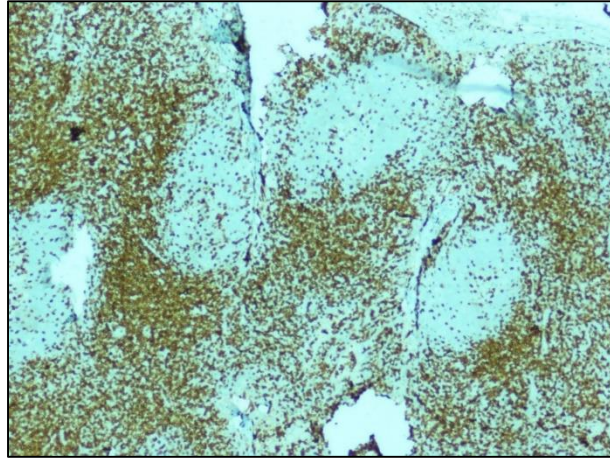


Fig. 4. Lymph node section showing CD-3 staining the paracortical cells.

Lymphocytes are less tightly packed in the medulla, forming irregular branching medullary cords between the reticulin networks (3).

LYMPHATIC AND VASCULAR SUPPLY

Vascular supply to the lymph node passes through the hilum. The arteries and veins give off straight branches as they course through the medulla, forming dense arcades and anastomosing loops at the cortex.

Afferent lymphatic channels enter the cortex, through which lymph permeates within the lymphoid tissue, reaching the medulla. The medullary sinuses filter lymph which is then collected at the hilum by the efferent lymphatic vessel (3).

LOCATION OF LYMPH NODES

There are up to 450 lymph nodes in an adult human body, predominantly in the neck, proximal regions of the limbs, mediastinum and abdomen.

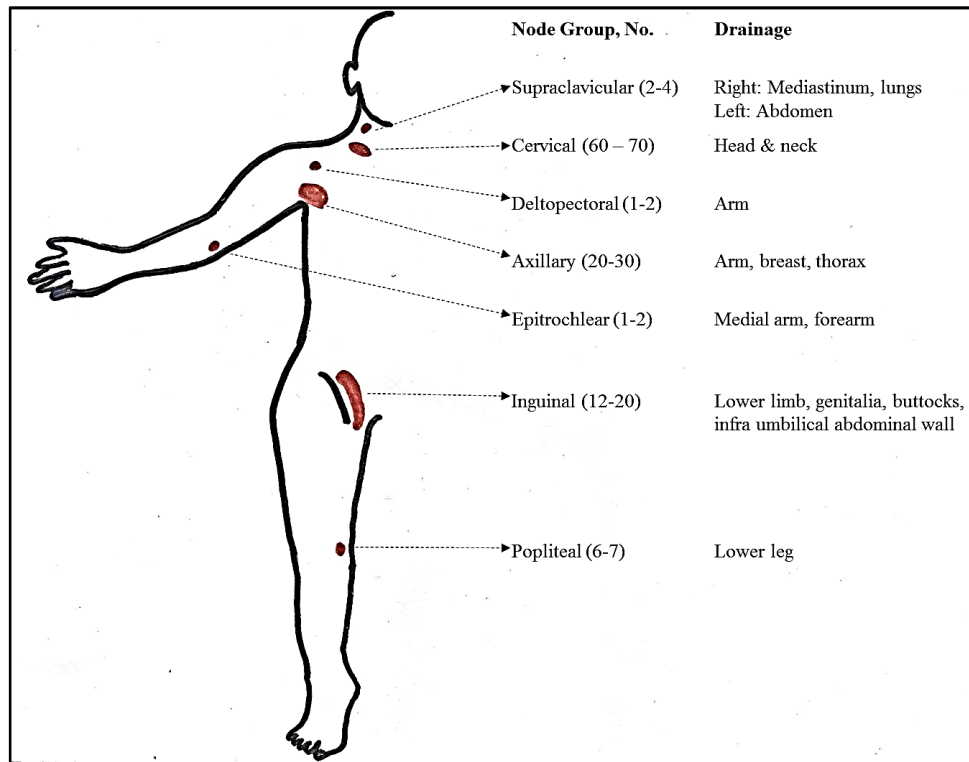


Fig. 5. Lymph node regions in the body. Adapted from (4).

CAUSES OF LYMPHADENOPATHY

‘Lymphadenopathy’ is a term used to describe disease of the lymph nodes. It can occur due to a myriad of causes. A clinically useful method to approach lymphadenopathy would be to classify it as localized, involving only one region, and generalized, in which more than one region is involved (5). Distinguishing between generalized and localized lymphadenopathy can aid in formulating a differential diagnosis.

A detailed and careful medical history and physical examination along with selected laboratory tests, aid the physician to decide whether the lymphadenopathy is normal or a finding that requires further evaluation (8).

Table 1. Causes of peripheral lymphadenopathy (5–7)

Cause	Examples
Infections	
Bacterial	
Localized	Skin infections, Streptococcal pharyngitis, plague, tularemia, diphtheria, chancroid, rat bite fever, cat scratch disease
Generalized	Lymphogranuloma venereum, typhoid, brucellosis, leptospirosis
Viral	Human immunodeficiency virus, Epstein-Barr virus, mumps, measles, herpes simplex virus, Cytomegalovirus, hepatitis B virus, dengue
Mycobacterial	Mycobacterium tuberculosis; atypical mycobacteria
Fungal	Cryptococcosis, histoplasmosis, coccidioidomycosis
Protozoal	Leishmaniasis, toxoplasmosis
Spirochetal	Lyme disease, secondary syphilis
Cancer	Head and neck squamous cell cancers, lymphoma, leukemia, metastasis
Lymphoproliferative	Autoimmune lymphoproliferative disease, Rosai-Dorfman disease, hemophagocytic lymphohistiocytosis, angioimmunoblastic lymphadenopathy with dysproteinemia
Immunologic	Drug reactions, serum sickness
Endocrine	Addison's disease , Hypothyroidism

Miscellaneous Sarcoidosis, histiocytosis, Kawasaki disease, Castleman's disease, chronic granulomatous disease, Kikuchi's disease, Churg-Strauss, inflammatory pseudotumor, systemic lupus erythematosis, dermatomyositis, rheumatoid arthritis, Still's disease, lipid storage disease, amyloidosis

Note: This table lists common conditions and is not all inclusive.

LOCALIZED LYMPHADENOPATHY

Cervical

Enlargement of cervical lymph nodes most commonly occurs with local infections in children as well as in adults, often due to streptococcal pharyngitis and viral upper respiratory infections. Lymph nodes are the favoured site for extra pulmonary tuberculosis, cervical being the most commonly involved nodal group (8). Cancers of the head and neck and of the upper aero-digestive tract metastasize to cervical nodes as part of their natural history. The occurrence of nodal metastasis has a profound effect on the management and prognosis of these patients (9).

Supraclavicular

There is a high risk of malignancy associated with supraclavicular lymphadenopathy. In two studies, in up to 50 per cent of cases with this presentation were found to have malignancy, the risk being highest above 40 years of age (11, 12). Right supraclavicular lymphadenopathy suggests cancer in the lungs, mediastinum or esophagus. Left

supraclavicular lymph node enlargement, commonly referred to as “Virchow’s node”, is associated with abdominal malignancies.

Axillary

The axillary nodes receive drainage from the upper extremity, breast and thoracic wall. Consequently, infections or malignancies involving these regions, cause this nodal group to enlarge. In breast cancer, involvement of 4 or more axillary nodes at the time of initial presentation is associated with a worse outcome (12).

Epitrochlear

A palpable epitrochlear node is always pathologic, causes ranging from infections involving the forearm or hand to lymphoma.

Inguinal

Inguinal adenopathy is often secondary to infections or trauma involving the lower extremity, sexually transmitted diseases and malignancies such as melanoma, squamous cell cancer, and lymphoma.

GENERALIZED LYMPHADENOPATHY

In generalised lymphadenopathy, three or more non-contiguous lymph node areas are involved (7).

Generalized lymphadenopathy may be a central feature of a number of common as well as rare systemic diseases, many of which can often be recognized by the clinical

presentation and presence of other findings. Biopsy is usually required to arrive at a diagnosis.

In an Indian study on the causes of peripheral lymphadenopathy in adults, out of 1724 cases, one-third was due to non-specific lymphadenitis (35.6%). The other common causes were tuberculosis (31.1%) and malignancy (25.9%) (13).

ASSESSMENT OF LYMPHADENOPATHY

CLINICAL ASSESSMENT

Lymphadenopathy may be an incidental finding in patients being examined for various reasons, or it could be a presenting sign or symptom of the patient's illness. A detailed medical history should reveal the setting in which lymph node enlargement is occurring.

Site and extent of lymphadenopathy, nodal size, texture, presence or absence of nodal tenderness and inflammatory signs over the node can be assessed on physical examination. Lymph nodes more than 1.0 cm in diameter are considered abnormal. Tender, warm and erythematous nodes are likely to be associated with a local infectious process, while hard, fixed nodes are highly suggestive of a malignancy (14). However, the accuracy of palpation in the detection of cervical lymph node metastasis is questionable. In a study by van den Brekel et al., 32% was the overall error of palpation in detecting affected nodes (15). Micrometastases in small nodes may give rise to high false negative rates that may be in the order of 20-30%. Similarly, normal nodes may vary in size up to 2.0 cm and can be readily palpable, and can give rise to false positive rates of up to 20%.

LABORATORY INVESTIGATIONS

In patients with lymphadenopathy, laboratory investigations must be tailored to elucidate the cause suspected from the medical history and clinical examination. Enlarged peripheral lymph nodes are often subjected to biopsy to obtain tissue for histopathological diagnosis and initiation of appropriate treatment.

LYMPH NODE BIOPSY

Biopsy should be promptly performed in patients in whom an underlying malignancy is suspected to be the cause of lymphadenopathy. Biopsy is also appropriate in a setting where the abnormal lymphadenopathy persists for more than four weeks. There are several methods available for direct examination of abnormal lymph nodes.

Open Biopsy

This is the best diagnostic test available as it provides intact tissue for histopathologic examination of abnormal nodal architecture as well as presence of abnormal cells.

Biopsy of peripheral lymph nodes is usually performed without the need for hospital admission, in an outpatient setting, and under local anaesthesia. If multiple nodal groups are involved, the most abnormal one is selected. The choice in descending order of preference, when no single node predominates, is supraclavicular, neck, axilla, and inguinal. The chance of nonspecific result and the frequency of the main complications of lymph node biopsy, i.e., infection and damage to neurovascular structures is greatest with axillary and groin nodes. Though there are more vital structures in the neck, these

can be relatively easily identified and avoided during surgery. Biopsy of the wrong node is not uncommon, causing false negative results.

It is important to inform the pathologist that the specimen is from a lymph node, so that proper stains, smears and cultures can be done. Many techniques require unfixed samples, making diagnosis difficult without them. For e.g., when lymphoma is suspected, special studies involving cytogenetic, immunohistochemical, molecular genetics, and cytogenetic techniques should be anticipated before the specimen is obtained (16).

Fine needle aspiration for cytology

Fine needle aspiration for cytology (FNAC) is most useful when cancer recurrence in a lymph node is suspected. Sampling error results in a substantial false-negative rate, while false-positive results are uncommon (10,17). A specific problem with the FNAC technique is the lack of information on tissue architecture in cases where lymphoma is suspected. In a study by Hehn et al. on the utility of FNAC in the diagnosis of lymphoma, only 29 per cent of FNA attempts at initial diagnosis and 41 per cent of FNACs in recurrent disease could yield a specific and complete histologic diagnosis (18).

FNA has a good role in evaluating lymphadenopathy in patients with HIV infection in whom coexistence of other diseases are suspected (19–21).

Nevertheless, FNA often assumes a larger role in centres where facilities for open biopsy is not available and when practised in a multidisciplinary setting having a specialized team of clinicians, radiologists, and pathologists (22,23).

Core Biopsy

Core biopsy is a relatively inexpensive, low morbidity alternative to open biopsy. Tissue can be obtained for special studies. It also provides some information on nodal architecture.

Ultrasound Guided FNAC / Biopsy

Real-time ultrasound (US) facilitates accurate biopsy (or FNAC) as it permits visualization of the needle within the lesion (24). Studies on thyroid nodules have shown that even in palpable cases, for obtaining adequate material for an accurate cytological assessment, US guidance is superior to manual palpation (24). However, for the achievement of optimal results with US guided procedures, with increased efficacy and decreased inadequacy rates, not only is a skilful aspiration technique and attention to the factors that affect sample adequacy required but also an awareness of the indications for and limitations of FNA biopsy. A strategy for post procedural management also needs to be in place (25).

US guided procedures are cheap, less invasive, associated with reduced morbidity, which is particularly relevant in patients with multiple comorbidities and in the elderly (26). Several studies have shown that US guided FNAC / FNAB can obtain sufficient sample, even in cases of lymphoma, without requirement for excision biopsy (27–29). US guided procedures are becoming increasingly popular and will soon become a key diagnostic investigation. Using larger bore needles as well as increasing the number of passes may improve the diagnostic yield from lymph nodes. The technique is of similar utility in superficial areas which were previously the domain of surgical biopsy (26).

IMAGING ASSESSMENT OF LYMPHADENOPATHY

Imaging has important therapeutic and prognostic significance in patients with lymphadenopathy by aiding in accurate identification and characterization of lymph nodes.

ULTRASOUND

Ultrasonography (US) has been used a cost effective and highly accurate diagnostic tool in the assessment of superficial lymph nodes for more than two decades. Reports from as early as the mid-eighties have shown its diagnostic potential (30,31). Gray-scale US assesses the size, shape, borders as well as internal architecture of lymph node. Sonographically, normal peripheral lymph nodes appear as slightly flattened, oval or reniform, hypoechoic structures with varying amounts of hilar fat (31). They are usually hypovascular but may show some hilar vascularity (32).

Ahuja et al. reported that in addition to the distribution and location of neck nodes, the size, shape, internal architecture, presence or absence of intranodal necrosis, hilar structure and presence or absence of calcification, are other useful grey-scale features that help distinguish between the various causes of lymphadenopathy (33).

TECHNICAL CONSIDERATIONS

Superficial lymph nodes should be assessed using linear array, high frequency transducers with a small footprint and large bandwidth transducers with central frequency above 10 MHz (34).

DIAGNOSTIC CRITERIA

Distribution

Metastatic lymph nodes are site-specific, a feature that helps to identify metastases and assists tumour staging.

Table 2. Common locations of abnormal lymph nodes in the neck (33)

Aetiology	Commonly involved lymph nodal groups
Tuberculosis	Supraclavicular fossa Posterior triangle
Metastases from	
Oropharynx, hypopharynx, larynx	Internal jugular
Oral cavity	Submandibular Upper cervical
Infraclavicular carcinomas	Supraclavicular Posterior triangle
Nasopharyngeal carcinoma	Upper cervical Posterior triangle
Papillary carcinoma of the thyroid	Internal jugular
Non-Hodgkin's lymphoma	Upper cervical Submandibular Posterior triangle

In cases where the primary tumour is not identified, the distribution pattern of metastatic nodes may suggest a primary location (33).

Size

Lymph node size using the axial or transverse nodal diameter was used earlier as an indicator of malignancy. Optimal size criterion varies with the nodal group involved and also the patient population (35). However, assessment of size alone cannot be relevant, as inflammatory nodes can be large, whilst metastatic nodes, very small. Using a lower cut-off for nodal size increases the sensitivity but considerably decreases the specificity and vice versa (33,34).

However, nodal size is of value in the follow up of patients with a known primary tumor. An increase in size on follow up examinations is highly suspicious of malignancy (36).

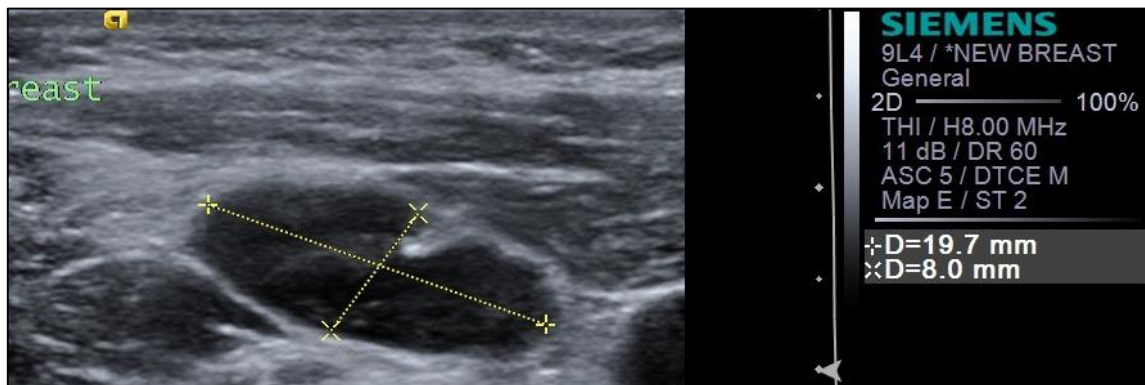


Fig. 6. US image showing short axis and long axis dimensions of a reactive axillary lymph node.

Shape

Classically, benign nodes are oval whereas malignant nodes are round. Nodal shape or 'roundness index' is defined by the ratio between the long axis diameter (L) and the

short axis diameter (S). In an oval benign node, the long axial diameter will be at least twice as great as the short axis diameter, described as $L/S > 2$ or $S/L < 0.5$. The value of L/S in a round, malignant node is less than 2 or < 1.5 or $S/L > 0.5$ (37,38).

Shape is however, misleading at times, as normal parotid and submandibular as well as abnormal tuberculous nodes can also be rounded (36,39).

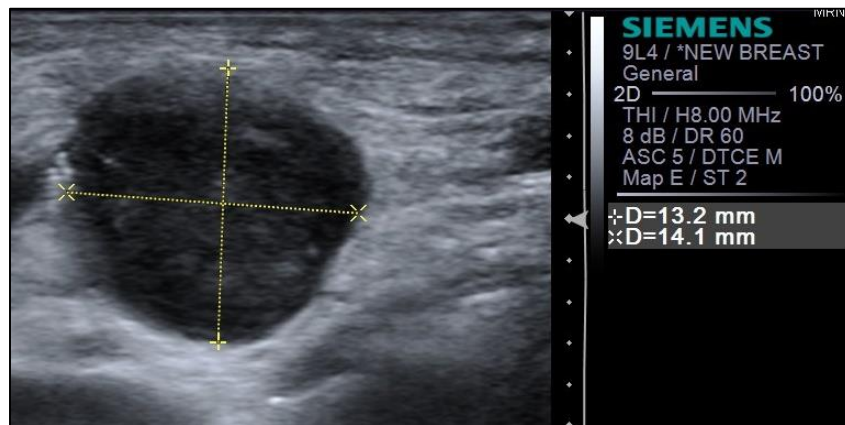


Fig. 7. US image of a tuberculous lymph node with a long axis to short axis ratio of 1.07

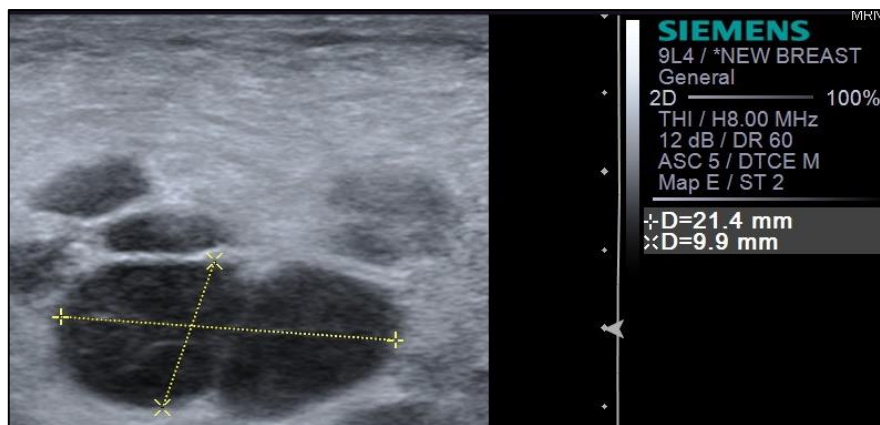


Fig. 8. US image of a malignant lymph node with a long axis to short axis ratio >2

Eccentric cortical hypertrophy indicates focal intranodal tumour infiltration and is another useful sign to identify malignant nodes (40).

Nodal Margin

Traditionally, malignant nodes have sharp borders, whereas benign nodes may have indistinct borders. The sharp border in malignant lymph nodes can be attributed to the mismatch in the acoustic impedance between the lymph nodes and surrounding tissue which occurs due to replacement of normal intranodal lymphoid tissues by infiltrating tumor cells. Reduced fatty infiltration also contributes to the difference in acoustic impedance between the lymph nodes and surrounding tissues. Active inflammation or edema of the surrounding soft tissues (periadenitis) in infective and inflammatory nodes causes them to have indistinct borders (41,42).

Sharpness of nodal border has limited imaging utility. However, presence of ill-defined borders in proven malignant nodes indicates extracapsular spread, a factor that aids in prognostication (33).

Structural changes

Hilum

The presence of a central echogenic hilum is a manifestation of the normal anatomy of a lymph node and is hence, considered a sign of benignity. However, it can also be seen in early nodal malignancy and can also be absent in benign conditions such as tuberculosis, limiting its applicability as a sole criterion for lymph node assessment (40,43).

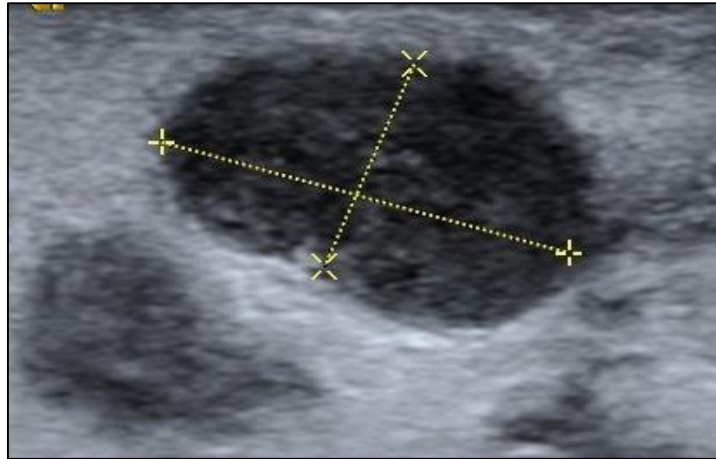


Fig. 9. US image of a cervical lymph node with absent hilum. HPE was reported as granulomatous inflammation.

Echogenicity

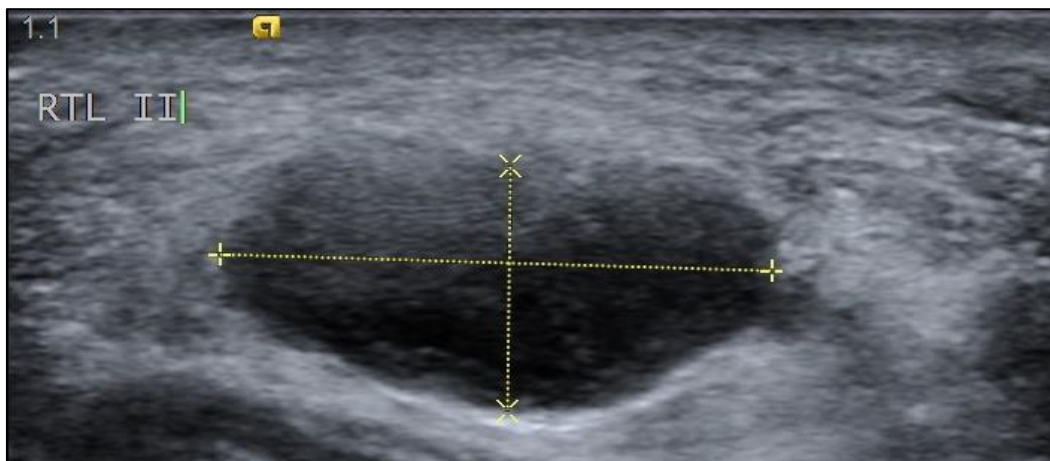


Fig. 10. US image of a hypoechoic tuberculous cervical lymph node.

Metastatic lymph nodes tend to be hypoechoic when compared to adjacent muscles (44). However, presence of thyroglobulin makes metastatic nodes from papillary carcinoma of thyroid hyperechoic (45). On the other hand, tuberculous lymph nodes after often hypoechoic due to the high incidence of intranodal necrosis (46).

Calcification

Nodal calcification, though rare in metastatic lymph nodes, is commonly seen in metastatic nodes from papillary and medullary forms of thyroid carcinoma. This occurs due to development of psammoma bodies, which are reported to be formed by intravascular tumor thrombi or due to calcification of infarcted tips of malignant papillae. (45) Intranodal calcification can also be seen post chemotherapy or irradiation and also in some cases of residual tuberculous lymphadenitis (45,46).

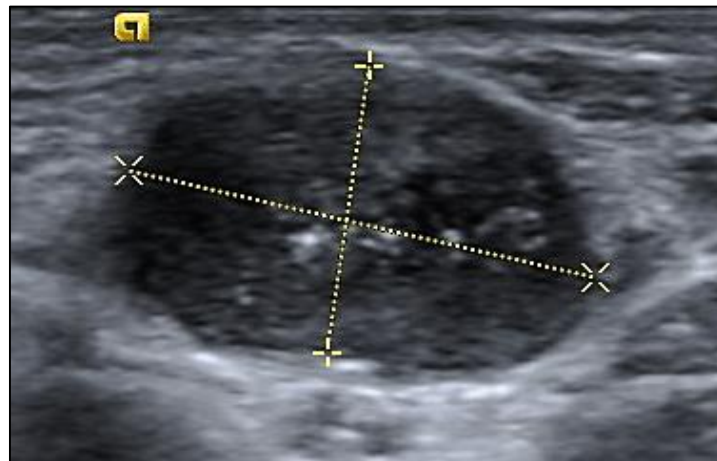


Fig. 11. US image of a cervical lymph node with intranodal micro calcifications.

HPE was reported as granulomatous inflammation.

Intranodal Necrosis

In the temporal profile of tumoral infiltration of a lymph node, nodal necrosis occurs as a late event. It encompasses two types - as an echogenic area (*coagulation necrosis*) or a cystic area (*cystic necrosis*). Cystic necrosis appears as an eccentric, anechoic area within the lymph nodes. It is commonly seen in metastatic nodes from papillary carcinoma of the thyroid and squamous cell carcinoma, and also in tuberculous lymphadenitis (41,45,46). Coagulation necrosis is uncommon and appears as an

isolated echogenic focus within the lymph node that does not communicate with the hilum or the perinodal fat. It may be found in both inflammatory and malignant nodes.

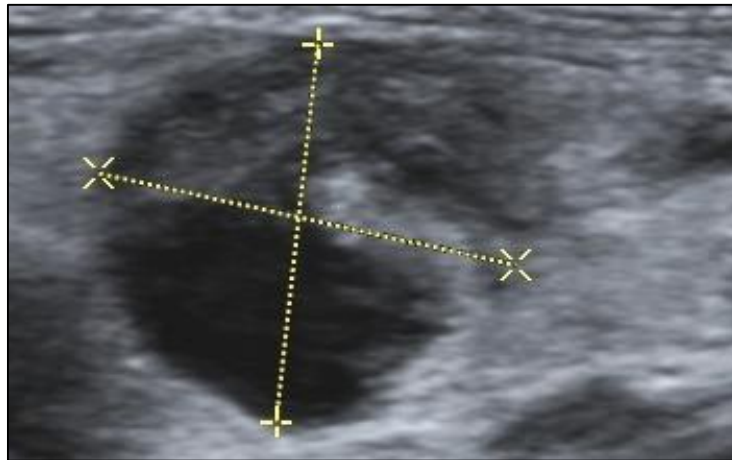


Fig. 12. US image of a cervical lymph node with focal necrotic area. HPE was reported as granulomatous inflammation.

Intranodal necrosis is always an abnormal finding, though, without disease specificity (33,34).

Ancillary findings

Matting

Matting is always pathological. In a study by Khanna et al., 83% of tuberculous nodes, 66% of metastatic nodes and 14% of cases with lymphoma were matted (38).

Perinodal edema

Peripheral halo or edema around a lymph node is always abnormal and occurs as an inflammatory response or due to tumor infiltrating into the adjacent soft tissue (46,47).

COLOUR DOPPLER

TECHNICAL CONSIDERATIONS

For an adequate assessment of superficial lymph nodes, the highest available colour Doppler (CD) frequency should be put to use. Wall filter settings should be low. Also, colour gain needs to be adjusted immediately below the level where nonvascular flickering within tissues occurs (34).

VASCULAR PATTERN

Absence or presence of flow

This parameter as a sole criterion has very low specificity. Small benign lymph nodes may not demonstrate vascularity. Malignant lymph nodes which are often vascular, may also lack Doppler signals when necrosis is present (42).

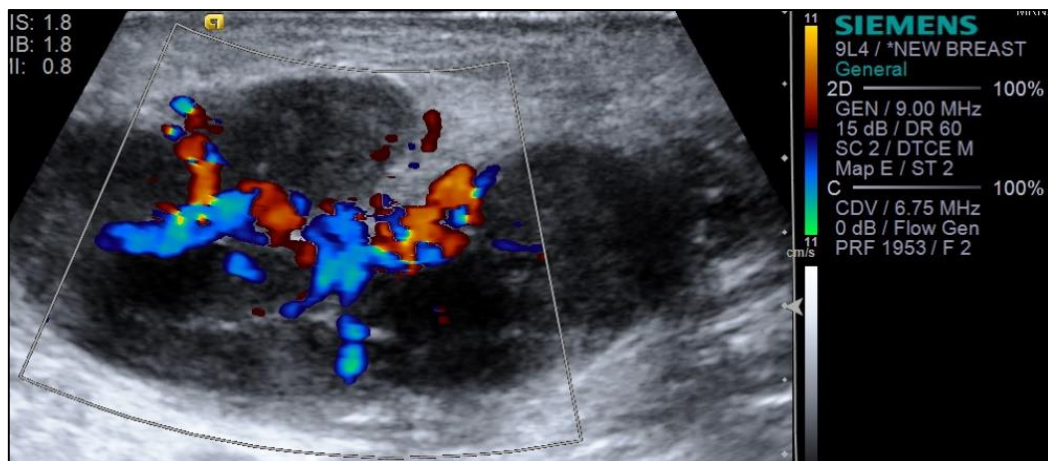


Fig. 13. Colour Doppler image of a metastatic lymph node demonstrating increased vascularity

Number, Location and Distribution of Vascular Pedicles

In benign nodes there is a single vascular pedicle that enters the hilum and branches radially throughout the node. Malignant nodes have multiple pedicles which invade the cortex and demonstrate a chaotic distribution pattern within the node (48,49). This chaotic pattern, is however, not unique to malignant nodes, and can also be seen in tuberculosis (33).

Vascular Resistance

In a normal lymph node, intranodal blood flow velocity increases with increase in its size. However, vascular resistance remains largely unchanged. In some studies the *pulsatility index* (PI) and *resistivity index* (RI) of reactive lymph nodes has been reported to be lower than that of metastatic lymph nodes (50–52).

Jayachandran et al., in their study of 80 adult Indian subjects, noted that for Doppler US, by vascular flow pattern there was 94.1% sensitivity, with a 100% specificity and an accuracy of 95.4% whereas by vascular indices the sensitivity was found to be 81.4%, specificity of 100%, and accuracy was 85.5%, which was a statistically significant correlation, ($P < 0.05$). They concluded that Doppler ultrasonography plays a definitive role as an adjunct to clinical evaluation in differentiating metastatic from reactive cervical lymph node involvement in patients with oral cancer as it aids in grading and staging of oral cancer (53).

However, in a study done by Adibelli et al. no such significant difference was found (42).

Owing to the considerable overlap of resistance parameters, in distinguishing malignant from benign lymph nodes, the role of Doppler in routine practice for evaluation of lymph nodes is of limited value (33,34).

Table 3. Classic ultrasound and colour Doppler US criteria in differentiating benign vs. malignant lymph nodes (27)

Criterion	Benign	Malignant
B mode		
Size	Small	Large
Shape	Oval	Rounded
Hilum	+	-
Echogenicity	Low or moderate	Markedly hypoechoic
Margins	Sharp	Irregular
Structural changes	-	+
Soft tissue edema	+/-	-
Doppler		
Flow	-	+
Vascular pedicle	Single	Multiple
Vessel location	Central	Peripheral
Vascular pattern	Regular	Chaotic
Flow impedance	Low	High

CONTRAST ENHANCED DOPPLER SONOGRAPHY

Reports suggest that the diagnostic accuracy of an US echo enhancer (contrast agent) in differentiating between benign vs. malignant lymphadenopathy is superior to conventional B-mode and conventional Doppler sonography (54,55). However, the short duration of contrast enhancement acts as a limiting factor, often necessitating the administration of more than one dose of contrast agent for an optimal assessment (33).

APPLICATION OF ULTRASOUND AND DOPPLER IN LYMPH NODE IMAGING

Conventional B-mode US is widely used to assess palpable lymph nodes in patients. It evaluates a multitude of parameters to discern whether a node is malignant or not.

Traditionally, imaging modalities such as US, computed tomography (CT) and magnetic resonance imaging (MRI) rely mainly on size measurements and topographic distribution for the differentiation of malignant from benign lymph nodes (56).

Lyshchik et al found that short-to-long-axis diameter ratio greater than 0.5 was the best grayscale criterion with 75% sensitivity, 81% specificity, and 79% overall accuracy (57).

Irrespective of the orientation of the node to the horizontal plane of the CT, US allows for measurement of the true axial and transverse diameter, giving it a significant advantage over CT scan (58) .

In a multivariate analysis of US findings as assessed by logistic regression analysis, performed by Chikui et al., suggested that the only sonographic features such as increases in short axial diameter, presence or absence of hilar echoes, and the presence

of normal hilar flow were predictive of reactive (presence of hilar flow and hilar echoes) and metastatic (increase in short axis length) lymph nodes. According to the multivariate analysis, colour-flow criteria did not provide any significant contribution in predicting metastatic nodes. However, the colour-flow criteria did appear to have improved the overall diagnostic accuracy for the less experienced observer (59).

ELASTOGRAPHY

Ultrasound elastography is a novel emerging imaging technique used for non-invasive assessment of viscoelastic properties of tissue. The word '*elastography*' was first coined by Ophir et al. in 1991 (59). The information displayed in the images on elastography acts as a surrogate for that obtained with manual palpation (60). Elastography images of a lesion are generated by an US machine along with a simultaneous acquisition of grey scale images, enabling comparison between the two (61).

COMMON TERMINOLOGY USED IN ELASTOGRAPHY (60–62)

Stress

Stress is defined as force per unit area, measured in Pascal (Newton/m²).

$$\text{Stress (kPa)} = \text{force/area}$$

Compression or longitudinal stress acts perpendicular to a surface causing the object to shorten. Stress when applied parallel to the surface causes deformation and is known as shear stress.

In elastography, stress can be applied in two ways, exogenous or endogenous. Exogenous stress is applied by the use of US transducers, vibrators or acoustic radiation force by using gentle intermittent freehand compression along the axis of the US beam. Endogenous stress comes from blood vessel, cardiac or respiratory motion.

Strain

The amount of deformation, i.e., change in original size and shape of an object, on applying stress is known as strain. Longitudinal strain causes change in length of an object while shear strain causes a change in its angles. The harder the object, the lower is its strain value. Strain is dimensionless and lacks any SI unit.

$$\text{Strain} = \text{change in length/original length}$$

A limitation of elastography that is similar to clinical palpation is that compression causes more displacement in tissue that is nearer to the applied force than in tissue that lies in a deeper plane.

Strain Rate

It is defined as the amount of strain that occurs in a unit of time, i.e., how quickly (or slowly) a material is being deformed.

Shear Modulus

Also known as modulus of rigidity, is a ratio between shear stress and shear strain.

Elasticity

Elasticity is the property of an object to regain its original form once stress is removed.

Viscosity

It is a measure of resistance of a fluid when it is subjected to stress.

Viscoelasticity

The ability of a material to exhibit both viscous and elastic properties, as in soft tissues, is viscoelasticity.

Hooke's Law

Within the elastic limits of an object, the stress applied on it is proportional to the strain.

Poisson's Ratio

It is the ratio of lateral strain over longitudinal strain. Poisson's ratio typically ranges between zero and 0.5.

Young's Modulus

It is proportionality constant between stress and strain and is a measure of the tissue's resistance to compression.

$$\text{Stiffness} = \text{stress/strain (Hooke's law)} \cong \text{Young's elastic modulus (kPa)}$$

ELASTOGRAPHY TECHNIQUES

Techniques of elastography (60,61,63) vary depending upon:

1. The method of tissue excitement (by using mechanical or ultrasonic force).
2. Tissue response to compression.
 - a. *Static (or quasistatic) method* - tissue response to a single constant compression is assessed
 - b. *Dynamic method* - where a time-varying force is applied, which can either be a short transient mechanical force or an oscillatory force with a fixed frequency
3. The mechanical parameters measured (stress, strain or modulus).

TYPES OF ELASTOGRAPHY

STRAIN ELASTOGRAPHY

Strain elastography could be performed using conventional US hardware and hence, was the first technique to appear on clinical US systems using a few software modifications.

The transducer is positioned in a manner similar to that of conventional US. Once the tissue of interest is identified on gray scale image, exogenous or endogenous compression is used to displace tissues. Tissue displacements along the beam axis are determined from the radiofrequency data received by comparing successive images using software cross-correlation methods. Then tissue strain is calculated for each spatial location. The resultant data can be graphically displayed as a two-dimensional map of relative tissue strain, called an elastograms (60,64).

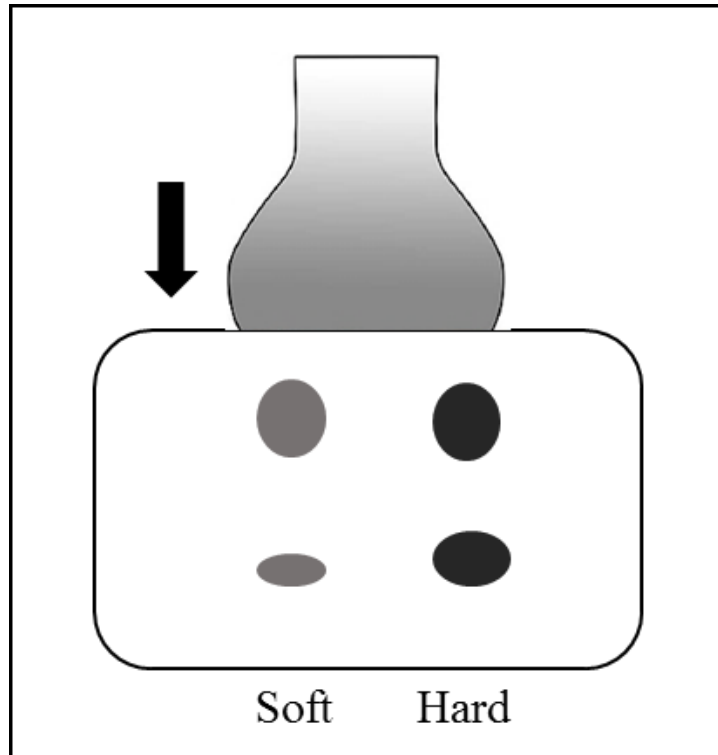


Fig. 14. Schematic diagram of strain elastography in which tissue displacement occurring along the axis of the applied force is measured.

For a given stress, soft lesions deform more than stiff lesions, and thus have higher strain (63).

A colour-coded scale is used in elastograms such that they are displayed as a semi-transparent overlay onto gray-scale images.

SHEAR WAVE ELASTOGRAPHY

Shear wave elastography is a quantitative method which has been recently introduced.

It utilizes a specially modified transducer to produce focused impulses of high intensity acoustic radiation (US), called push pulses, at specific locations within the tissue of interest. This produces shear waves, whose velocities can be tracked by a series of normal intensity impulses using US correlation methods (64).

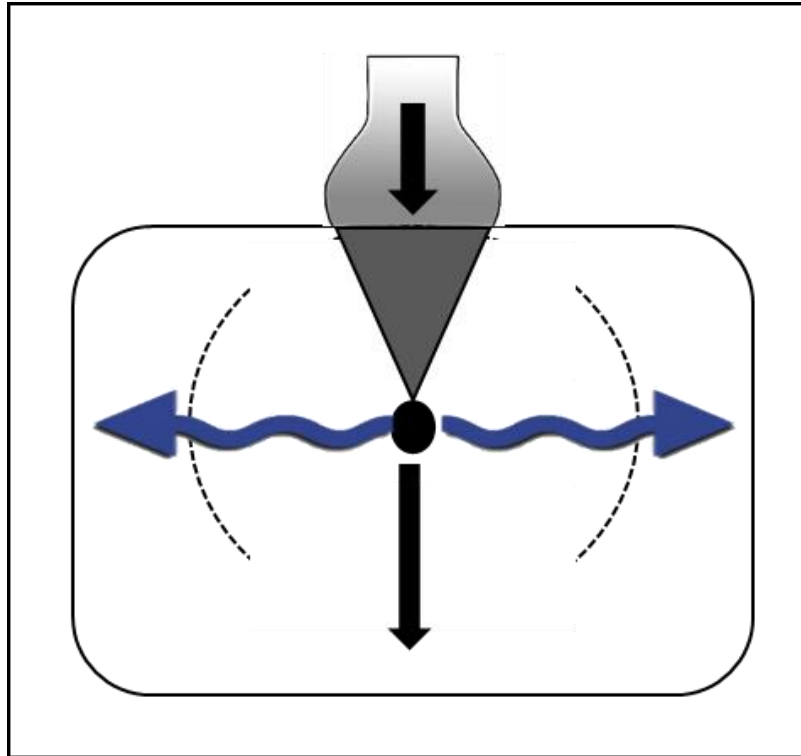


Fig. 15. Schematic diagram of stress elastography in which shear waves generated by the tangential sliding of the tissue particles, traveling perpendicularly to the direction of the applied force are measured.

Shear waves can propagate in solids but not in true liquids. They travel with a velocity proportional to the square root of the tissue stiffness given according to the following formula:

$$E = 3\rho c^2$$

Where E - tissue stiffness, i.e. Young's elastic modulus (kPa),

c - Shear wave velocity (m/s), and

ρ - Density (kg/m^3)

As both strain elastography and shear wave elastography are operator dependent, careful attention to practical technique is required. Precompression is a term used to

describe tissue elasticity that varies with the amount of resting pressure applied. Thus, minimal pressure should be applied on the skin with the transducer during acquisition. Misleading elastograms can be produced when excessive precompression is applied as it increases the overall stiffness of tissues while lowering relative stiffness contrast between different tissues (65).

Shear wave elastography may be less operator dependent than strain imaging because it does not require freehand compressions (63).

APPLICATION OF ELASTOGRAPHY TECHNIQUES IN LYMPH NODE IMAGING

The basic principle of elastography is that malignant tissue is stiffer and deforms less when compared to a benign tissue which is softer. Conventional elastography uses a semi quantitative method of assessing relative tissue stiffness using elasticity scores based on the degree of strain a tissue undergoes in response to an external compressive force (66).

Only a few studies with sample sizes between 51 to 141 and comprising a variety of benign and malignant pathological entities have evaluated USE as a diagnostic tool for detection of malignancy in cervical lymph nodes (67). These studies have shown that lymph node elastography modality improves the specificity of conventional US in characterizing palpable lymph nodes.

In a study by Alam et al., elastographic patterns of cervical lymph nodes were determined based on the percentage of the lymph node area with high elasticity and the

distribution pattern. They examined eighty five cervical lymph nodes (metastatic, n= 53; reactive, n = 32) from 37 patients by both elastography and B-mode US in a prospective study. While pattern 1 was considered as being an absent or very small hard area, pattern 5 was defined a hard area occupying the entire lymph node. The cut-off line was set between patterns 2 and 3 for reactive versus metastatic nodes. Patterns 3–5 were considered metastatic. The sum of scores for five criteria: shape, short-axis diameter, border (regular or irregular), hilum (present or absent) and echogenicity (homogeneous or inhomogeneous) was used to arrive at the B-mode sonographic diagnosis. The cut-off line being set between scores 6 and 7 for reactive versus metastatic; scores 5 and 6 were considered reactive, while scores 7–10, metastatic. It was found that the specificity, sensitivity and accuracy of B-mode US were 59%, 98%, and 84%, respectively; 100%, 83%, and 89% for elastography; and 94%, 92%, and 93% for the combined evaluation of both (67).

Ghajarzadeh M et al. did a systematic review to determine the diagnostic accuracy of US elastography in the evaluation of cervical lymph nodes. A total number of 936 cervical LNs was evaluated (502 malignant and 434 benign). The sensitivity of the strain ratio (SR) measurements and the scoring system for the differentiation of benign and malignant LNs were 0.83 (95% CI: 0.78-0.87) and 0.76 (95% CI: 0.71-0.8). The specificities were 0.84 (95% CI: 0.79-0.88) and 0.8 (95% CI: 0.75-0.84), respectively. Area under the curve for SR measurement was 0.95 (SE = 0.02) and 0.86 (standard error [SE] = 0.03) for the scoring system (68).

Lyshchik et al. evaluated one hundred forty-one peripheral neck lymph nodes (60 metastatic, 81 metastasis free) in 43 consecutive patients. Patients referred for surgical

treatment of suspected hypopharyngeal or thyroid cancer were examined with gray-scale US, power Doppler US, and US elastography. The following lymph node characteristics were evaluated at gray-scale and power Doppler US: echogenicity, calcifications, short-axis diameter, short-to-long-axis diameter ratio, and vascularity. Using a four-point rating scale, US elastograms for lymph node visibility, relative brightness, margin definition and margin regularity were evaluated. In addition, strain measurements of lymph nodes and surrounding neck muscles were done on elastograms, and the strain index, i.e., the muscle-to-LN strain ratio, was calculated. With 98% specificity, 85% sensitivity, and 92% overall accuracy, a strain index greater than 1.5 had high utility in the classification of metastatic nodes, results that were significantly better than those obtained by using short-to-long-axis diameter ratio greater than 0.5, the best gray-scale criterion, with had a specificity of 81%, sensitivity of 75%, and overall accuracy of 79% (57).

Nazarian et al. observed that diagnostic techniques used for lymph node detection must be sensitive enough to allow detection and removal of all cancer deposits and specific enough to avoid unnecessary treatment. However, since no imaging technique is perfect, tissue diagnosis is almost always needed for definitive staging. Though US guided FNAC / FNAB is both specific and sensitive for diagnosing nodal metastases, it could still yield false-negative results. The study found that US elastography has the potential to improve the accuracy of percutaneous biopsy and/or nodal dissection. It also increases the accuracy of imaging findings on follow-up of post-operative cases, especially when metastatic infiltration causes lymph nodes to harden before they increase in size (69).

Tan et al. performed B-mode US, power Doppler imaging, and US elastography in 128 cervical lymph nodes of 107 consecutive patients. Only nodes that could be unequivocally matched between sonography and pathology were analysed. Using histopathological analysis as the reference standard, the results of B-mode US, power Doppler imaging, and US elastography were interpreted separately to assess cervical nodes. There was a marked difference ($P = .000$) found in the strain ratio between 58 benign (median, 1.44; range, 0.62-3.90) and 70 malignant nodes (median, 2.71; range, 1.36-36.09). Receiver-operating characteristic curves showed that > 1.5 strain ratio had high utility in classifying enlarged cervical lymph nodes, with sensitivity of 92.5%, specificity of 53.4%, and a Youden's index of 0.463. They found these results to be significantly better than those obtained using a ratio of long-axis to short-axis diameter > 2 , their best gray-scale criterion, which yielded a sensitivity of 58.6%, specificity of 70%, and a Youden's index of 0.286. The highest kappa values for inter observer agreement was using elastography. They concluded that US elastography holds much promise as an adjunct modality in screening and monitoring lymphadenopathy (70).

In their study Teng et al. examined the single node most suspicious of malignancy from each of the 89 subjects. They examined these lymph nodes using B-mode US, power Doppler and US elastography imaging. Elastography evaluation methods included the 4 scoring scale of elastographic classification. When $\geq 80\%$ area of the lymph node plane section was green or red (soft), a score of 1 was given. A score of 2 indicated that $< 80\%$ and $\geq 50\%$ of the node was red or green. A score of 3 was assigned for nodes with $< 80\%$ and $\geq 50\%$ blue areas (hard), and a score of 4 was to indicate that $\geq 80\%$ area of the nodal section was blue. Lesions with a score of 1 or 2 were classified as

probably benign, while scores of 3 and 4 were indicative of probable malignancy. They also used the strain ratio (SR) of neck muscle to cervical lymph node as another kind of elastographic evaluation method. The cut-off point of SR was calculated to be 1.78 using receiver-operating characteristic curves, with values ≥ 1.78 indicative of malignancy. Among the gray-scale US parameters, short-axis diameter was found to be the most accurate with sensitivity, specificity and accuracy of 94.20%, 40.50% and 71.90% respectively, while the values were 67.3%, 75.7% and 70.8% respectively, for power Doppler imaging. Of the two elastographic criteria used, the 4 scoring method showed sensitivity, specificity and accuracy values of 88.4%, 35.1% and 66.3%, respectively, while 98.1%, 64.9% and 84.3% were the values for SR. The study concluded that except short-axis diameter the sensitivity of SR was significant higher than all the other diagnostic criteria examined and that the accuracy of SR was the highest. This showed that elastography does aid in differentiating benign and malignant cervical lymph nodes (71).

Arda et al. studied fifty-one patients (12 men, 39 women) referred for fine-needle aspiration or surgical biopsies of suspected cervical lymph nodes with gray scale US, power Doppler US, and real-time US elastography. During Doppler US examination, vascularity and resistance index (RI) values were evaluated. US elastograms for lymph nodes were evaluated using a five-group elastographic colour coding pattern. Pattern 1 was for a very small or an absent hard area; pattern 2 for hard area $< 45\%$; pattern 3 for hard area $\geq 45\%$; pattern 4 for central soft and peripheral hard areas; and lastly, pattern 5, hard area occupying the entire solid component with or without the presence of a soft rim. Strains of nodes and surrounding muscles were measured, and the muscle-to-LN

ratio (strain index) was calculated on elastograms. A strain index higher than 2.45 and colour patterns 4 and 5 had high utility in the classification of malignant lymph nodes with sensitivity of 93.8% and specificity of 89.5% with 89.5% positive and 93.8% negative predictive values respectively ($p < 0.001$). The results were significantly better than those obtained by using Doppler US characterization using $RI > 0.57$ which had sensitivity, specificity, positive and negative predictive values of 78.9%, 90.6%, 83.3% and 87.9%, respectively ($p < 0.001$). The mean strain index value of benign lymph nodes was 1.4 ± 0.97 , and the mean strain index values of malignant lymph nodes were 10.9 ± 14.9 (72).

Overall, preliminary evidence suggests that US elastography may be a useful imaging adjunct in aiding differentiation between benign and malignant peripheral lymph nodes, although further research is required (73).

ACOUSTIC RADIATION FORCE IMPULSE IMAGING

Acoustic radiation force impulse (ARFI) as a method of mechanical tissue excitation was first proposed by Sugimoto in 1990 (74). ARFI based elasticity imaging methods use short duration acoustic radiation force known as push pulses to transiently deform soft tissue which returns to its original position once the pulse is stopped. This dynamic displacement response of tissues can be measured by US and is used to estimate the tissue's mechanical properties. These measured data can be reconstructed to provide both qualitative images and quantitative elasticity metrics, providing complimentary information to both diagnose as well as longitudinally monitor disease progression (61,64). This method of excitation is coupled directly within the organ of interest. This

can be advantageous when compared with external methods which couple with the organ of interest through the intervening tissues (64). Images related to tissue stiffness can be either qualitative or quantitative.

VIRTUAL TOUCH IMAGING (VTI)

It provides a qualitative as well as a semi-quantitative assessment by forming images portraying the relative differences in tissue stiffness.

In VTI mode, the gray-scale US and VTI images are displayed simultaneously, side by side, in a split-screen mode. Comparison between the lesion and the surrounding tissue is used to classify the gray-scale value in VTI image into two values (black or white) which can be scored accordingly (55, 58).

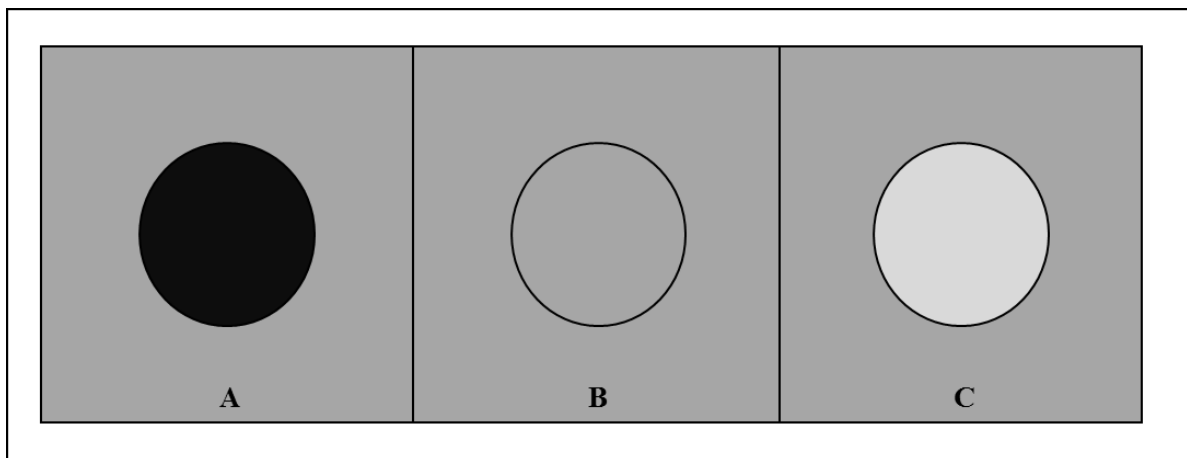


Fig. 16. Schematic diagram of brightness pattern on virtual touch imaging, A: darker than surrounding; B: equal to surrounding; C: lighter than surrounding tissue.

In addition, VTI area ratio (VAR) gives a ratio of the areas of the nodules on both VTI and B-mode images. It is proposed that the area ratio of malignant lesions is more than that of benign lesions (75).

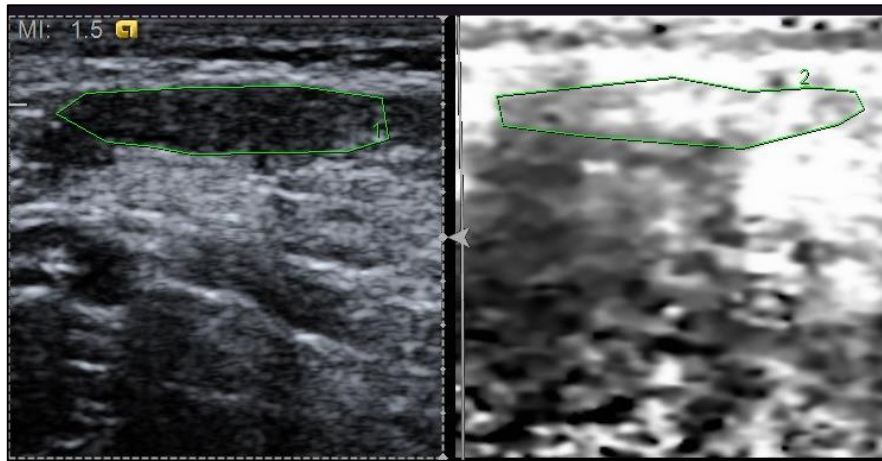


Fig. 17. US and corresponding VTI image of a reactive lymph node demonstrating the brightness of the node compared to surrounding tissue.

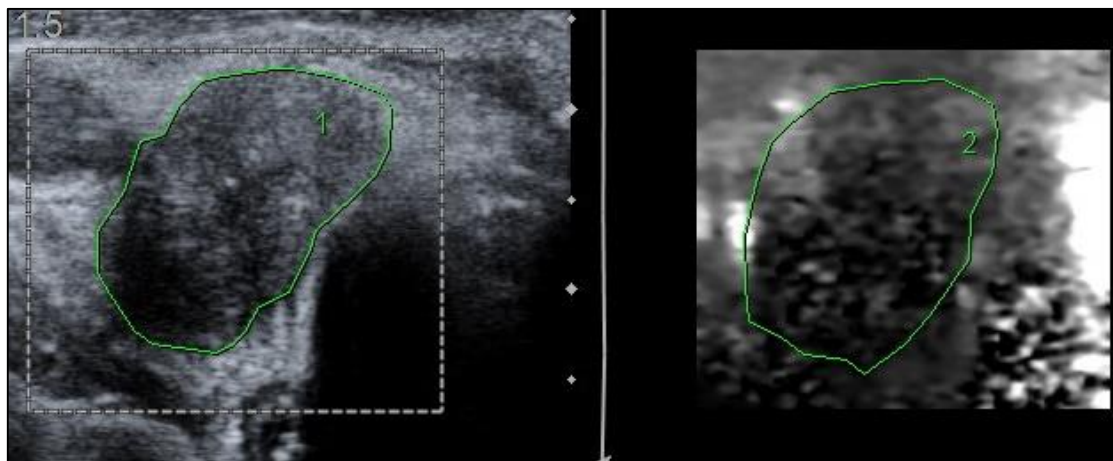


Fig. 18. US and corresponding VTI image of a malignant lymph node demonstrating that the node is darker than the surrounding tissue. HPE was reported as papillary thyroid carcinoma with nodal involvement.

VIRTUAL TOUCH QUANTIFICATION (VTQ)

It provides a quantitative estimate of the underlying tissue elasticity by displaying the shear wave velocity using reconstruction methods.

The operator first positions a fixed, 5 mm x 5 mm, sized box, the ROI, over the tissue of interest on the gray-scale image. Once the ARFI capture mode is triggered, the value of the mean shear wave velocity of the ROI is estimated and displayed (63).

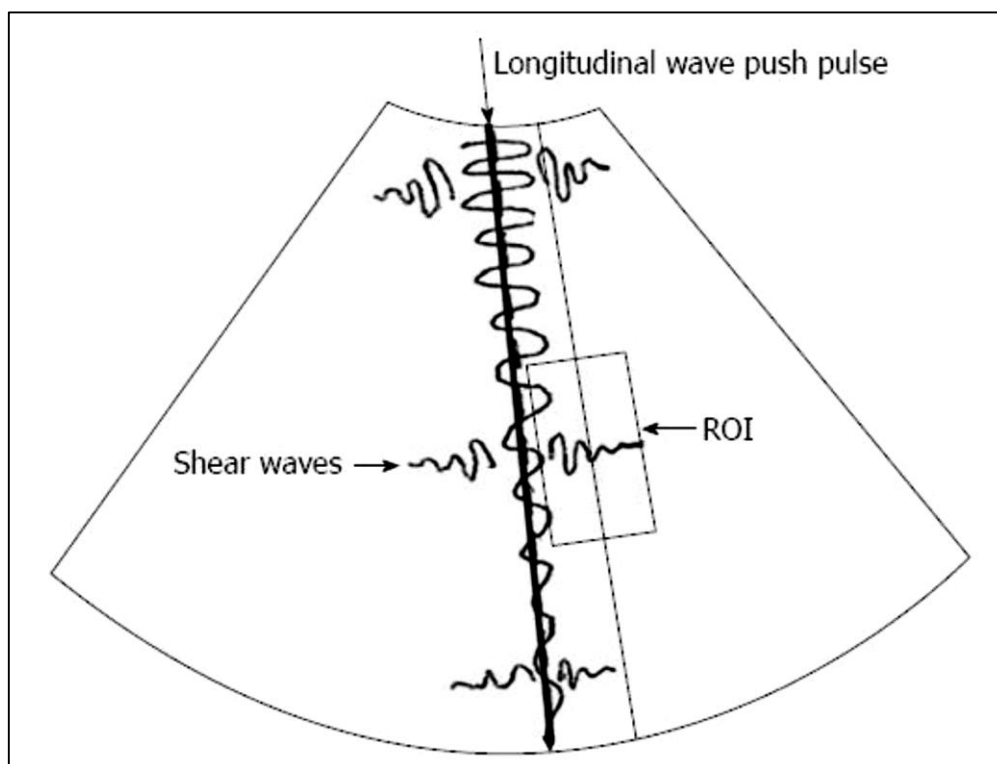


Fig. 19. Technical scheme of virtual touch quantification. ROI: Region of interest.

APPLICATION OF ARFI IN IMAGING PERIPHERAL LYMPH NODES

ARFI uses short acoustic radiation forces to create local tissue displacements which are dependent on the elastic properties of the tissue. Shear waves generated by the acoustic radiation force travel faster in stiffer tissues while they are slower in softer tissues.

There are two basic components in ARFI elastography, one is Virtual Touch Imaging

(VTI) (5) which gives a qualitative depiction of tissue stiffness on a grey-scale and the other is Virtual Touch Quantification (VTQ) which provides quantitative assessment of tissue stiffness in meters per second. Area ratios can be calculated using VTI mode while shear wave velocity is obtained from VTQ mode. This new modality aims to improve lesion characterization especially in cases of indeterminate lesions, thereby avoiding unnecessary biopsies.

Though the application of ARFI imaging in the liver has been standardized for a while now, its use in other organs is still limited to research phase, with very few studies being currently available on the evaluation of peripheral lymph nodes.

Fujiwara et al. studied used ARFI to compare the stiffness of forty two lymph nodes (reactive = 22; metastatic = 20) in 19 patients (6 women, 13 men; mean age, 63.68 ± 14.9 y; range, 23-85 y) with cervical lymphadenopathy. They evaluated the shear wave velocity (SWV, m/s) of each lymph node by ARFI imaging. Reactive lymph nodes had a SWV of 1.52 ± 0.48 m/s, while SWV of metastatic/malignant lymph nodes was 2.46 ± 0.75 m/s. Using a cut-off SWV > 1.9 m/s was found to be very useful in the classification of metastatic lymph nodes, with 81.8% sensitivity, 95.0% specificity and 88.0% overall accuracy. The area under the ROC curve was 0.923 (95% confidence interval, 0.842-1.000). They thus concluded that ARFI imaging was useful in differentiating reactive and malignant/metastatic cervical lymph nodes (76).

Meng et al. evaluated the virtual touch quantification (VTQ) component of ARFI in their study. The VTQ values were analysed in 181 cervical lymph nodes (87 benign, 94 malignant) of 123 patients (mean age 40.8 years, range 1-81 years). Using a cut-off value of 2.595 m/s, the mean VTQ values of the benign lesions was found to be $2.01 \pm$

0.95 m/s and that of malignant lesions was 4.61 ± 2.56 m/s ($p < 0.001$). Malignancy could be predicted using the receiver operating characteristic curves of VTQ with the cut-off value with 82.9% sensitivity, 93.1% specificity and areas under the curve of 0.906 (95% CI 0.857-0.954). ARFI was reported to be a feasible complement to B-mode US to potentially improve the characterization of cervical lymph nodes (77).

Virtual touch imaging (VTI) was analysed by Che et al. in 81 patients (mean age, 46.6 years; range, 5-82 years) with 81 lymph nodes (36 benign nodes and 45 metastatic nodes). Bright regions on the VTI images defined tissue that was more elastic than dark areas. Most metastatic nodes were obviously darker than the surrounding tissue while most benign lymph nodes were either the same in brightness or slightly darker or when compared with surrounding tissue. For metastatic lymph nodes the mean area ratio of (1.39 ± 0.20) was statistically higher than the mean area ratio of benign lymph nodes (1.05 ± 0.15 ; $P < 0.001$). The cut-off level for area ratio of metastatic lymph nodes was estimated to be 1.16. Using receiver operating characteristic curves with this cut-off value, the area ratio predicted malignancy with 91.1% sensitivity and 83.3% specificity (78).

Xu et al. used US, SE and ARFI including VTI and VTQ to perform a multivariate analysis in the pre-operative evaluation of 222 consecutive patients with papillary thyroid carcinoma. In the analysis, VTI area ratio (VAR) > 1 emerged to be the best predictor for central lymph node metastasis (CLNM). ROC analyses showed that the sensitivity, specificity and areas under the curve were 0.600-0.630, 47.7 %-93.2 %, and 26.9 %-78.4 % for US, respectively. For VAR > 1 they were 0.784, 83.0 %, and 73.9 %, respectively. A combination of US characteristics without and with VAR, the

sensitivity and specificity were 77.6 %, 11.2 % and 83.0 %, 100.0 %, and, respectively ($p < 0.001$).

They concluded that in predicting cervical lymph node metastasis in patients with papillary carcinoma of thyroid, ARFI elastography showed superior performance over conventional US, particularly when combined with US (75).

Xu et al. also performed another prospective study to propose a new rating system using a risk model including conventional US as well as ARFI imaging for predicting central lymph node metastasis in patients with papillary thyroid microcarcinoma (PTMC). US and ARFI including VTI and VTQ was used to evaluate a total of 252 patients with PTMCs preoperatively. Univariate and multivariate analyses of various risk factors of independent variables for CLNM were performed. The results showed that multiple suspicious foci, capsule involvement, rare internal flow on US, and $VAR > 1$ on ARFI imaging were the risk factors for predicting CLNM and thus has a potential to avoid unnecessary nodal dissection in the central compartment (79).

It can thus be concluded that ARFI has great potential when combined with US I predicting malignancy/metastasis within peripheral lymph nodes.

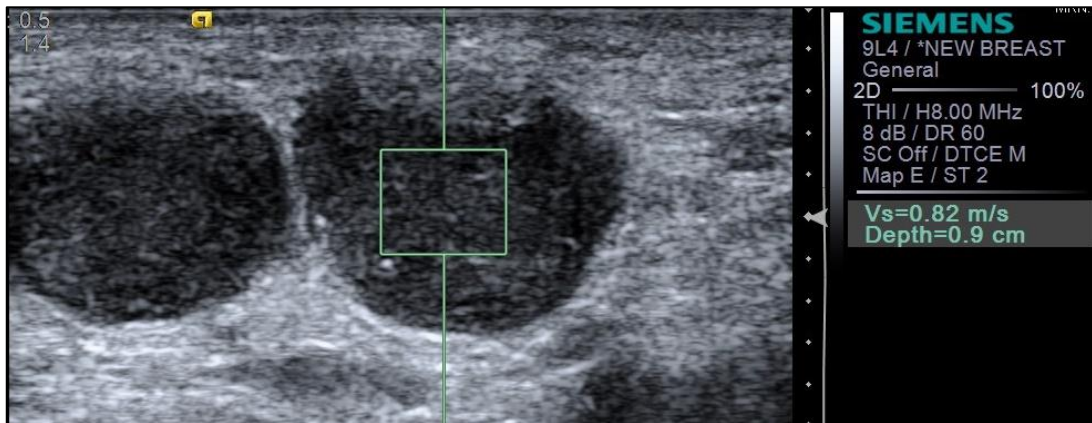


Fig. 20. Tuberculous round, hypoechoic lymph node with SWV 0.8 m/s.

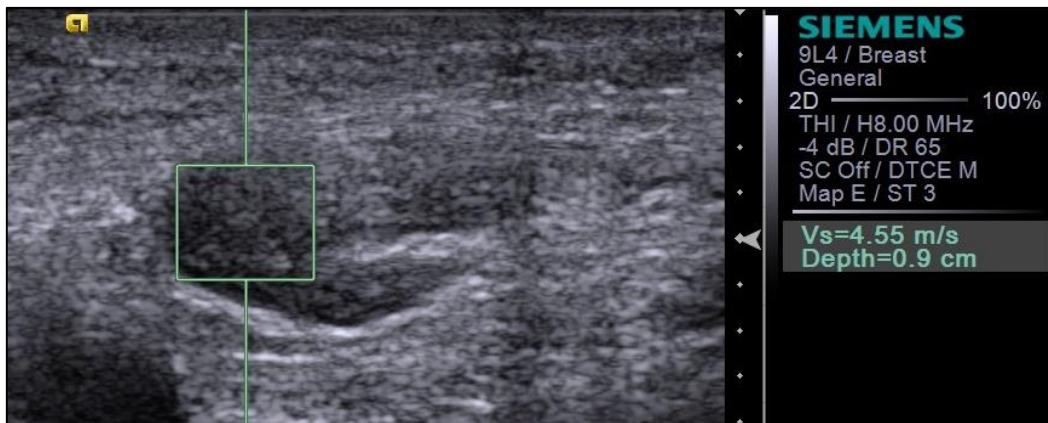


Fig. 21. Reniform, hypoechoic lymph node with preserved central hilum; SWV 4.5m/s; HPE was reported as Kikuchi disease.

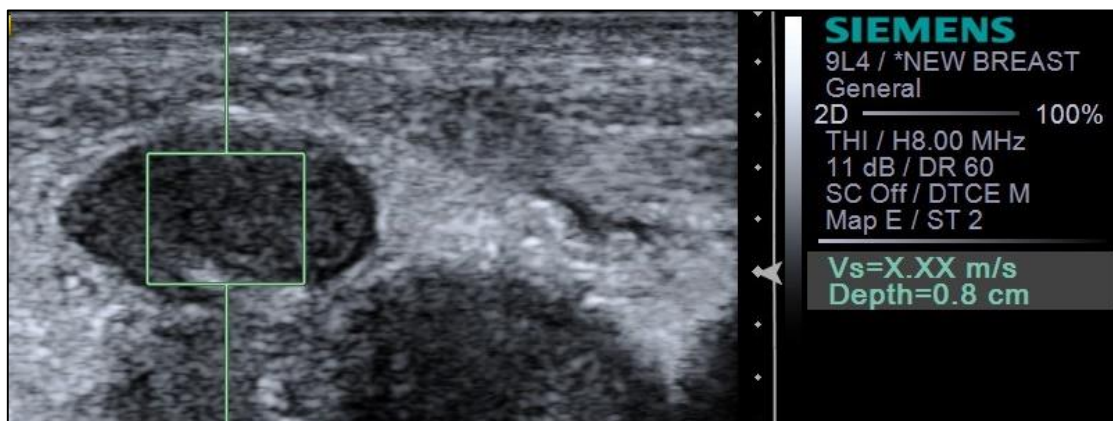


Fig. 22. VTQ of an oval, hypoechoic lymph node with SWV X.XX m/s. HPE was reported as metastatic squamous cell carcinoma.

ADVANTAGES OF ARFI (59,63,64,74)

Compared to conventional elastography techniques, the advantages of ARFI are:

1. Highly operator independent
2. Interacts directly with tissue of interest and not the intervening structures
3. Images formed are more homogeneous
4. Better contrast resolution
5. Deeper tissue not accessible by conventional elastography can be assessed

DISADVANTAGES OF ARFI (61,64,74)

1. Image quality can be degraded by physiological or transducer motion
2. Attenuation of the push pulses at a depth of more than 10 cm renders these areas inappropriate for assessment.
3. Peak temperature rise associated with a single pulse varies from 0.02 to 0.2°C, limiting the duration of pulses and frame rates to within the standard diagnostic limits of mechanical and thermal index (80).
4. Current ARFI systems are not yet equipped to generate real-time elastograms. Although this method can quantitatively estimate and display the shear wave velocity, it cannot be used to calculate the elastic modulus (63).

Table 4. Summary of studies on the use of elastography in the assessment of lymph nodes (81)

Study	LN per patients		Sensitivity	Specificity	Accuracy
	(Malignant)	Cut-off	(%)	(%)	(%)
Strain elastography					
Lyshchik et al. (57)*	141/43 (43%)	ES (2/3)	NA	NA	NA
		SR (1.5)	85	98	92
Alam et al. (67)*	85/37 (62%)	ES (2/3)	83	100	89
Rubaltelli et al. (82)	53/53 (53%)	ES (2/3)	75	80	77
Zhang et al. (83)**	155/82 (56%)	ES (2/3)	74.40	97.10	84.50
		SR (2.4)	78.40	98.50	87.1
Bhatia et al. (84)**	74/74 (50%)	ES (2/3)	62.20	83.80	73
Tan et al. (70)**	128/107 (55%)	ES (2/3)	NA	NA	NA
		SR (1.5)	92.50	53.40	75
Ishibashi et al.** (85)	71/19 (44%)	ES (2/3)	83.9	82.5	83.1
Teng et al. (71)**	89/89 (58%)	ES (2/3)	88.40	35.10	66.30
		SR (1.8)	98.10	64.90	84.30
Lenghel et al. (86)**	69/42 (57%)	ES (3/4)	66.70	96.70	81.2
Lo et al. (87)**	131/131 (41%)	ES (2/3)	66.70	57.10	61.10
Acoustic radiation force impulse imaging					
Fujiwara et al. (76)**	42/19 (48%)	>1.9 m/s	95	81.80	88
Meng et al. (77)**	181/123 (52%)	>2.6 m/s	82.90	93.10	87.8

AUC, area under the curve; EM, elastic modulus; ES, elastographic scale; LN, lymph node; NA, not acquired; SR, strain ratio; SWS, shear wave speed; *, prospective study; **, retrospective study

OTHER IMAGING MODALITIES

Cross sectional imaging modalities have been routinely used for the evaluation of lymph nodes, though more commonly to detect and characterize lymph nodes in regions that are inaccessible to percutaneous US.

Investigations and review of literature by Kau et al revealed that the accuracy of MRI (85%) and CT scanning (84.9%) was much superior to palpation (69.7%) and US (72.7%). The accuracy of US guided FNAC was 89%, in the same range with positron emission tomography (PET) (90.5%) (88).

In a study by Yuasa et al., by using appropriate diagnostic criteria for the CT and US evaluation of cervical lymph nodes in oral squamous cell carcinoma, it was found that the positive predictive value (PPV) for US was 96.5% and the negative predictive value (NPV) was 88.1% However, 25.5% of all lymph nodes could not be classified as either benign or metastatic. PPV for CT was 90.8% and NPV was 70.4% and 65.7% of all lymph nodes could not be classified as either benign or metastatic (89).

Golder et al. noted that recognition of lymph node involvement is one of the most challenging topics of diagnostic radio-oncology. In addition to size, shape and contours, the intrinsic nodal architecture, its vessels and its metabolic activity also need to be assessed and used for diagnostic conclusions. Though the specificity of conventional US is moderate, it is highly sensitive in detecting enlarged lymph nodes. Alterations of intranodal angio-architecture due to tumor infiltration are not specific enough to allow reliable diagnosis by colour Doppler ultrasound. Power Doppler US improved distinction between reactive, inflamed and metastatic nodes. Though CT is most widely

used to evaluate deep seated intrathoracic and intra-abdominal nodes, diffuse lymphadenopathy secondary to metastases or systemic lymphoma cannot be discriminated from infectious or granulomatous diseases. As PET offers functional information on tissue activity, it provides superior information on staging. The sensitivity and specificity of PET is better than CT for revealing neoplastic involvement. Dual modality scanners (CT + PET) enable precise localization of diseased lymph nodes and provide unique information about the residual tumor activity. MRI is comparable to CT in identifying lymph nodes. However, it has not been useful in reliable follow up of disease activity. MR lymphography has opened a new chance to avoid overstaging due to peritumoural inflammation as well as understaging due to microscopic tumor invasion(90). The expansion of such and other advanced techniques will lessen the need for invasive lymph node diagnosis (90).

A meta-analysis from seventeen articles showed the highest areas under the curve (AUC) for US guided FNAC (AUC=0.98) and US (AUC=0.95). MRI-USPIO (ultra-small super paramagnetic iron oxide contrast agent) (AUC=0.89) and CT (AUC=0.88) also had similar results. MRI showed an AUC=0.79. US guided FNAC showed the highest diagnostic odds ratio (DOR=260) compared to MRI (DOR=7), CT (DOR=14), MRI-USPIO (DOR=21), and US (DOR=40). Thus it was concluded that US guided FNAC showed promise in being the most accurate imaging modality in detecting cervical lymph node metastases (91).

In another meta-analysis comparing imaging modalities for the detection of cervical lymph node metastasis in head and neck cancer patients with clinically N0 neck, there was no difference in sensitivity and specificity among the evaluated imaging modalities,

except CT was superior to US in specificity. On a per-neck basis, 66% (45~77%), 52% (95% confidence interval [CI], 39%~65%), 65% (34~87%), and 66% (47~80%), were the pooled estimates for sensitivity for US, CT, MRI, and PET respectively. In terms of specificity, the pooled estimates for US, CT, MRI, PET were 78% (71~83%), 93% (87%~97%), 81% (64~91%), and 87% (77~93%), respectively. Thus, the authors observed that these modern imaging modalities offered similar diagnostic accuracy to clinically define and diagnose N0 neck. They suggested that the use of PET for nodal surveillance should not be routine as it did not provide better sensitivity and specificity, though being the more expensive imaging option. They opined that CT or MRI is preferred for clinically N0 neck pre-operative evaluation because CT and MRI had similar diagnostic sensitivities to PET and US. Furthermore, CT and MRI can also evaluate the status of primary tumor at the same time. They also added that in comparison to other imaging modalities, US was inexpensive and a more convenient tool to monitor nodal status. It could also be used with real-time guided FNAC. However, it may not allow adequate assessment of the primary tumor lesion and some deep-seated lymph nodes (92).

METHODOLOGY

STUDY DESIGN: Test of diagnostic accuracy

STUDY TYPE: Prospective study approved by the Institutional Review Board.

SETTING: Christian Medical College, Vellore is a tertiary care centre in Tamil Nadu, India. The institution was established in 1900 and is now a 2800 bedded multispecialty hospital. The annual outpatient footfall is around 2 million and there are around 1,30,000 admissions each year. The Department of Radiology was established in the year 1936. What was initially a conventional radiography setup evolved into digitalization in the year 2000 with the introduction of the Picture Archiving and Communication Systems (PACS). The department is staffed by 90 radiologists and 120 radiographers. A number of diagnostic as well as interventional radiological procedures are performed on a routine basis

STUDY POPULATION RECRUITMENT

SAMPLE SIZE

nMaster Sample Size Calculator software, version 2.0, developed by the Dept. of Biostatistics, Christian Medical College, Vellore, was used to calculate the sample size. The required sample size to show that ARFI has sensitivity and specificity of about 93% and 91% with 95% confidence limits with 8% precision was found to be 49 malignant and 51 benign cases(78). However, due to a change in the flow of patients, a total of

86 cases could be performed within the defined period. Of this, 8 of patients did not undergo any interventional procedure after the initial imaging and hence, had to be excluded from the study due to lack of a confirmatory tissue diagnosis. Study will be ongoing till a total of 100 cases are completed.

INCLUSION CRITERIA:

1. Patients with peripheral lymphadenopathy
2. Patients with a valid histopathological or cytological report after ARFI

EXCLUSION CRITERIA

1. Lymph nodes < 7 mm
2. Necrotic or cystic node with no solid component
3. Nodes with large areas of calcification avoiding which the ARFI box cannot be placed
4. Patients without a tissue diagnosis or an inadequate sample

SAMPLING AND CONSENT

The study was conducted on 86 patients who were referred to the Department of General Surgery and Department of Radiodiagnosis, Christian Medical College, Vellore for FNAC/biopsy/excision of peripheral lymph nodes between September 2015 and August 2016. All patients who met the inclusion criteria were included in the study. An informed consent was obtained from the patient prior to the study as per the Institutional Review Board guidelines in accordance with the ethical guidelines of the Declaration

of Helsinki. The patient information sheet and consent forms are attached in Annexure 2 & 3. Personal data, imaging and histopathological findings were entered into a coded proforma (Annexure 1).

TIMING

The study period was from September 2015 to August 2016. The time period between the index study (ARFI) and the reference standard was a maximum of 2 weeks. All imaging examinations were performed prior to any intervention. The primary investigator was blinded from the results of the biopsy till the end of the study.

STANDARD OPERATING PROCEDURES

Ultrasound and ARFI imaging of peripheral lymph nodes was performed using a high multi-frequency linear probe (4-9 MHz) on Siemens ACUSON S2000™. All patients were examined in supine position. For cervical and supraclavicular lymph nodes, the neck was extended by placing a pillow under the upper back. Axillary lymph nodes were examined after extending the upper limb. Examination of inguinal lymph nodes did not warrant any special manoeuvre.

ULTRASOUND & COLOUR DOPPLER OF PERIPHERAL LYMPH NODES

The patients were initially examined using B-mode ultrasonography. In cases with only a single enlarged lymph node, images were acquired directly.

In cases where more than one lymph node in a nodal group were involved, assuming that all nodes were affected by similar pathology, the single most representative node

was isolated based on its size- the largest node that would fit the elastographic window and also allow the comparative evaluation of adjacent muscles.

After the selection of the most representative lymph node, it was examined for the following gray-scale parameters:

1. Site
2. Size - long axis diameter, short axis diameter, ratio of long axis to short axis
3. Shape - reniform/round/conglomerate/irregular/other
4. Margins – circumscribed/lobulated/irregular/indistinct/other
5. Echogenicity - hyperechoic/isoechoic/hypoechoic/complex
6. Hilum – present or absent
7. Calcification - presence (micro/macro, focal/diffuse) or absence
8. Necrosis – presence (focal/diffuse) or absence

Using colour Doppler, nodal vascularity was assessed – for its presence or absence and pattern (normal hilar or altered).

These parameters were interpreted individually to be compared with the final diagnosis.

ULTRASOUND ARFI OF PERIPHERAL LYMPH NODES

Using light pressure to ensure good skin contact and with suspended respiration, Virtual Touch Imaging (VTI) was performed. With the VTI mode turned on, once the lesion was entirely placed within the region of interest (ROI), a B-mode image was obtained on the left hand side of the screen and VTI image was obtained on the right hand side. The area of the lesion was measured and ratio calculated on both B-mode and VTI.

Using the same technique of light pressure and suspended respiration, VTQ was performed by placing the region of interest (ROI) (size 6 mm x 6 mm) entirely within the lesion at a maximum depth of 4 cm and Shear Wave Velocity within the lesion and in the perilesional tissue at the same depth (not less than 1cm from the lesion) was measured 5 times each and average of both will be calculated.

In certain cases, a VTQ 'X.XX m/s' was obtained on repeat imaging and even after manoeuvring the ROI to a different area on the same node. This implied that the VTQ values were outside the range of assessment by the machine (<0 m/s or > 8.5 m/s). Such lymph nodes were assigned based on their appearance on grey scale, as 'too soft' for cystic lesions and 'too hard' for entirely solid lesions.

FINAL DIAGNOSIS

The final diagnosis was established using fine needle aspiration cytology or histopathology findings. The FNAC/biopsy was performed from the most representative lymph node. The findings of ultrasound examination were then compared with the cytological/histopathological diagnosis.

PERSONNEL

1. Initial B mode Ultrasound and ARFI was performed by the principal investigator who was unaware of the clinical suspicion
2. Lymph node biopsy / FNAC was performed by a general surgeon or a radiologist
3. Histopathological / cytological examination was performed by the pathologist who was blinded to the US and ARFI findings

4. Execution and interpretation of both Index and Reference test were overseen by the guide and co-investigators involved in the study.

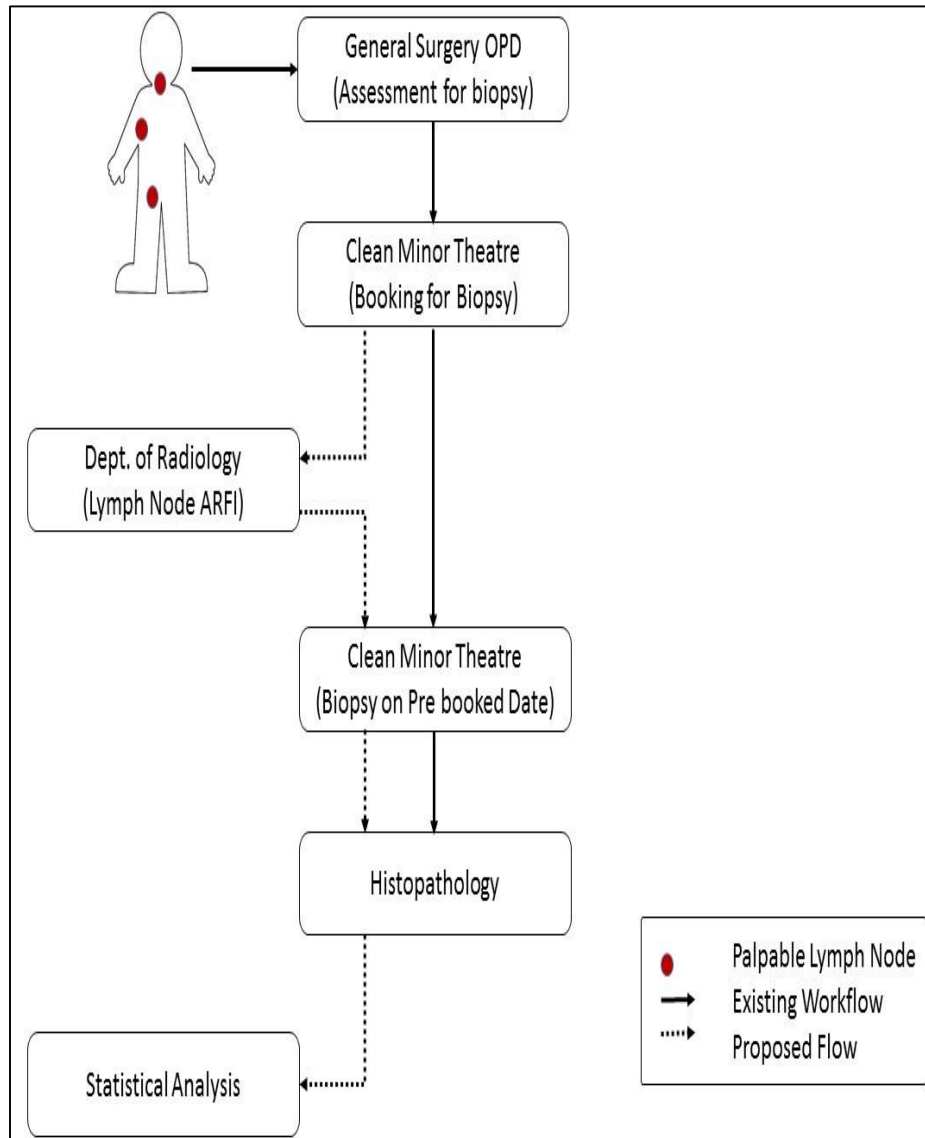


Fig. 23. Diagrammatic algorithm of workflow during the study.

STATISTICAL ANALYSIS

Data entry was done using Epidata version 3.0 software. Statistical analysis was performed using SPSS software, version 24. Receiver operating characteristic curves were employed to compare the diagnostic performances of ultrasound, colour Doppler, and both VTI and VTQ parameters of ARFI. A *p-value* of <0.01 was considered statistically significant. Positive predictive values, likelihood ratios and odds ratios for malignant and benign lymph nodes were determined.

PATIENT DEMOGRAPHICS

1. AGE DISTRIBUTION

The mean age of the patient population was 38 years (range 16 to 75 years).

2. SEX DISTRIBUTION

Of the 78 patients examined, there were 32 males and 46 females.

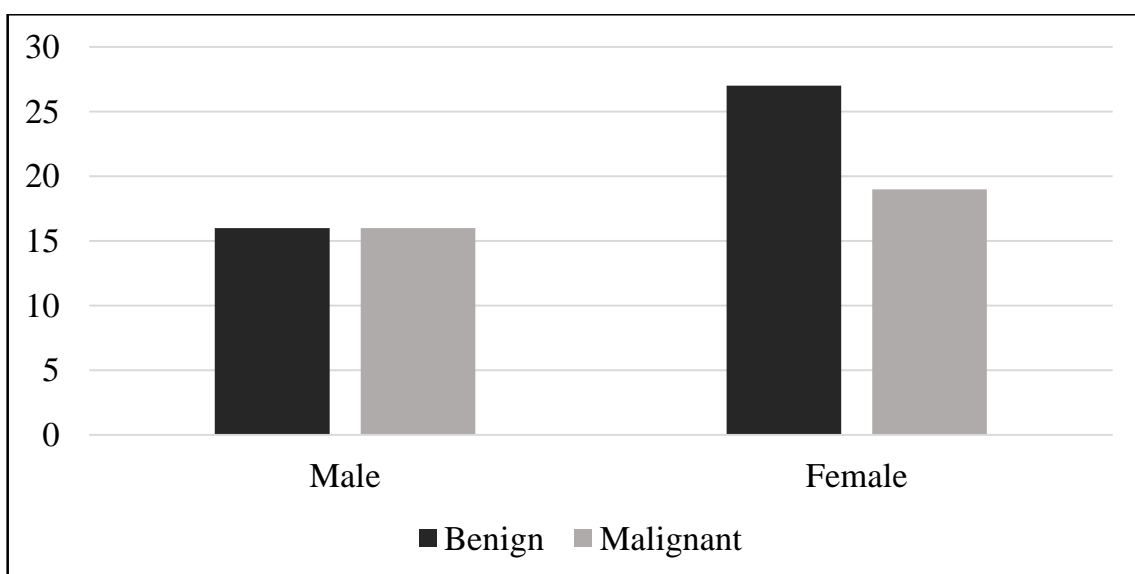


Fig. 24. Sex distribution of patients vs. histology.

There was no statistically significant correlation between gender of a patient and the presence of malignancy (Chi-square statistic 0.5769, *p-value* 0.45).

NODAL CHARACTERISTICS

1. LOCATION AND DISTRIBUTION

Of the 78 nodes imaged, 30 belonged to the cervical group, 19 to the supraclavicular, 22 to the axillary and 7 to the inguinal group.

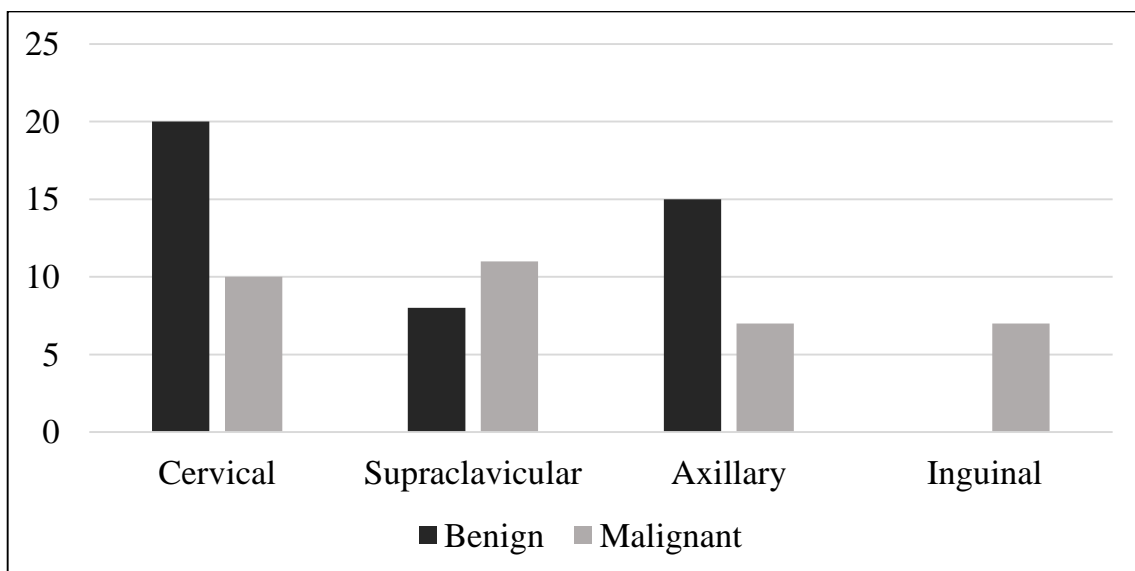


Fig. 25. Nodal location vs. histopathology.

A statistically significant correlation could not be found between the histopathology and involvement of cervical, supraclavicular and axillary nodes.

All the inguinal lymph nodes examined were found to be malignant. This could be explained by the fact that selection of inguinal node for biopsy would have been done only in those cases where the clinical suspicion was extremely high (nodal size > 1.5cm,

established primary malignancy in the lymph node territory) as inguinal nodes are otherwise known to have a low diagnostic yield (6).

2. HISTOPATHOLOGY

There were 43 benign and 35 malignant lymph nodes

Table 5. Histopathology of benign lymph nodes

Histopathology	Number of Nodes
Reactive change	13 (30.2%)
Tuberculosis	20 (46.5%)
Granulomatous inflammation	6 (14%)
Non-specific hyperplasia	3 (7%)
Kikuchi disease	1 (2.3%)
Total	43

Table 6. Histopathology of malignant lymph nodes

Histopathology	Number of Nodes
Lymphoma	19 (54.3%)
Metastasis	
Adenocarcinoma	4 (11.4%)
Squamous cell carcinoma	2 (5.7%)

Breast	6 (17.1%)
Papillary thyroid	2 (5.7%)
Ewing	1 (2.9%)
Urothelial	1 (2.9%)
<hr/>	
Total	35
<hr/>	

3. PALPATION

The sensitivity of clinical palpation in determining the presence of malignancy in a lymph node was 37.5% (low Chi-square statistic, *p-value* > 0.01)

ULTRASOUND CHARACTERISTICS

A statistically significant correlation could not be established between the examined US characteristics and the presence of malignancy (low Chi-square test statistic, *p-value* > 0.01).

Table 7. Ultrasound Characteristics of Examined Lymph Nodes

	Benign	Malignant / Metastatic
	(n = 43)	(n = 35)
<hr/>		
Short axis diameter		
≤ 1 cm	21 (48.8%)	14 (40%)
> 1 cm	22 (51.2%)	21 (60%)

Long axis to short axis ratio

< 2	24 (55.8%)	25 (71.5%)
> 2	19 (44.2%)	10 (28.5%)

Hilum

Present	23 (53.5%)	17 (48.6%)
Absent	20 (46.5%)	18 (51.4%)

Necrosis

Absent	37 (86.1%)	34 (97.1%)
Present	6 (13.9%)	1 (2.9%)

Calcification

Absent	37 (86.1%)	34 (97.1%)
Present	6 (13.9%)	1 (2.9%)

Table 8. Ultrasound Characteristics of Examined Lymph Nodes (Recoded Data)

	Benign	Malignant / Metastatic
	(n = 43)	(n = 35)
Shape		
Reniform	30 (69.8%)	20 (57.1%)
Round	9 (20.8%)	11 (31.5%)
Conglomerate	2 (4.7%)	0
Irregular	2 (4.7%)	4 (11.4%)

Shape recoded

Normal	30 (69.8%)	20 (57.1%)
Abnormal	13 (30.2%)	15 (42.9%)

Margin

Circumscribed	37 (86.1%)	30 (85.7%)
Lobulated	0	0
Irregular	1 (2.3%)	4 (11.4%)
Indistinct	5 (11.6%)	1 (2.9%)

Margin recoded

Normal	37 (86.1%)	30 (85.7%)
Abnormal	6 (13.9%)	5 (14.3%)

Echopattern

Hyperechoic	2 (4.7%)	2 (5.7%)
Isoechoic	1 (2.3%)	0
Hypoechoic	24 (55.7%)	25 (71.5%)
Normal	13 (30.2%)	8 (22.8%)
Complex	3 (6.9%)	0

Echopattern recoded

Normal	14 (32.6%)	8 (22.8%)
Abnormal	29 (67.4%)	27 (77.2%)

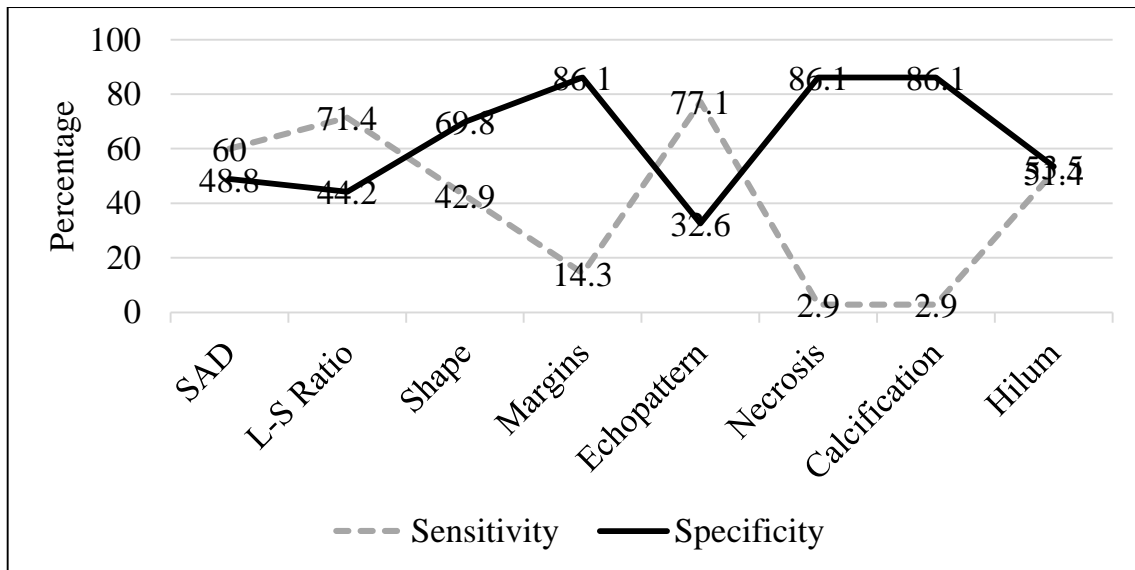


Fig. 26. Statistical parameters of ultrasound characteristics.

The diagnostic accuracy of L-S ratio, considered the best US parameter in literature, was 56.4%, with a sensitivity of 71.4%, specificity of 44.2%, PPV of 51% and NPV of 66%. Using short axis diameter of ≥ 1 cm predicted malignancy with a sensitivity of 60%, soecificity of 49% and an accuracy of 54%. Though an altered nodal echotexture had a sensitivity of 77%, a large number of benign nodes also appeared hypoechoic. Presence of intra nodal necrosis or calcification was highly indicative of a pathological process, however, these were not specific to any benign or malignant entity.

COLOUR DOPPLER CHARACTERISTICS

There was a strong correlation between the presence of altered nodal vascularity (absent, decreased or increased) and malignancy (Chi- square test statistic 8.10, *p-value* 0.004).

CD had a sensitivity of 85.7%, specificity of 44.2%, PPV of 56% and NPV of 79%, with an overall accuracy of 62.8% in detecting malignancy.

Table 9. Colour Doppler Characteristics of Examined Lymph Nodes

	Benign	Malignant / Metastatic
	(n = 43)	(n = 35)
Hilar vascularity		
Normal	19 (44.2%)	5 (14.3%)
Absent	12 (27.9%)	8 (22.8%)
Altered	12 (27.9%)	22 (62.9%)
Hilar vascularity recoded		
Normal	19 (44.2%)	5 (14.3%)
Abnormal	24 (55.8%)	30 (85.7%)

A combination of US & CD increased the specificity to 69% & the overall diagnostic accuracy to 65.4%.

ARFI PARAMETERS

1. VTI

NODAL AREA ON VTI

The mean area of lymph nodes on US (GAR) was 1.7 cm² (standard deviation \pm 1.07) for benign and 2.3cm² (standard deviation \pm 1.71) for malignant entities.

The mean area on VTI (VAR) was 1.5 cm² (standard deviation \pm 1.08) for benign and 2.6 cm² (standard deviation \pm 1.74) for malignant lymph nodes. Area \geq 1.4 cm² on VTI

predicted malignancy with a sensitivity of 74%, specificity of 63% and accuracy of 68%.

AREA RATIO

The mean area ratio (AR) of benign nodes was 0.88 (standard deviation ± 0.2) and of malignant nodes was 1.17 (standard deviation ± 0.14).

A cut-off area ratio (AR) of ≥ 1 between the lymph node area on VTI (VAR) and area on US (GAR) improved the diagnostic accuracy to 86%, with a sensitivity of 97% and specificity of 77%, PPV of 77% and NPV of 97% with a positive likelihood ratio of 4.2 (Chi-square statistic 32.03, *p-value* <0.01).

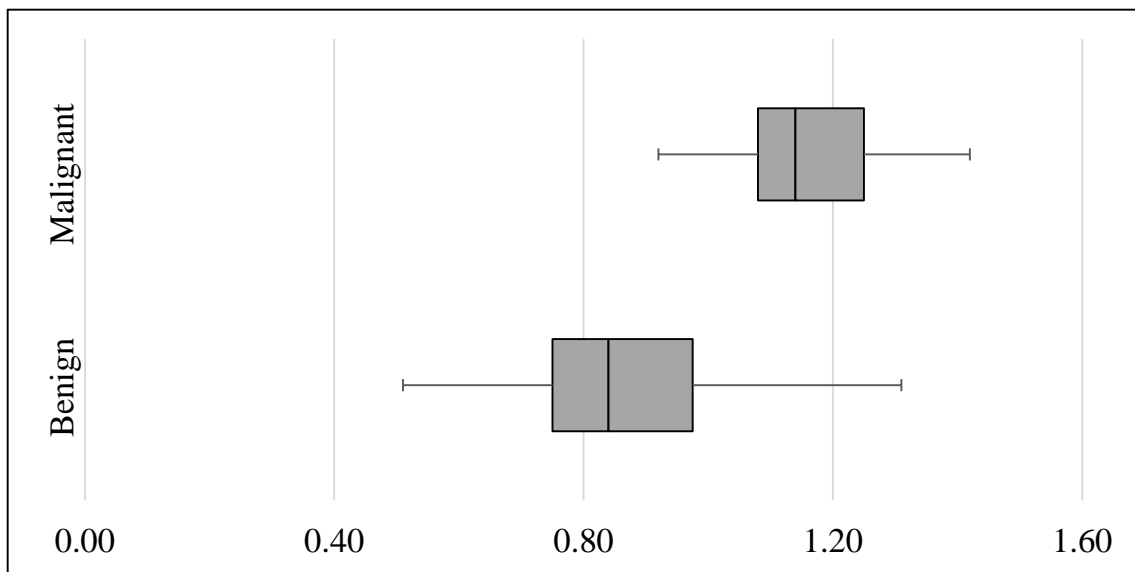


Fig. 27. Box and whisker plot of area ratio of lymph nodes on virtual touch imaging.

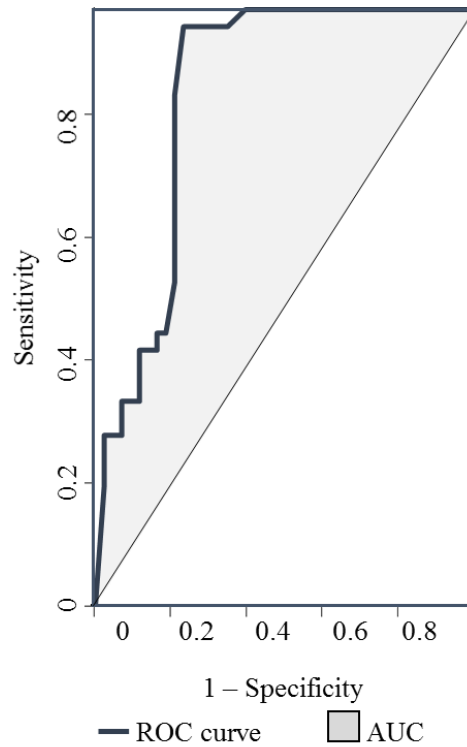


Fig. 28. Receiver operating characteristic curve of area ratio on virtual touch imaging.

The ROC curve of AR demonstrated an area under the curve of 0.86 (95% CI 0.63 - 0.82).

BRIGHTNESS PATTERN

Assuming that benign lymph nodes are brighter or occasionally slightly darker than surrounding tissue, malignant nodes being much darker (78), brightness pattern on VTI detected malignancy with a sensitivity of 74% and specificity of 77% (Chi-square statistic 20.22, *p-value* <0.01). The PPV was 72%, NPV was 79% with a positive likelihood ratio of 3.2 and diagnostic accuracy of 76%.

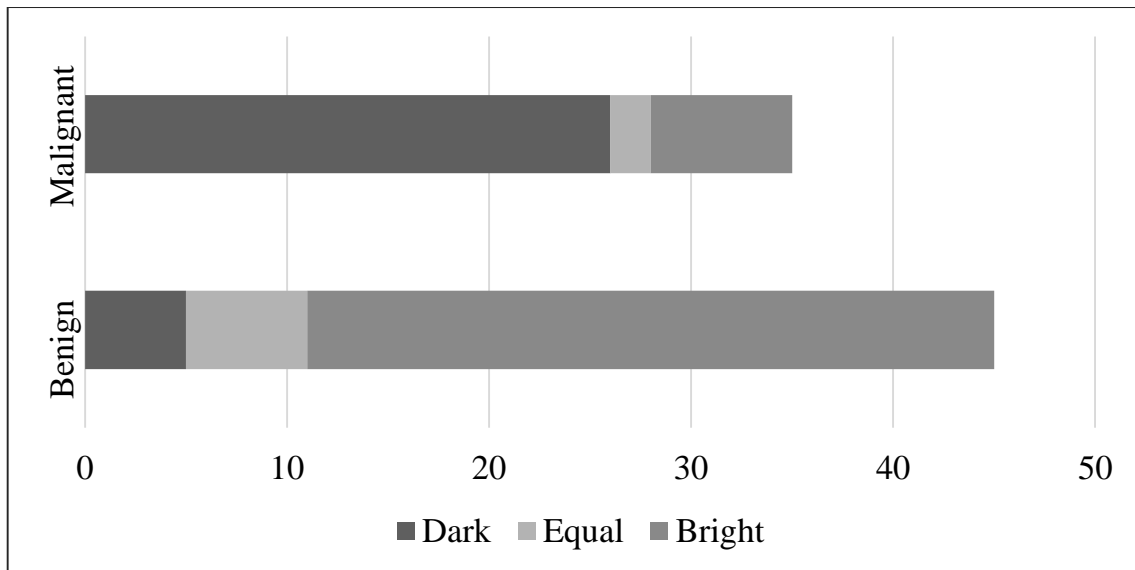


Fig. 29. Brightness pattern of lymph nodes on virtual touch imaging.

COMBINATION OF VTI PARAMETERS

Combined use of AR and brightness pattern markedly improved the sensitivity to 99% and specificity to 95%.

Table 10. VTI Characteristics of Examined Lymph Nodes

	Benign (n = 43)	Malignant / Metastatic (n = 35)
VTI Area		
< 1.4	25 (58.1%)	8 (22.9%)
≥ 1.4	18 (41.9%)	27 (77.1%)
VTI Area Ratio		
< 1	28	1 (2.9%)
≥ 1	15 (34.9%)	34 (97.1%)

VTI Brightness Pattern (Compared to surrounding)

Obviously less	4 (9.3%)	12 (34.2%)
Less	6 (13.9%)	14 (40%)
Equal	11 (25.6%)	1 (2.9%)
More	15 (34.9%)	1 (2.9%)
Obviously more	7 (16.3%)	7 (20%)

VTI Brightness Pattern (recoded)

< Surrounding	10 (23.3%)	26 (74.3%)
≥ Surrounding	33 (76.7%)	9 (25.7%)

2. VTQ

SHEAR WAVE VELOCITY OF LESION

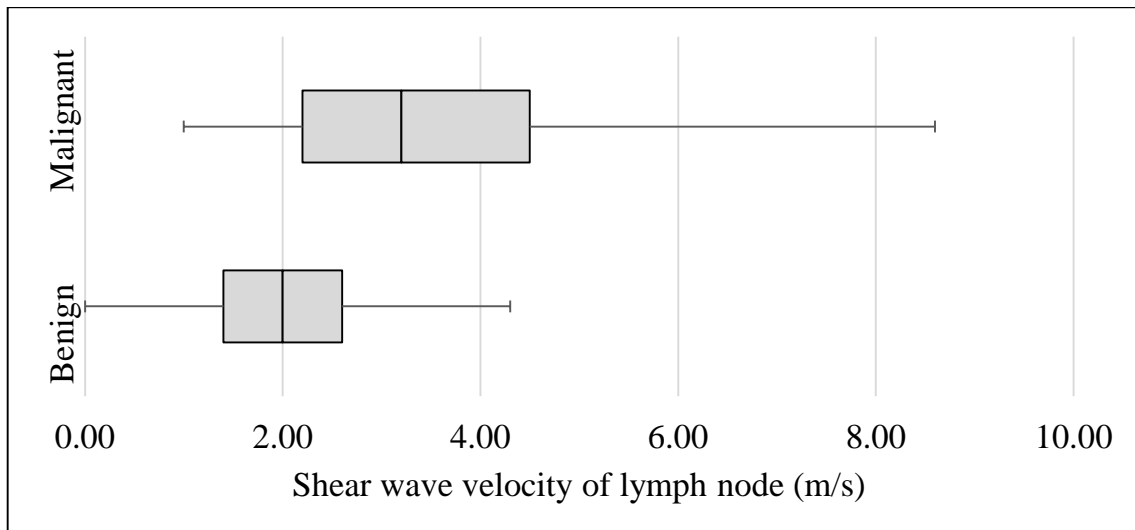


Fig. 30. Box plot of shear wave velocity of lymph nodes on virtual touch quantification.

The mean shear wave velocity (SWV) of benign lesions was 2.02 m/s (standard deviation ± 0.94) and 3.7 m/s (standard deviation ± 2.27) for malignant lesions.

Using a nodal SWV cut-off value of ≥ 2.4 cm² predicted malignancy with a sensitivity of 71%, specificity of 70%, accuracy of 70%, PPV of 66%, NPV of 75% and a positive likelihood ratio of 2.4 (Chi-square statistic 11.37, *p-value* <0.01).

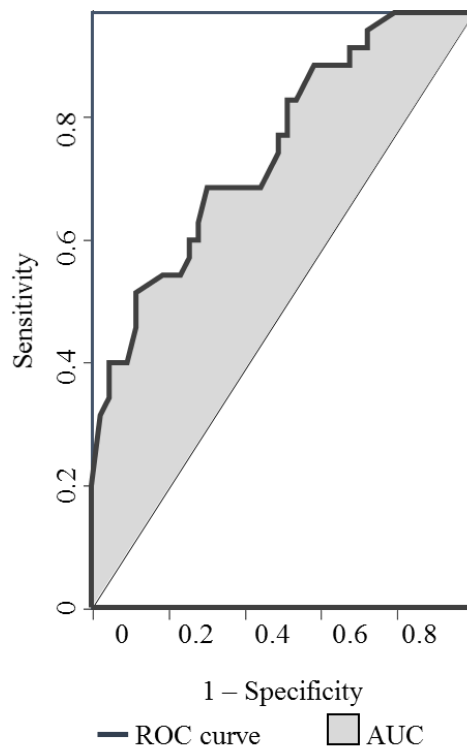


Fig. 31. ROC curve of mean shear wave velocity of lymph node.

The receiver operating characteristic curve demonstrated an area under the curve of 0.78 (95% CI: 0.69– 0.87).

6 lymph nodes displayed SWV of X.XX m/s. On grey scale, 5 of these appeared solid while one had necrotic areas within. All 5 nodes that were solid on grey scale appeared darker than surrounding on VTI and were therefore considered ‘too hard’. The lymph node with necrotic areas within was bright on VTI, hence it was assigned as ‘too soft’.

Excluding these nodes from the analysis reduced the sensitivity to 66%, specificity to 69%, AUC to 0.73 (95% CI: 0.64 – 0.83) and the mean SWV to 2.45 m/s (standard deviation \pm 1.08) (benign - 2.08 m/s \pm 0.92, malignant - 2.98 m/s \pm 1.09). Hence, these nodes were included for analysis (76).

SHEAR WAVE VELOCITY OF SURROUNDING TISSUE

Mean SWV of surrounding tissue was 1.98 m/s (standard deviation \pm 0.84).

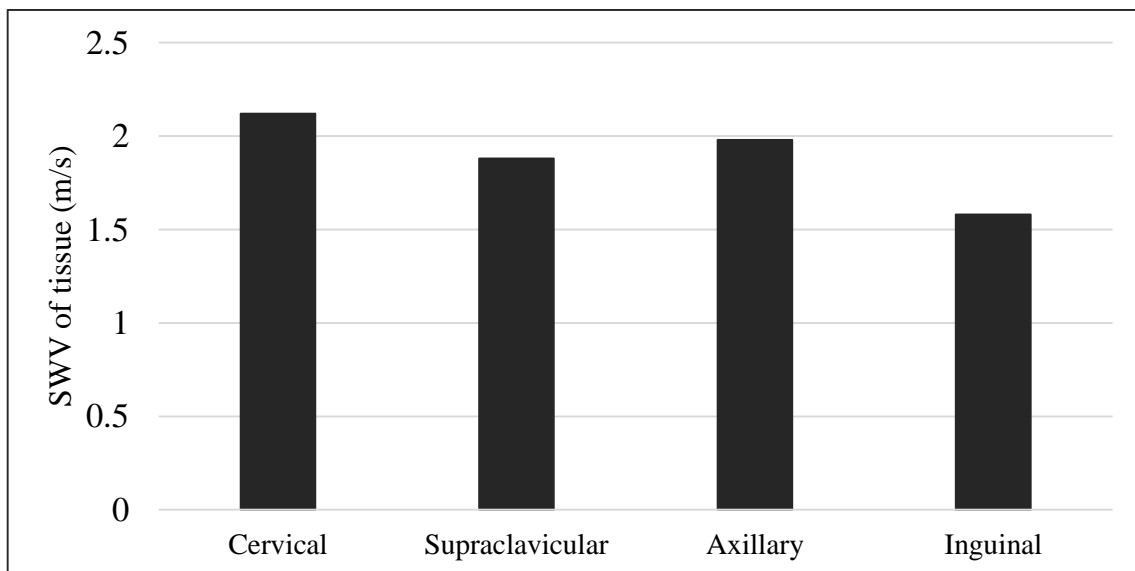


Fig. 32. Bar graph depicting the mean shear wave velocity of tissue surrounding lymph node at a particular site.

SHEAR WAVE VELOCITY RATIO

The mean shear wave velocity ratio (SWVR) of benign nodes was 1.1 m/s (standard deviation \pm 0.64) and of malignant nodes was 2.4 m/s (standard deviation \pm 1.71).

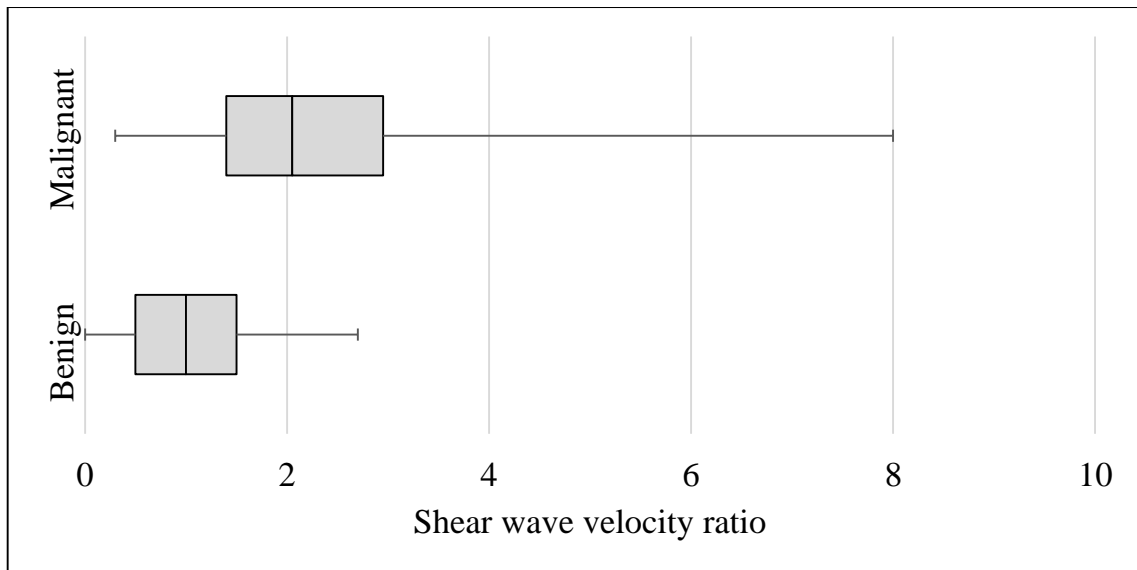


Fig. 33. Box and whisker plot of shear wave velocity ratio between lymph node and surrounding tissue.

A cut-off SWVR (AR) of ≥ 1.5 between the SWV of lymph node vs. the surrounding tissue had an improved diagnostic accuracy of 74%, with a specificity to 79% (Chi-square statistic 10.31, p -value <0.01). The sensitivity of SWVR was 68%.

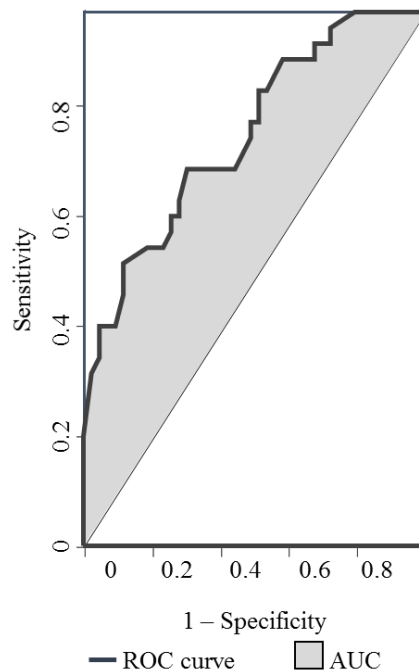


Fig. 34. ROC curve of mean SWV ratio of lymph node to surrounding tissue.

The area under the receiver operating characteristic curve of mean shear wave velocity ratio of lymph node to surrounding tissue was 0.82 (95% CI: 0.74 – 0.90).

Table 11. VTQ Characteristics of Examined Lymph Nodes

	Benign	Malignant / Metastatic
	(n = 43)	(n = 35)
VTQ SWV of Lesion		
< 2.4	30 (69.8%)	11 (31.5%)
≥ 2.4	13 (30.2%)	24 (68.5%)
VTQ SWV Ratio		
< 1.5	28 (65.1%)	10 (28.5%)
≥ 1.5	15 (34.9%)	25 (71.5%)

COMBINATION OF VTQ PARAMETERS

Parallel use of both SWVL and SWVR had a sensitivity to 91% and specificity to 94%, which was significantly more than the individual parameters.

OVERALL ARFI PARAMETERS

The sensitivity and specificity could further be increased to 99.9% and 99.7% respectively when VTI and VTQ were used together.

CASE BASED IMAGING FINDINGS & HPE CORRELATION

CASE 1. 40 year old lady, post treatment for carcinoma breast, now presented with palpable right cervical lymph node.

IMAGING FINDINGS:

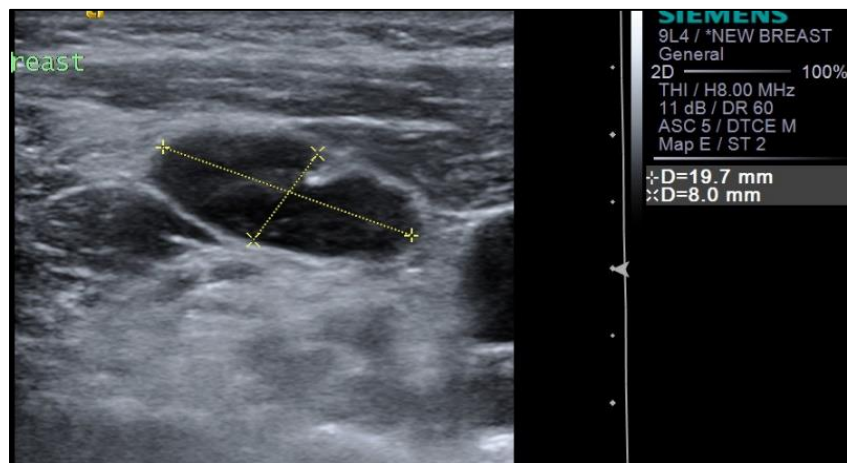


Fig. 35. US: hypoechoic reniform node with preserved central fatty hilum.

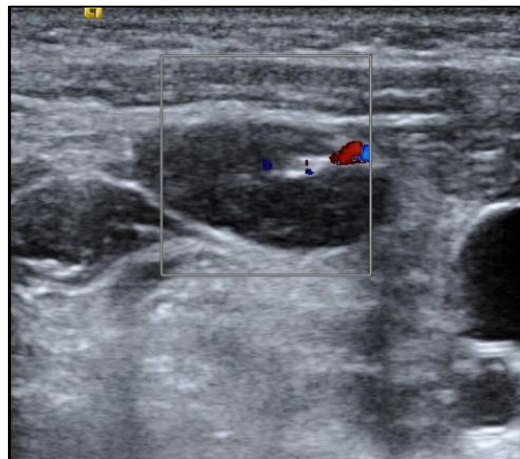


Fig. 36. CD: normal hilar vascularity.

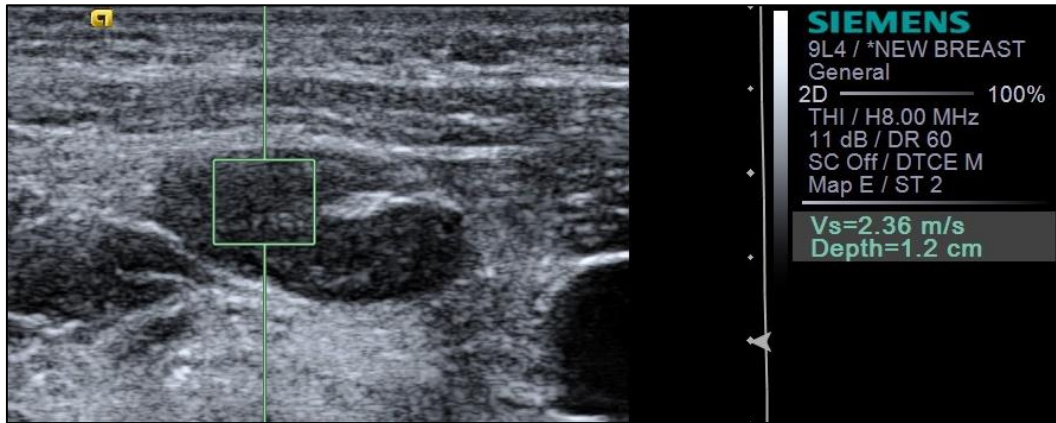


Fig. 37. VTQ of lymph node with SWV 2.4 m/s

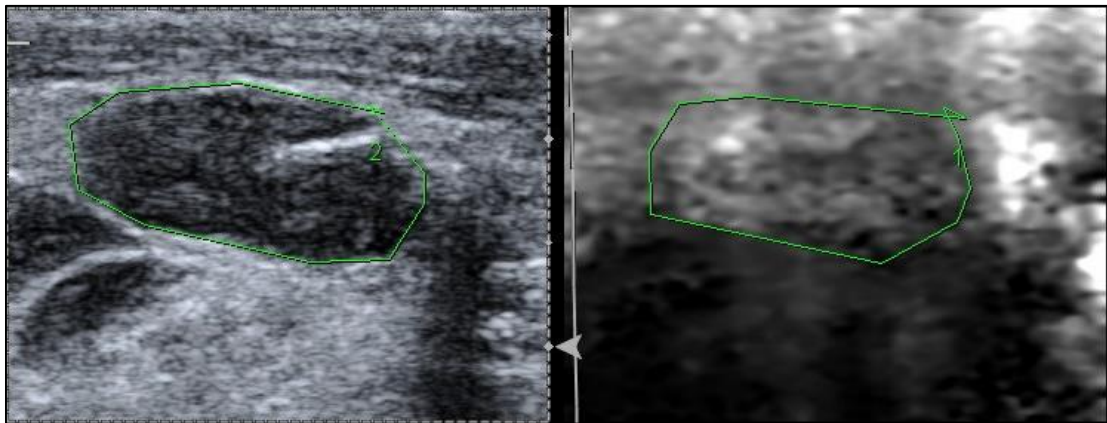


Fig. 38. VTI: Lymph node brightness is equal to surrounding tissue.

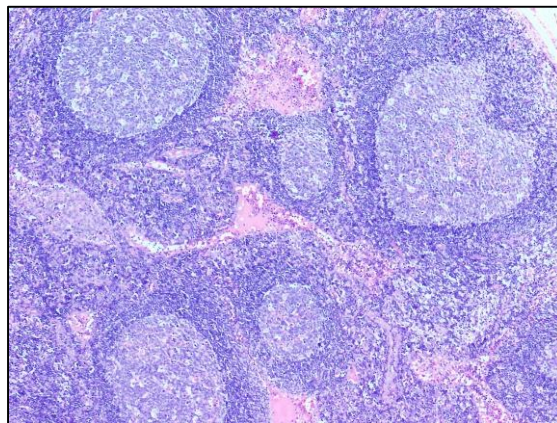


Fig. 39. H&E stain, 40x, reactive changes with sinus histiocytosis.

FINAL DIAGNOSIS ON HPE: Reactive hyperplasia of lymph node

CASE 2. 55 year old lady with non-tender cervical lymphadenopathy.

IMAGING FINDINGS:

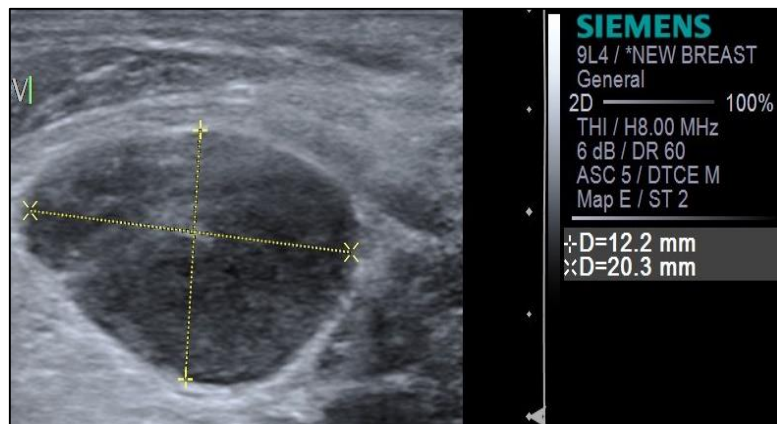


Fig. 40. US: hypoechoic oval lymph node.



Fig. 41. Increased hilar vascularity.

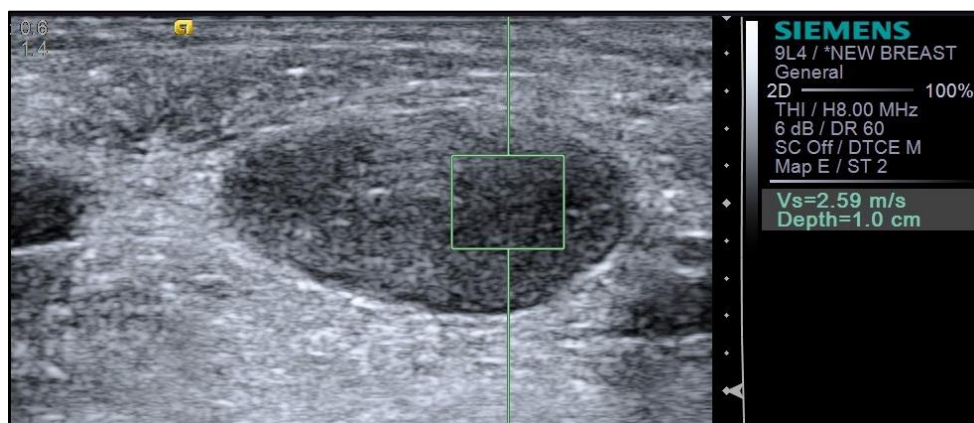


Fig. 42. VTQ: SWV of lymph node 2.6 m/s.

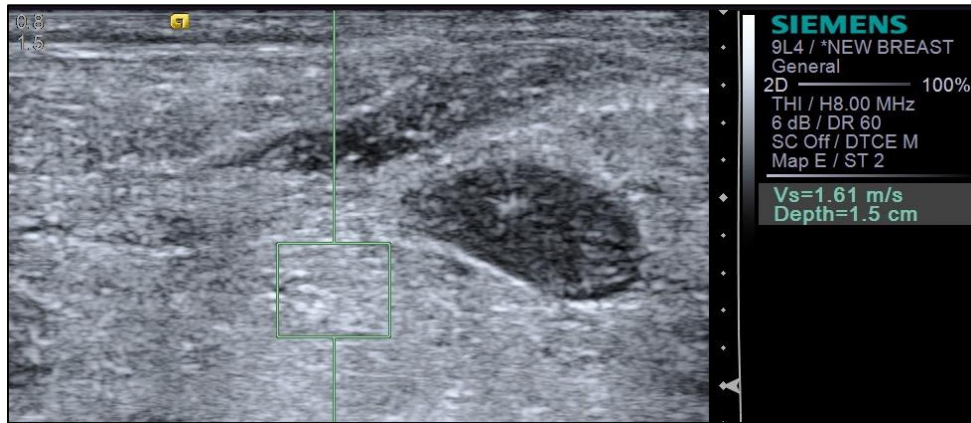


Fig. 43. VTQ: SWV of surrounding tissue 1.5 m/s.

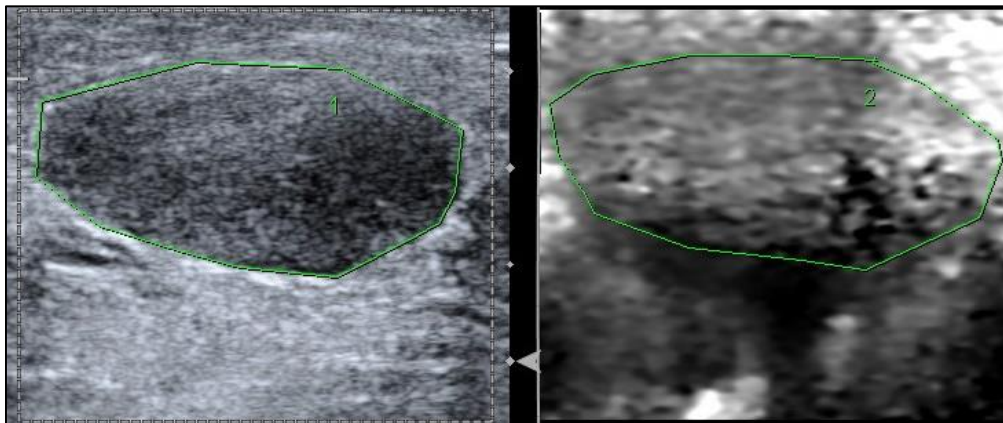


Fig. 44. VTI: Equal brightness with increased area ratio.

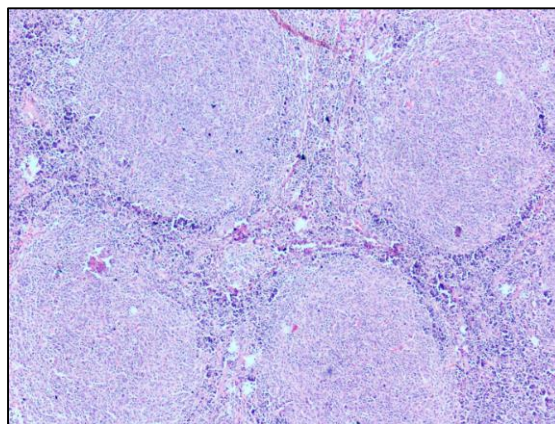


Fig. 45. H&E stain, 40x, lymph node with neoplastic follicles arranged back to back, composed predominantly of centrocytes and very occasional centroblasts (0-5/ hpf).

FINAL DIAGNOSIS ON HPE: Lymphoma

CASE 3. 55 year old lady with constitutional symptoms for few months.

IMAGING FINDINGS:

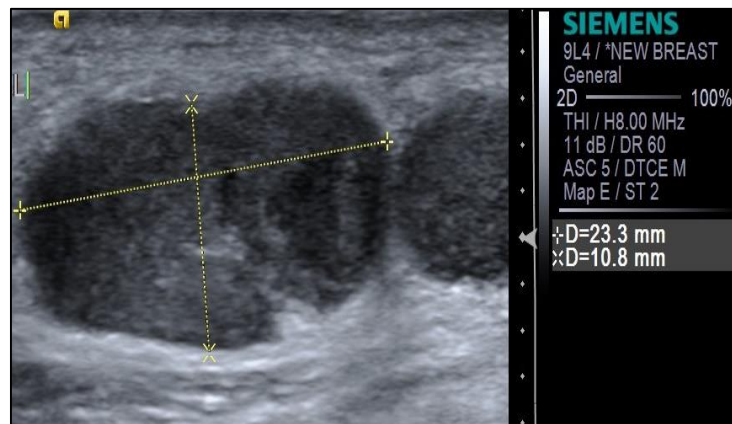


Fig. 46. US: Hypoechoic oval lymph node with slightly lobulated contour.

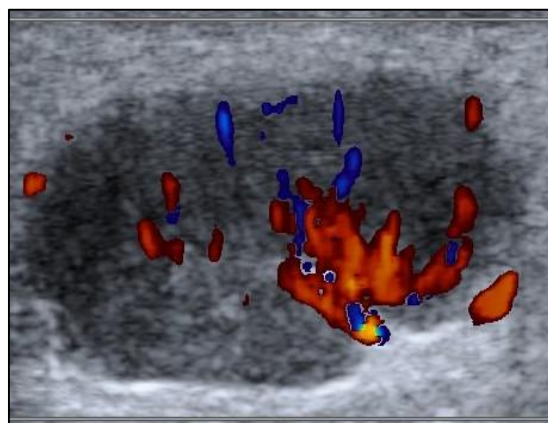


Fig. 47. CD: Significantly increased nodal and perinodal vascularity.

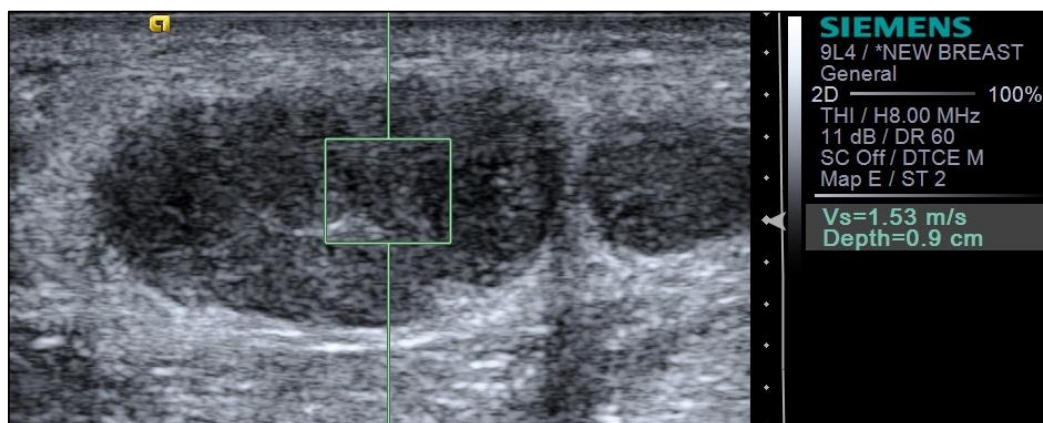


Fig. 48. VTQ: SWV of lymph node 1.5 m/s.

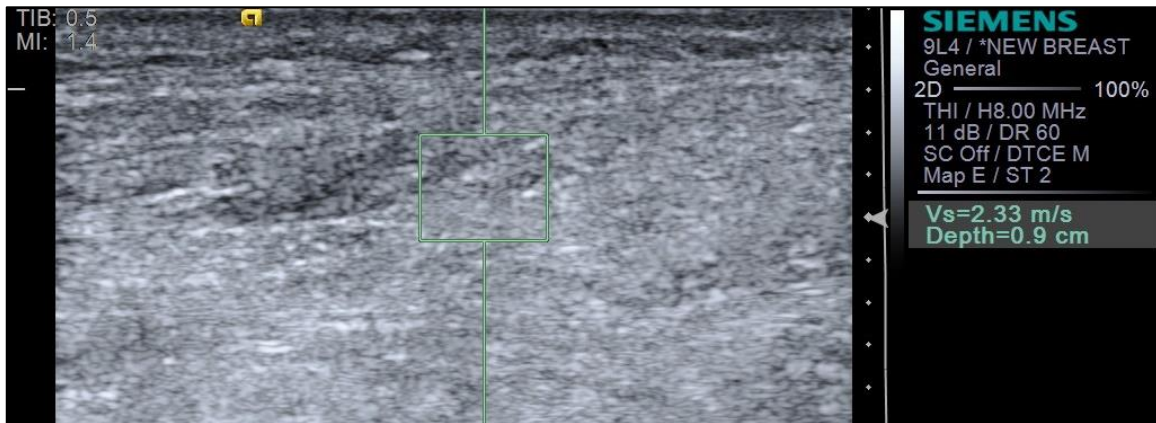


Fig. 49. VTQ: SWV of surrounding tissue is 2.3 m/s.

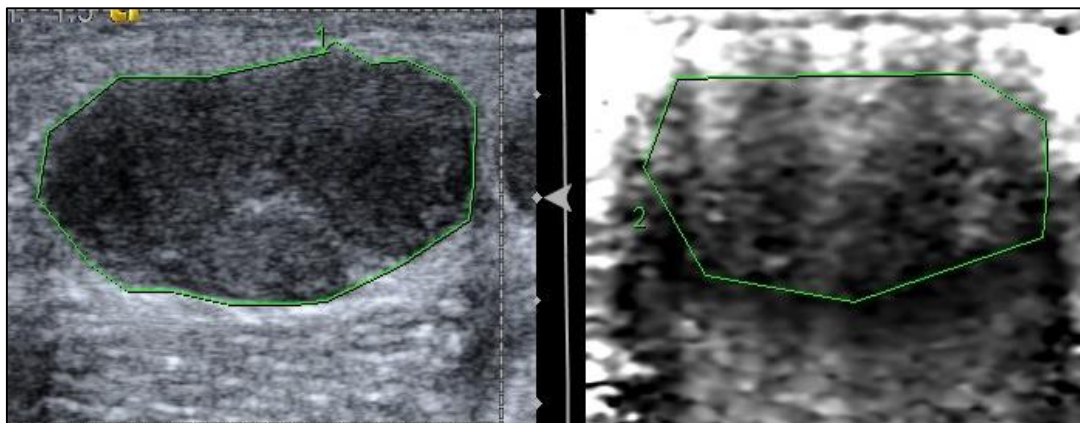


Fig. 50. VTI: brightness pattern similar to surrounding with decreased area ratio.

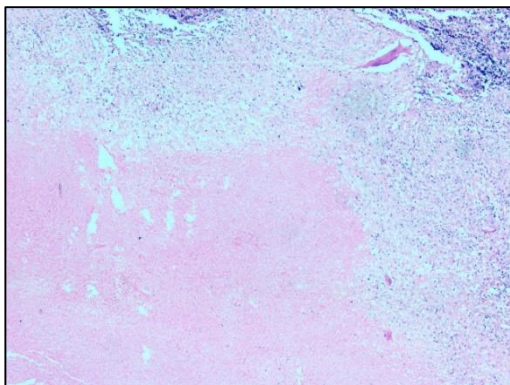


Fig. 51. Large areas of caseous necrosis.
H&E, 40x.

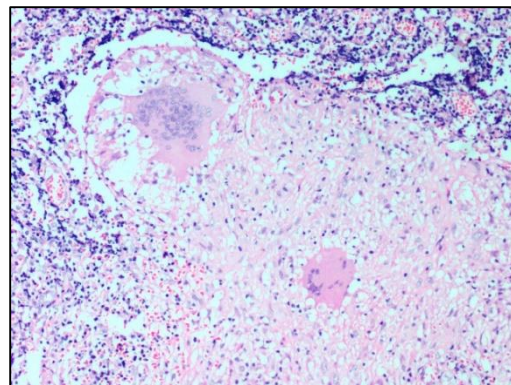


Fig. 52. Epithelioid granulomas with
Langhan's giant cells, H&E, 400x.

FINAL DIAGNOSIS ON HPE: Tuberculosis

CASE 4. 60 year old lady with palpable left axillary lymph node.

IMAGING FINDINGS:

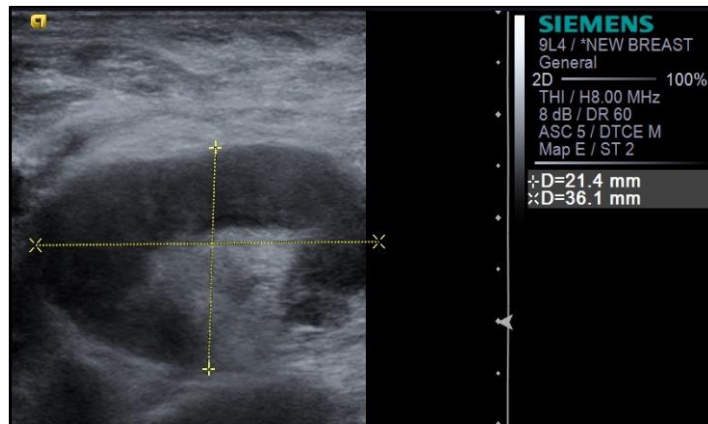


Fig. 53. US: Enlarged lymph node with preserved central fatty hilum.

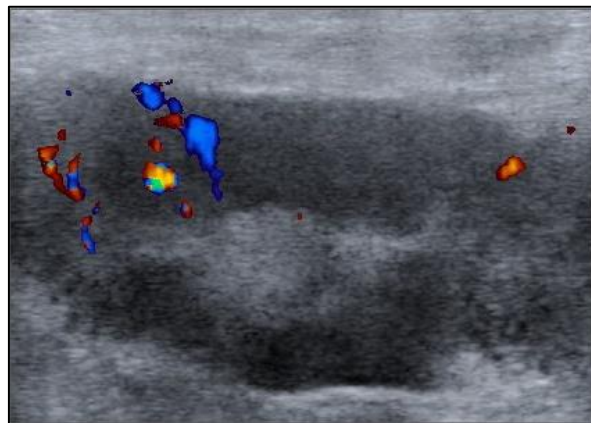


Fig. 54. CD: Altered nodal vascularity.

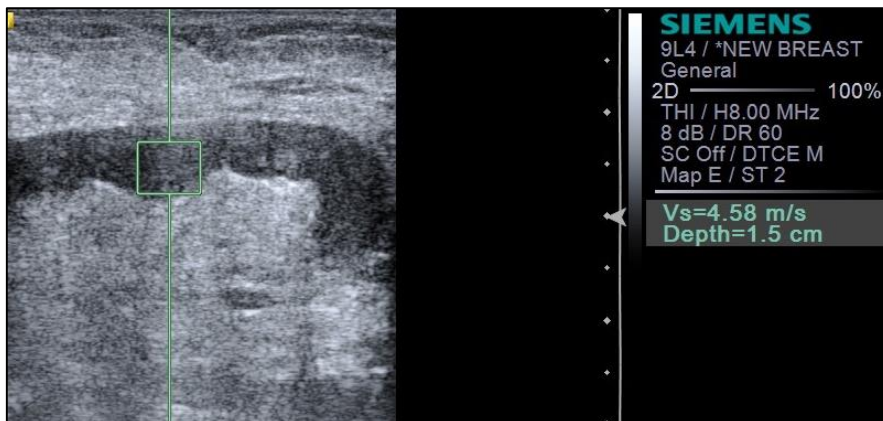


Fig. 55. VTQ: SWV of lymph node is 4.6 m/s.

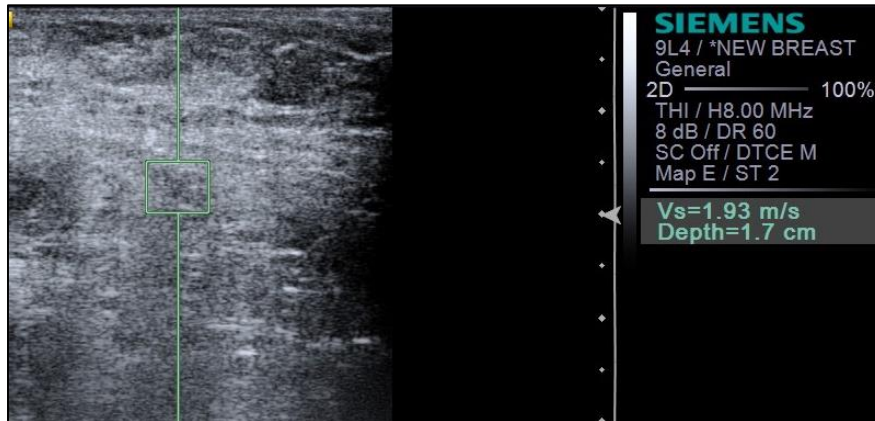


Fig.56. VTQ: SWV of tissue surrounding the node is 1.9 m/s.

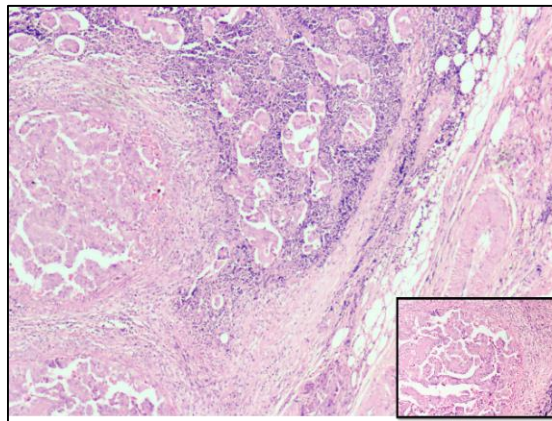


Fig. 57. H&E, 40x; Complex glandular structures and occasional papillary lined by atypical columnar to cuboidal cells; Inlet: papillary structure.

FINAL DIAGNOSIS: Metastatic adenocarcinoma

DISCUSSION

A total of 86 patients were enrolled in this study of which 78 were included in the final analysis. There were 32 men and 46 women. The average age of the patients was 36 years. Age, gender and site of the lymph node did not have any effect on the disease outcome.

Tuberculosis was present in a significant proportion of benign lymph nodes (20 of 43). Lymphoma was the most common etiology of nodal involvement by neoplastic process (19 of 35).

LS ratio had a sensitivity of 71% and a specificity of 44% while SAD had a sensitivity of 60% and specificity of 49%. Overall diagnostic accuracy of US parameters ranged from 49% to 58%. An altered hilar vascularity favoured malignancy with a sensitivity of 86%, specificity of 44% and accuracy of 63%. Concurrent use of US parameters and CD improved the sensitivity to 96% and specificity to 69%.

The mean lymph nodal area on VTI was $1.5 \text{ cm}^2 (\pm 1.08)$ for benign and $2.6 \text{ cm}^2 (\pm 1.74)$ for malignant nodes. VTI area $\geq 1.4 \text{ cm}^2$ had a sensitivity of 74%, specificity of 63% and accuracy of 68% in predicting malignancy. Cut-off area ratio of ≥ 1 had an improved sensitivity of 97%, specificity of 77%, accuracy of 86% and AUC 0.86. Benign nodes had a mean area ratio of $0.88 (\pm 0.2)$ while for malignant node the mean ratio was $1.17 (\pm 0.14)$. VTI brightness pattern detected malignancy with a sensitivity of 74%, specificity of 77% and diagnostic accuracy of 76%. Combining both VTI parameters increased the sensitivity to 99% and specificity to 95%.

On VTQ, the mean shear wave velocity of benign lesions was 2.02 m/s (\pm 0.94) and of malignant lesions was 3.7 m/s (\pm 2.27). Cut-off value of \geq 2.4 cm² predicted malignancy with a sensitivity of 71%, specificity of 70%, accuracy of 70% and AUC 0.78. Using \geq 1.5 cut-off SWVR had a sensitivity of 68%, specificity of 79%, accuracy of 74% and AUC 0.82. Concomitant use of both SWVL and SWVR increased the sensitivity to 91% and specificity to 94%.

Combining VTI and VTQ increased the sensitivity to 99.9% and specificity to 99.7%. It was also found that three parameters, LS ratio on US, hilar vascularity and brightness pattern, when used together, had a sensitivity of 99% in differentiating benign from malignant lymph nodal pathology. This was also the least time consuming method which did not require repeat imaging values (as occurs in mean VTQ) or any form of mathematical calculation (as required for AR in VTI or SWVR in VTQ).

An in-depth analysis revealed that though ARFI parameters could reliably differentiate between benign and malignant lymph nodes, the same statement does not hold true in differentiating simple reactive nodal hyperplasia (*'leave-alone'* lesions) from other sinister benign or malignant pathologies.

The cause for the overlap in US and ARFI findings between benign and malignant nodes can be partly attributed to the high prevalence of tuberculosis in India, mirrored in the patient population visiting our set-up, as in this study it was found that tuberculous lymph nodes often displayed US and ARFI characteristics similar to neoplastic nodes, also increasing the mean nodal stiffness.

LIMITATIONS

1. The fact that the study was conducted in a tertiary care centre attributed to a selection bias wherein more number of clinically aggressive lesions were referred for ARFI and biopsy.
2. The calculated sample size was 100. However, due to the rate of flow of patients and other unforeseen circumstances in patient enrolment (eg., mismatch between the list of cases booked for biopsy in Clean Minor Theatre vs. the actual biopsies performed in a particular day, incorrect / inadequate patient contact details on the Hospital Information System), only 86 cases could be done. Recruitment of cases will continue till the required sample size is met.

TECHNICAL FACTORS:

1. In few cases, especially in the posterior triangle of the neck, lymph nodes were too superficial and beyond the adjustable focus of the transducer.
2. It was technically challenging to fit the entire footprint of the probe in large and very superficial lymphadenopathy.
3. The shape of the ROI box while performing VTQ cannot be altered.
4. VTQ values of X.XX m/s were assigned stiffness values based on their appearance on grey scale and VTI as the real stiffness could not be determined.
5. Transmitted pulses from neighbouring large arteries (carotid in the neck, axillary in the armpit and femoral in the groin) could have led to erroneous values.
6. A reasonable amount of breath-holding was required while evaluating neck and axillary nodes.

CONCLUSION

1. ARFI is a relatively new promising US-based technique which is operator independent, allowing evaluation of tissue hardness without external compression.
2. ARFI parameters have a higher diagnostic accuracy when compared to clinical palpation, US or CD in the differentiation of benign from malignant lymph nodes.
3. The performance of VTI was superior to VTQ.
4. Area ratio on VTI emerged as the best ARFI imaging parameter.
5. In VTQ, the diagnostic performance of SWVR bettered that of SWVL.
6. Calculating the area ratio on VTI had the best diagnostic accuracy.
7. A combination of LS ratio, vascularity on CD and brightness pattern on VTI could be recommended as a standard protocol in differentiating benign from malignant lymph nodes.

Overall, establishing the correct diagnosis of the cause of lymphadenopathy is of paramount importance as it forms the basis of effective treatment.

Imaging techniques like ARFI, by being a feasible complement to US, can potentially improve the characterization of lymph nodes and play a crucial role in non-invasive evaluation of lymphadenopathy.

BIBLIOGRAPHY

1. Hall JE. Guyton and Hall Textbook of Medical Physiology Elsevieron VitalSource. Elsevier Health Sciences; 2015. 1171 p.
2. Kumar V, Abbas AK, Fausto N, Aster JC. Robbins & Cotran Pathologic Basis of Disease. Elsevier Health Sciences; 2009. 7658 p.
3. Standring S. Gray's Anatomy: The Anatomical Basis of Clinical Practice. Churchill Livingstone/Elsevier; 2008. 1551 p.
4. Robert H Fletcher. Evaluation of peripheral lymphadenopathy in adults. In: Laurence A Boxer, editor. UpToDate. Waltham, MA;
5. Habermann TM, Steensma DP. Lymphadenopathy. Mayo Clin Proc. 2000 Jul;75(7):723–32.
6. Ferrer R. Lymphadenopathy: differential diagnosis and evaluation. Am Fam Physician. 1998 Oct 15;58(6):1313–20.
7. Kasper D, Fauci A, Hauser S, Longo D, Jameson J, Loscalzo J. Harrison's Principles of Internal Medicine 19/E (Vol.1 & Vol.2). McGraw Hill Professional; 2015. 3983 p.
8. Pandit S, Choudhury S, Das A, Das SK, Bhattacharya S. Cervical Lymphadenopathy—Pitfalls of Blind Antitubercular Treatment. J Health Popul Nutr. 2014 Mar;32(1):155–9.
9. Chong V. Cervical lymphadenopathy: what radiologists need to know. Cancer Imaging. 2004 Jun 25;4(2):116–20.
10. Chau I, Kelleher MT, Cunningham D, Norman AR, Wotherspoon A, Trott P, et al. Rapid access multidisciplinary lymph node diagnostic clinic: analysis of 550 patients. Br J Cancer. 2003 Feb 10;88(3):354–61.
11. Fijten GH, Blijham GH. Unexplained lymphadenopathy in family practice. An evaluation of the probability of malignant causes and the effectiveness of physicians' workup. J Fam Pract. 1988 Oct;27(4):373–6.
12. Jatoi I, Hilsenbeck SG, Clark GM, Osborne CK. Significance of axillary lymph node metastasis in primary breast cancer. J Clin Oncol Off J Am Soc Clin Oncol. 1999 Aug;17(8):2334–40.
13. Mohan A, Reddy MK, Phaneendra BV, Chandra A. Aetiology of peripheral lymphadenopathy in adults: analysis of 1724 cases seen at a tertiary care teaching hospital in southern India. Natl Med J India. 2007 Apr;20(2):78–80.

14. Bernard M Karnath. Approach to the Patient with Lymphadenopathy. *Hosp Physician*. 2005 Jul;
15. Magnetic Resonance Imaging vs Palpation of Cervical Lymph Node Metastasis | Jun 01, 1991 | *JAMA Otolaryngology–Head & Neck Surgery* | JAMA Network [Internet]. [cited 2016 Jul 10]. Available from: <http://archotol.jamanetwork.com/article.aspx?articleid=619762>
16. Weiss LM, O'Malley D. Benign lymphadenopathies. *Mod Pathol Off J U S Can Acad Pathol Inc*. 2013 Jan;26 Suppl 1:S88-96.
17. Steel BL, Schwartz MR, Ramzy I. Fine needle aspiration biopsy in the diagnosis of lymphadenopathy in 1,103 patients. Role, limitations and analysis of diagnostic pitfalls. *Acta Cytol*. 1995 Feb;39(1):76–81.
18. Hehn ST, Grogan TM, Miller TP. Utility of fine-needle aspiration as a diagnostic technique in lymphoma. *J Clin Oncol Off J Am Soc Clin Oncol*. 2004 Aug 1;22(15):3046–52.
19. Bottles K, McPhaul LW, Volberding P. Fine-needle aspiration biopsy of patients with acquired immunodeficiency syndrome (AIDS): experience in an outpatient clinic. *Ann Intern Med*. 1988 Jan;108(1):42–5.
20. Reid AJ, Miller RF, Kocjan GI. Diagnostic utility of fine needle aspiration (FNA) cytology in HIV-infected patients with lymphadenopathy. *Cytopathol Off J Br Soc Clin Cytol*. 1998 Aug;9(4):230–9.
21. Ellison E, Lapuerta P, Martin SE. Fine needle aspiration (FNA) in HIV+ patients: results from a series of 655 aspirates. *Cytopathol Off J Br Soc Clin Cytol*. 1998 Aug;9(4):222–9.
22. Fanny M-L, Beyam N, Gody JC, Zandanga G, Yango F, Manirakiza A, et al. Fine-needle aspiration for diagnosis of tuberculous lymphadenitis in children in Bangui, Central African Republic. *BMC Pediatr*. 2012;12:191.
23. Zardawi IM. Fine needle aspiration cytology in a rural setting. *Acta Cytol*. 1998 Aug;42(4):899–906.
24. Yokozawa T, Fukata S, Kuma K, Matsuzuka F, Kobayashi A, Hirai K, et al. Thyroid cancer detected by ultrasound-guided fine-needle aspiration biopsy. *World J Surg*. 1996 Sep;20(7):848–853; discussion 853.
25. Kim MJ, Kim E-K, Park SI, Kim BM, Kwak JY, Kim SJ, et al. US-guided Fine-Needle Aspiration of Thyroid Nodules: Indications, Techniques, Results. *RadioGraphics*. 2008 Nov 1;28(7):1869–86.
26. Burke C, Thomas R, Inglis C, Baldwin A, Ramesar K, Grace R, et al. Ultrasound-guided core biopsy in the diagnosis of lymphoma of the head and neck. A 9 year experience. *Br J Radiol*. 2011 Aug;84(1004):727–32.

27. Vandervelde C, Kamani T, Varghese A, Ramesar K, Grace R, Howlett DC. A study to evaluate the efficacy of image-guided core biopsy in the diagnosis and management of lymphoma--results in 103 biopsies. *Eur J Radiol.* 2008 Apr;66(1):107–11.
28. Pfeiffer J, Kayser G, Technau-Ihling K, Boedeker CC, Ridder GJ. Ultrasound-guided core-needle biopsy in the diagnosis of head and neck masses: indications, technique, and results. *Head Neck.* 2007 Nov;29(11):1033–40.
29. Screatton NJ, Berman LH, Grant JW. Head and neck lymphadenopathy: evaluation with US-guided cutting-needle biopsy. *Radiology.* 2002 Jul;224(1):75–81.
30. Gritzmann N, Czembirek H, Hajek P, Karnel F, Frühwald F. [Sonographic anatomy of the neck and its importance in lymph node staging of head and neck cancer]. *RöFo Fortschritte Auf Dem Geb Röntgenstrahlen Nukl.* 1987 Jan;146(1):1–7.
31. Marchal G, Oyen R, Verschakelen J, Gelin J, Baert AL, Stessens RC. Sonographic appearance of normal lymph nodes. *J Ultrasound Med Off J Am Inst Ultrasound Med.* 1985 Aug;4(8):417–9.
32. Ying M, Ahuja A. Sonography of neck lymph nodes. Part I: normal lymph nodes. *Clin Radiol.* 2003 May;58(5):351–8.
33. Ahuja A, Ying M. Sonography of neck lymph nodes. Part II: abnormal lymph nodes. *Clin Radiol.* 2003 May;58(5):359–66.
34. Dudea SM, Lenghel M, Botar-Jid C, Vasilescu D, Duma M. Ultrasonography of superficial lymph nodes: benign vs. malignant. *Med Ultrason.* 2012 Dec;14(4):294–306.
35. van den Brekel MW, Castelijns JA, Stel HV, Golding RP, Meyer CJ, Snow GB. Modern imaging techniques and ultrasound-guided aspiration cytology for the assessment of neck node metastases: a prospective comparative study. *Eur Arch Oto-Rhino-Laryngol Off J Eur Fed Oto-Rhino-Laryngol Soc EUFOS Affil Ger Soc Oto-Rhino-Laryngol - Head Neck Surg.* 1993;250(1):11–7.
36. Ahuja AT, Ying M, Ho SY, Antonio G, Lee YP, King AD, et al. Ultrasound of malignant cervical lymph nodes. *Cancer Imaging.* 2008 Mar 25;8(1):48–56.
37. Sohn Y-M, Kwak JY, Kim E-K, Moon HJ, Kim SJ, Kim MJ. Diagnostic approach for evaluation of lymph node metastasis from thyroid cancer using ultrasound and fine-needle aspiration biopsy. *AJR Am J Roentgenol.* 2010 Jan;194(1):38–43.

38. Khanna R, Sharma AD, Khanna S, Kumar M, Shukla RC. Usefulness of ultrasonography for the evaluation of cervical lymphadenopathy. *World J Surg Oncol*. 2011;9:29.
39. Ahuja AT, Ying M. Sonographic evaluation of cervical lymph nodes. *AJR Am J Roentgenol*. 2005 May;184(5):1691–9.
40. Vassallo P, Wernecke K, Roos N, Peters PE. Differentiation of benign from malignant superficial lymphadenopathy: the role of high-resolution US. *Radiology*. 1992 Apr;183(1):215–20.
41. J I, T A, T T, K S, S S. Ultrasonic evaluation of cervical lymph node metastasis of squamous cell carcinoma in oral cavity. *Bull Tokyo Med Dent Univ*. 1989 1989;36(4):63–7.
42. Shozushima M, Suzuki M, Nakasima T, Yanagisawa Y, Sakamaki K, Takeda Y. Ultrasound diagnosis of lymph node metastasis in head and neck cancer. *Dento Maxillo Facial Radiol*. 1990 Nov;19(4):165–70.
43. Evans RM, Ahuja A, Metreweli C. The linear echogenic hilus in cervical lymphadenopathy--a sign of benignity or malignancy? *Clin Radiol*. 1993 Apr;47(4):262–4.
44. The Journal of Laryngology & Otology - A practical approach to ultrasound of cervical lymph nodes - Cambridge Journals Online [Internet]. [cited 2016 Jul 14]. Available from: <http://journals.cambridge.org/action/displayAbstract?fromPage=online&aid=1059396>
45. Ahuja AT, Chow L, Chick W, King W, Metreweli C. Metastatic cervical nodes in papillary carcinoma of the thyroid: ultrasound and histological correlation. *Clin Radiol*. 1995 Apr;50(4):229–31.
46. Ahuja A, Ying M, Evans R, King W, Metreweli C. The application of ultrasound criteria for malignancy in differentiating tuberculous cervical adenitis from metastatic nasopharyngeal carcinoma. *Clin Radiol*. 1995 Jun;50(6):391–5.
47. Sugama Y, Kitamura S. Ultrasonographic evaluation of neck and supraclavicular lymph nodes metastasized from lung cancer. *Intern Med Tokyo Jpn*. 1992 Feb;31(2):160–4.
48. Gritzmann N. Sonography of the neck: current potentials and limitations. *Ultraschall Med Stuttg Ger* 1980. 2005 Jun;26(3):185–96.
49. Gritzmann N, Hollerweger A, Macheiner P, Rettenbacher T. Sonography of soft tissue masses of the neck. *J Clin Ultrasound JCU*. 2002 Aug;30(6):356–73.

50. Ariji Y, Kimura Y, Hayashi N, Onitsuka T, Yonetsu K, Hayashi K, et al. Power Doppler sonography of cervical lymph nodes in patients with head and neck cancer. *AJNR Am J Neuroradiol.* 1998 Feb;19(2):303–7.
51. Choi MY, Lee JW, Jang KJ. Distinction between benign and malignant causes of cervical, axillary, and inguinal lymphadenopathy: value of Doppler spectral waveform analysis. *AJR Am J Roentgenol.* 1995 Oct;165(4):981–4.
52. Na DG, Lim HK, Byun HS, Kim HD, Ko YH, Baek JH. Differential diagnosis of cervical lymphadenopathy: usefulness of color Doppler sonography. *AJR Am J Roentgenol.* 1997 May;168(5):1311–6.
53. Jayachandran S, Sachdeva S. Diagnostic accuracy of color doppler ultrasonography in evaluation of cervical lymph nodes in oral cancer patients. *Indian J Dent Res.* 2012;23(4):557.
54. Moritz JD, Ludwig A, Oestmann JW. Contrast-enhanced color Doppler sonography for evaluation of enlarged cervical lymph nodes in head and neck tumors. *AJR Am J Roentgenol.* 2000 May;174(5):1279–84.
55. Willam C, Mäurer J, Schroeder R, Hidajat N, Hell B, Bier J, et al. Assessment of vascularity in reactive lymph nodes by means of D-galactose contrast-enhanced Doppler sonography. *Invest Radiol.* 1998 Mar;33(3):146–52.
56. New ultrasound techniques for lymph node evaluation. - PubMed - NCBI [Internet]. [cited 2016 Jul 17]. Available from: <http://www.ncbi.nlm.nih.gov/pubmed/23946589>
57. Lyshchik A, Higashi T, Asato R, Tanaka S, Ito J, Hiraoka M, et al. Cervical Lymph Node Metastases: Diagnosis at Sonoelastography—Initial Experience 1. *Radiology.* 2007;243(1):258–267.
58. Senchenkov A, Staren ED. Ultrasound in head and neck surgery: thyroid, parathyroid, and cervical lymph nodes. *Surg Clin North Am.* 2004 Aug;84(4):973–1000.
59. Ophir J, Céspedes I, Ponnekanti H, Yazdi Y, Li X. Elastography: a quantitative method for imaging the elasticity of biological tissues. *Ultrason Imaging.* 1991 Apr;13(2):111–34.
60. Hall TJ. AAPM/RSNA Physics Tutorial for Residents: Topics in US. *RadioGraphics.* 2003 Nov 1;23(6):1657–71.
61. Veenu Singla, Tulika Singh, Anindita Sinha. Ultrasound Elastography: Principles and Applications. In: *Diagnostic Radiology. (Recent Advances and Applied Physics in Diagnostic Imaging).*
62. Gao L, Parker KJ, Lerner RM, Levinson SF. Imaging of the elastic properties of tissue--a review. *Ultrasound Med Biol.* 1996;22(8):959–77.

63. Bhatia KSS, Lee YYP, Yuen EHY, Ahuja AT. Ultrasound elastography in the head and neck. Part I. Basic principles and practical aspects. *Cancer Imaging*. 2013 Jul 22;13(2):253–9.
64. Palmeri ML, Nightingale KR. Acoustic radiation force-based elasticity imaging methods. *Interface Focus*. 2011 Aug 6;1(4):553–64.
65. Barr RG, Zhang Z. Effects of precompression on elasticity imaging of the breast: development of a clinically useful semiquantitative method of precompression assessment. *J Ultrasound Med Off J Am Inst Ultrasound Med*. 2012 Jun;31(6):895–902.
66. Bamber J, Cosgrove D, Dietrich C, Fromageau J, Bojunga J, Calliada F, et al. EFSUMB Guidelines and Recommendations on the Clinical Use of Ultrasound Elastography. Part 1: Basic Principles and Technology. *Ultraschall Med - Eur J Ultrasound*. 2013 Apr 4;34(2):169–84.
67. Alam F, Naito K, Horiguchi J, Fukuda H, Tachikake T, Ito K. Accuracy of Sonographic Elastography in the Differential Diagnosis of Enlarged Cervical Lymph Nodes: Comparison with Conventional B-Mode Sonography. *Am J Roentgenol*. 2008 Aug 1;191(2):604–10.
68. Ghajarzadeh M, Mohammadifar M, Azarkhish K, Emami-Razavi SH. Sonoelastography for Differentiating Benign and Malignant Cervical Lymph Nodes: A Systematic Review and Meta-Analysis. *Int J Prev Med*. 2014 Dec;5(12):1521–8.
69. Nazarian LN. Science to practice: can sonoelastography enable reliable differentiation between benign and metastatic cervical lymph nodes? *Radiology*. 2007 Apr;243(1):1–2.
70. Tan R, Xiao Y, He Q. Ultrasound elastography: Its potential role in assessment of cervical lymphadenopathy. *Acad Radiol*. 2010 Jul;17(7):849–55.
71. Teng D-K, Wang H, Lin Y-Q, Sui G-Q, Guo F, Sun L-N. Value of ultrasound elastography in assessment of enlarged cervical lymph nodes. *Asian Pac J Cancer Prev APJCP*. 2012;13(5):2081–5.
72. Kemal Arda, Nazan Ciledag, Pelin Demir Gumusdag. Differential diagnosis of malignant cervical lymph nodes at real-time ultrasonographic elastography and Doppler ultrasonography. *Hung Radiol Online*. 2010;
73. Bhatia KSS, Lee YYP, Yuen EHY, Ahuja AT. Ultrasound elastography in the head and neck. Part II. Accuracy for malignancy. *Cancer Imaging*. 2013 Jul 22;13(2):260–76.
74. Sugimoto T, Ueha S, Itoh K. Tissue hardness measurement using the radiation force of focused ultrasound. In: *Ultrasonics Symposium, 1990 Proceedings, IEEE 1990*. 1990. p. 1377–80 vol.3.

75. Xu J-M, Xu X-H, Xu H-X, Zhang Y-F, Guo L-H, Liu L-N, et al. Prediction of cervical lymph node metastasis in patients with papillary thyroid cancer using combined conventional ultrasound, strain elastography, and acoustic radiation force impulse (ARFI) elastography. *Eur Radiol.* 2015 Nov 11;
76. Thitaikumar A, Krouskop TA, Garra BS, Ophir J. Visualization of bonding at an inclusion boundary using axial-shear strain elastography: a feasibility study. *Phys Med Biol.* 2007 May 7;52(9):2615–33.
77. Fujiwara T, Tomokuni J, Iwanaga K, Ooba S, Haji T. Acoustic radiation force impulse imaging for reactive and malignant/metastatic cervical lymph nodes. *Ultrasound Med Biol.* 2013 Jul;39(7):1178–83.
78. Meng W, Xing P, Chen Q, Wu C. Initial experience of acoustic radiation force impulse ultrasound imaging of cervical lymph nodes. *Eur J Radiol.* 2013 Oct;82(10):1788–92.
79. Che D, Zhou X, Sun M-L, Wang X, Jiang Z, Changjun-Wu null. Differentiation of metastatic cervical lymph nodes with ultrasound elastography by virtual touch tissue imaging: preliminary study. *J Ultrasound Med Off J Am Inst Ultrasound Med.* 2015 Jan;34(1):37–42.
80. Xu J-M, Xu H-X, Li X-L, Bo X-W, Xu X-H, Zhang Y-F, et al. A Risk Model for Predicting Central Lymph Node Metastasis of Papillary Thyroid Microcarcinoma Including Conventional Ultrasound and Acoustic Radiation Force Impulse Elastography. *Medicine (Baltimore).* 2016 Jan;95(3):e2558.
81. Choi YJ, Lee JH, Baek JH. Ultrasound elastography for evaluation of cervical lymph nodes. *Ultrasonography.* 2015 Feb 10;34(3):157–64.
82. Rubaltelli L, Stramare R, Tregnaghi A, Scagliori E, Cecchelerio E, Mannucci M, et al. The role of sonoelastography in the differential diagnosis of neck nodules. *J Ultrasound.* 2009 Jun 21;12(3):93–100.
83. Zhang Y, Lv Q, Yin Y, Xie M, Xiang F, Lu C, et al. The value of ultrasound elastography in differential diagnosis of superficial lymph nodes. *Front Med China.* 2009 Jul 17;3(3):368–74.
84. Bhatia KSS, Cho CCM, Yuen Y-H, Rasalkar DD, King AD, Ahuja AT. Real-time qualitative ultrasound elastography of cervical lymph nodes in routine clinical practice: interobserver agreement and correlation with malignancy. *Ultrasound Med Biol.* 2010 Dec;36(12):1990–7.
85. Ishibashi N, Yamagata K, Sasaki H, Seto K, Shinya Y, Ito H, et al. Real-time tissue elastography for the diagnosis of lymph node metastasis in oral squamous cell carcinoma. *Ultrasound Med Biol.* 2012 Mar;38(3):389–95.

86. Lenghel LM, Bolboaca SD, Botar-Jid C, Baciut G, Dudea SM. The value of a new score for sonoelastographic differentiation between benign and malignant cervical lymph nodes. *Med Ultrason*. 2012 Dec;14(4):271–7.
87. Lo W-C, Cheng P-W, Wang C-T, Liao L-J. Real-time ultrasound elastography: an assessment of enlarged cervical lymph nodes. *Eur Radiol*. 2013 Sep;23(9):2351–7.
88. Kau RJ, Alexiou C, Stimmer H, Arnold W. Diagnostic Procedures for Detection of Lymph Node Metastases in Cancer of the Larynx. *ORL*. 2000;62(4):199–203.
89. Yuasa K, Kawazu T, Nagata T, Kanda S, Ohishi M, Shirasuna K. Computed tomography and ultrasonography of metastatic cervical lymph nodes in oral squamous cell carcinoma. *Dento Maxillo Facial Radiol*. 2000 Jul;29(4):238–44.
90. Golder WA. Lymph Node Diagnosis in Oncologic Imaging: A Dilemma Still Waiting to Be Solved. *Oncol Res Treat*. 2004 May 7;27(2):194–9.
91. de Bondt RBJ, Nelemans PJ, Hofman P a. M, Casselman JW, Kremer B, van Engelshoven JMA, et al. Detection of lymph node metastases in head and neck cancer: a meta-analysis comparing US, USgFNAC, CT and MR imaging. *Eur J Radiol*. 2007 Nov;64(2):266–72.
92. Liao L-J, Lo W-C, Hsu W-L, Wang C-T, Lai M-S. Detection of cervical lymph node metastasis in head and neck cancer patients with clinically N0 neck-a meta-analysis comparing different imaging modalities. *BMC Cancer*. 2012;12:236.

ANNEXURE 1. DATA COLLECTION SHEET

Department of Radiodiagnosis, Christian Medical College, Vellore

Role of Acoustic Radiation Forced Impulse Imaging (ARFI) Elastography in

Characterization of Superficial Lymph Nodes

PROFORMA

Serial no:

Hospital No.:

Age:

Sex:

Clinical information:

I. Prior surgery / FNA / RT on the same site: Yes / No

II. Clinical palpation: 1 - Hard 2 – Firm 3 – Soft

III. Site:

	Right	Left
Cervical (Level)		
Supraclavicular		
Axillary		
Inguinal		

Imaging findings:

1. **B-mode USG:**

I. Short Axis Diameter: _____mm II. Long Axis Diameter: _____mm

II. Short: Long Axis:

III. Shape

1. Reniform
2. Round
3. Conglomerate
4. Irregular
5. Other_____

IV. Margin

1. Circumscribed
2. Lobulated
3. Irregular
4. Indistinct
5. Other_____

V. Echo pattern

1. Hyperechoic
2. Isoechoic
3. Hypoechoic
4. Complex

VI. Hilum

1. Present
2. Absent

VII. Necrosis

1. Absent
2. Present

a. Focal (<50%)

b. Diffuse (>50%)

VIII. Calcification

1. Absent
2. Macrocalcification Focal / Diffuse
3. Microcalcification Focal / Diffuse

2. Colour Doppler

1. Normal
2. Absent
3. Altered

3. ARFI Elastography

a. VTTI

I. Area

- a. Area 1 (VTI) = _____
- b. Area 2 (Grey) = _____
- c. Area Ratio = _____

II. Brightness Pattern

1. Obviously less than surrounding
2. Less than surrounding
3. Equal
4. More than surrounding
5. Obviously more than surrounding

b. VTTQ

I. SWV of Lesion (SWVL)

SWVL1	SWVL2	SWVL3	SWVL4	SWVL5	Mean

II. SWV of Surrounding tissue (SWV)

SWV1	SWV2	SWV3	SWV4	SWV5	Mean

III. Mean SWV ratio of lesion to surrounding tissue: _____

4. Histopathology

I. Benign

a. Reactive

b. Diseased

i. TB

ii. Others_____

II. Malignant

a. Lymphoma

b. Metastasis

i. Squamous

ii. Adeno

ANNEXURE 2A. PATIENT INFORMATION SHEET – ENGLISH

**DEPARTMENT OF RADIOLOGY, CHRISTIAN MEDICAL COLLEGE,
VELLORE**

PATIENT INFORMATION SHEET

**Study Title: Role of Acoustic Radiation Force Impulse (ARFI) Imaging in
Differentiating Benign and Malignant Lymph Nodes**

You are requested to participate in a study to see if a new ultrasound technique called ARFI can help in predicting whether a lymph node is benign or cancerous before you undergo biopsy. The final diagnosis will be given by microscopic examination of the tissue. By using this imaging technique we may be able to predict the nature of the lymph node which could aid in appropriate selection of lymph nodes prior to biopsy.

What is ARFI? How does it differentiate benign from cancerous lesions?

ARFI is a type of ultrasound which can measure the hardness of tissues. It is known that cancerous tissues are harder than benign tissues and ARFI uses this stiffness information to predict whether a lesion is likely to be benign or cancerous.

Does ARFI have any side effects?

No, ARFI is comparable to the conventional ultrasound used in routine imaging. There is no radiation exposure.

If you take part what will you have to do?

If you agree to participate in this study, you will have to come for ARFI study before your lymph node biopsy is performed. This study will take about 10-15minutes. There will be no change in any treatment or other investigations advised by your doctor. No blood test will be required for this study.

Will you have to pay for the ARFI study?

No, you will not be charged for the ARFI study. All other investigations will continue in the usual manner as advised by your doctor.

What happens after the study is over?

You may or may not benefit immediately from this study since the final results of this study will interpreted at the end of 1 year. If we come to a conclusion that the study is beneficial, we will be able to use information in assessing patients with similar conditions in future.

Will your personal details be kept confidential?

The results of this study will be published in a medical journal but your identity will not be revealed in any manner. However, the images may be reviewed by other specialists associated with the study without your additional permission.

If you have any further questions, please contact Dr Reettika Chanda (Ph. 0416 307 3012) or E-mail: reetikachanda@gmail.com

ANNEXURE 2B. PATIENT INFORMATION SHEET – BENGALI

রেডিওলজি বিভাগ, খ্রীষ্টান মেডিকেল কলেজ, ভেল্লেরে

রোগী তথ্য পত্র

সৌম্য এবং ঘাতক লিম্ফ নোডের অন্তরে আর্ফি আলট্রাসাউন্ডের ভূমিকা

আপনাকে সৌম্য এবং ঘাতক লিম্ফ নোডে অন্তর করতে আর্ফি আলট্রাসাউন্ডের ভূমিকা বিষয় অধ্যয়নে ভাগ নিতে অনুরোধ করা হচ্ছে। আর্ফি, আলট্রাসাউন্ডের এমন বিশিষ্ট পদ্ধতি যেতে বায়প্লীর পূর্ব হী লিম্ফ নোডে ক্যান্সারের উপস্থিতির অনুমান লাগানো যেতে পারে। এর অন্তিম নির্ণয় টিসুর আণুবীক্ষণিক পরীক্ষার পর করা যাবে। আর্ফির উপযোগ করে বায়প্লীর জন্য উপযুক্ত বেছে নিতে সুবিধা হবে।

আর্ফি কি?

এতে সৌম্য এবং ঘাতক লিম্ফ নোডে অন্তর কি ভাবে করা যায়?

ইহার দ্বারা সৌম্য এবং ঘাতক লিম্ফ নোডের মধ্যে পার্থক্য কি ভাবে করা যায়?

আর্ফি আলট্রাসাউন্ডের এমন একটা পদ্ধতি যাহার দ্বারা গাঠের সংকুচন কে মাপা যেতে পারে। ইহা ধরে নেওয়া হয় যে সামান্য কোশিকার তুলনায় ক্যান্সারের কোশিকা বেশি শক্ত হয়। আর্ফি প্রয়োগের মাধ্যমে কোশিকার শক্ত ভাবের মাপ করা হয় এবং এই অনুমান করা যেতে পারে যে উহার মধ্যে ক্যান্সারের সম্ভাবনা কতটা আছে।

আর্ফির কি কোনো পার্শ্বক্রিয়া আছে?

আর্ফির কোনো দুপ্তভাব নেই। আর্ফির তুলনা সামান্য আলট্রাসাউন্ডের সাথে করা যেতে পারে। ইহার দ্বারা কোনো প্রকারের হানিকারক বিকিরণ বেরয়ে না।

এই অধ্যাযানে অংশগ্রহন করার জন্য আপনার কি করার প্রয়োজন?

যদি আপনি এই অধ্যাযানে অংশগ্রহন করতে রাজি হন, তাহলে আপনাকে নিজের লিম্ফ নোড বায়স্পীর পূর্বে রাদীয়লোপ্য বিভাগে গিয়ে সেই লিম্ফ নোডের করিয়ে নিতে হবে। এই প্রাক্রিয়ায়ে কেবল মাত্র ১৫ - ২০ মিনিট সময় লাগবে। আপনার ডাক্তারের নির্দেশানুসারে অন্যান্য প্রক্রিয়া এবং চিকিত্সায়ে কোনো পরিবর্তন হবে না। আর্ফির জন্য কোনো রক্ত পরীক্ষার আবশ্যকতা নেই।

লিম্ফ নোড আর্ফির জন্য কোনো ধনরাশি জামা করতে হয়ে কি?

আপনার জন্য এই পরীক্ষা নিঃশুঙ্ক। ডাক্তার দ্বারা নির্ধারিত অন্যান্য সব পরীক্ষার প্রক্রিয়া সামান্য ভাবে চলবে।

অধ্যায়নের শেষে কি হবে?

এই অধ্যায়ন এক বছর ধরে চলবে। এই অধ্যায়নের মাধ্যমে সুফল নিষ্কর্ষ পাওয়া গেলে এর প্রয়োগ আমরা আপনার মত ই অন্য

লিম্ফ নোড বৃদ্ধির রুগীদের চিকিত্সাতে করতে পারব।

আপনার ব্যক্তিগত বিবরণ কে গুপ্ত রাখা হবে কি?

এই অধ্যায়নের পরিণাম মেডিকেল বুলেটিনে প্রকাশিত করা হবে। সকল অংশগ্রহনকারীদের পরিচয় গুপ্ত রাখা হবে। তবে,

এই অধ্যায়নের সঙ্গে জড়িত অন্যান্য বিশেষজ্ঞগন অতিরিক্ত অনুমতি ছাড়া এই আর্ফির ছবিগুলোর বিশ্লেষণ করতে পারবে।

আপনি যদি এই বিষয় আরও তথ্য জানতে চান তবে ডাঃ ঋতিকা চন্দ সঙ্গে যোগাযোগ করুন।

ফোন নং 0416 307 2027 ইমেল: reetikachanda@gmail.com

ANNEXURE 2C. PATIENT INFORMATION SHEET – HINDI

रेडियोलॉजी विभाग, क्रिस्चियन मेडिकल कॉलेज, वेल्लोर

रोगी जानकारी पत्र

सौम्य एवं घातक लिम्फोमा (लिम्फ नोड) के अंतर में आर्फी (ARFI) अल्ट्रासाउंड की भूमिका

सविनय निवेदन है की आप सौम्य एवं घातक लिम्फ नोड में अंतर करने में आर्फी अल्ट्रासाउंड की क्षमता के अध्ययन में भाग लें। आर्फी, अल्ट्रासाउंड की एक ऐसी विशिष्ट पद्धति है जिससे बायोप्सी के पूर्व ही गाँठ में कैंसर की उपस्थिति का अनुमान लगाया जा सकता है। इसका अंतिम निर्णय कोशिका के सूक्ष्म परिक्षण द्वारा दिया जायेगा। आर्फी के प्रयोग से बायोप्सी के लिए उपयुक्त लिम्फ नोड का चुनाव करने में सुविधा होगी।

आर्फी क्या है? इससे सौम्य एवं घातक लिम्फ नोड में अंतर कैसे किया जाता है?

आर्फी अल्ट्रासाउंड की एक ऐसी तकनीक है जिससे गाँठ के संकुचन को नापा जा सकता है। यह माना जाता है कि सामान्य ऊतक की तुलना में कैंसर के ऊतक ज़्यादा सख्त होते हैं। आर्फी के प्रयोग से ऊतक की सख्ती का माप कर यह अनुमान लगाया जा सकता है कि उसमें कैंसर की कितनी संभावना है।

क्या आर्फी का कोई गौण प्रभाव है?

आर्फी का कोई गौण प्रभाव नहीं है। आर्फी की तुलना सामान्य अल्ट्रासाउंड के साथ की जा सकती है। इससे हानिकारक विकिरण नहीं निकलते हैं।

अध्ययन में भाग लेने पर आपको क्या करना होगा?

अगर आप इस अध्ययन में भाग लेने के लिए सहमत हैं, तो आपको अपने लिम्फ नोड बायोप्सी के पूर्व रेडियोलॉजी विभाग में आकर उस लिम्फ नोड का आर्फी अल्ट्रासाउंड करवाना पड़ेगा। जांच के लिए केवल 15 मिनट लगेंगे। आपके डॉक्टर के निर्देशानुसार अन्य जांच एवं उपचार में कोई बदलाव नहीं होगा। आर्फी के लिए किसी रक्त परीक्षा की आवश्यकता नहीं है।

क्या लिम्फ नोड आर्फी के लिए किसी धनराशि का भुगतान करना होगा?

आपके लिए यह जांच निःशुल्क है। डॉक्टर द्वारा सुझाये गए अन्य सभी जांच प्रक्रिया सामान्य रूप से चलेंगी।

अध्ययन के अंत में क्या होगा?

इस अध्ययन का आवर्तकाल एक साल है। अध्ययन के अंत में लाभकारी निष्कर्ष मिलने पर इसका उपयोग हम आप ही के समान अन्य

लिम्फ नोड वृद्धि के मरीजों की चिकित्सा में कर पाएंगे।

क्या आपके व्यक्तिगत विवरण को गुप्त रखा जाएगा?

इस अध्ययन का परिणाम मेडिकल बुलेटिन में प्रकाशित की जायेगी। भाग लेने वाले सभी व्यक्तियों की पहचान गोपनीय राखी जायेगी।

हालाँकि, इस अध्ययन से जुड़े अन्य विशेषज्ञ, बिना किसी अतिरिक्त अनुमति के, इन आर्फी की छवियों का विश्लेषण कर पाएंगे।

इस अध्ययन से जुड़े अन्य किसी विवरण के लिए डॉ. ऋत्तिका चंदा से सम्पर्क करें।

फ़ोन न. 0416 307 2027 ईमेल: reetikachanda@gmail.com

ANNEXURE 2D. PATIENT INFORMATION SHEET – TAMIL

ரேழ்வாண்கி துறை, கிரிஸ்து மருத்துவ கல்லூரி, வேலூர்.

சுகவலரிடம் சூப்பதல் சுகவல துறை

ஆய்வு தகவல்: Acoustic Radiation Force Impulse (ARFI),
 எந்தும் கருவிமீன் மீலம் ரெநி கட்டிணை
 4ந்ருநீராய் கட்டிவணையும் 4ந்ருநீராய் அல்லாத
 கட்டிவணையும் எவ்வாறு உணைப்படுகிறது என்பதை
 பருவிய ஓடு ஆய்வு

இந்த ஆய்வில் கண்டு வகண்டிக்கும் மீலம் ரெநி கட்டிணை
 4ந்ருநீராய் கட்டிவணையும் 4ந்ருநீராய் அல்லாத கட்டிவணையும் இது
 பரிசீலனை விசயத்திற்கு முன்பு ரெநி கட்டிணை எவ்வாறு ARFI
 உருவாகிறது என்பதை அறிவலாம். ரெநி கட்டிணை அல்லாத கட்டிவணையும்
 பரிசீலனைக்கு முன்பு ARFIவை பயன்படுத்தி ரெநி கட்டிவணை
 தன்மைவை கண்டறிந்து எந்த உணை ரெநி கட்டிவணை இது பரிசீலனை
 குட படுகின்றன என்பதை கண்டறிவலாம்.

1. ARFI எந்தென எனது? அது எவ்வாறு ரெநி கட்டிவணை
 4ந்ருநீராய் கட்டிவணையும் 4ந்ருநீராய் அல்லாத கட்டிவணையும் உணைப்படுகிறது
 ARFI என்பது ஒரு உணைவை அல்லாத அண்டி ரெநி கட்டிவணை
 இது மீலம் திசுவின் கட்டிவணைவை அண்டிவலாம். 4ந்ருநீராய்
 திசுவின் உணைவை 4ந்ருநீராய் அல்லாத திசுவை வில கட்டிவணை கிடுக்டும்.
 இந்த உணைவை ARFI மூக்கு உருவாகிறது.

2. ARFI இது பக்க விணைவுகள் உண்டா?
 இவை இதுவும் அல்லாத அண்டி ரெநி கட்டிவணை போன்ற
 ஒரு கருவி இதற்கும் கதிர்வீச்சு விணைவுகள் கிடைவாது.

3. திருத்த ஆய்வில் கலந்து கொண்டிருக்கிற குறியீடுகள் என்ன செயல்படும்?

திருத்த ஆய்வில் கலந்து கொண்டிருக்கிற குறியீடுகள் என்ன செயல்படும்? திருத்த ஆய்வில் கலந்து கொண்டிருக்கிற குறியீடுகள் என்ன செயல்படும்? திருத்த ஆய்வில் கலந்து கொண்டிருக்கிற குறியீடுகள் என்ன செயல்படும்?

4. ARFI ஆய்வில் கலந்து கொண்டிருக்கிற குறியீடுகள் என்ன செயல்படும்?

திருத்த ஆய்வில் கலந்து கொண்டிருக்கிற குறியீடுகள் என்ன செயல்படும்? திருத்த ஆய்வில் கலந்து கொண்டிருக்கிற குறியீடுகள் என்ன செயல்படும்?

5. ஆய்வில் முடிவில் என்ன நடக்கும்?

திருத்த ஆய்வில் முடிவில் என்ன நடக்கும்? திருத்த ஆய்வில் முடிவில் என்ன நடக்கும்? திருத்த ஆய்வில் முடிவில் என்ன நடக்கும்?

6. உங்களை பற்றிய தகவல் / அபாயம் என்னிடம் படுமா?

திருத்த ஆய்வில் முடிவில் என்ன நடக்கும்? திருத்த ஆய்வில் முடிவில் என்ன நடக்கும்? திருத்த ஆய்வில் முடிவில் என்ன நடக்கும்?

ANNEXURE 3A. CONSENT FORM – ENGLISH

CONSENT TO TAKE PART IN STUDY

Study Title: Role of Acoustic Radiation Force Impulse (ARFI) imaging in differentiating benign and malignant lymph nodes

Study Number: _____

Participant's Name: _____

Father's/Husband's Name: _____

Age: _____ Sex: Male / Female

Hospital No.: _____

I declare the following: (please tick the boxes)

(i) I have read and understood the information sheet provided to me regarding this study and have had the opportunity to ask questions.

(ii) I understand that my participation in the study is voluntary and that I am free to withdraw at any time, without giving any reason, without my medical care or legal rights being affected.

(iii) I understand that the study staff and the Ethics Committee will not need my permission to look at my health records both in respect of the current study and any further research that may be conducted in relation to it. I agree to this access. However, I understand that my identity will not be revealed in any information released to third parties or published.

(iv) I agree not to restrict the use of any data or results that arise from this study provided such a use is only for scientific purpose(s).

(v) I agree to take part in the above study.

Participant's

Signature: _____

Date: ____/____/____

Investigator's

Signature: _____

Date: ____/____/____

ANNEXURE 3B. CONSENT FORM – BENGALI

সূচিত সহমতি প্রপত্র

অধ্যায়ন শীর্ষক: সৌম্য এবং ঘাতক লিফ নোডের অন্তরে আর্ফি আলট্রাসাউন্ডের ভূমিকা

অধ্যায়ন সংখ্যা: _____

অনশগ্রাহকের নাম: _____

বাবা/ স্বামীর নাম: _____

বয়স: _____ লিঙ্গ: স্ত্রী / পুরুষ

হাসপাতাল নম্বর: _____

আমি ঘোষণা করছি যে: (নিম্নলিখিত প্রত্যেকটি সন্থায়ে সঠিক চিহ্ন দিন)

১. দেওয়া রোগী তথ্য পত্র আমি ধ্যানপূর্বক পড়েছি এবং বুঝে নিয়েছি। অধ্যায়ন সম্বন্ধিত জিজ্ঞাসা করার পর্যাপ্ত সুযোগও প্রদান করা হয়েছে।

২. আমি বুঝেছি যে এই অধ্যয়নে অংশগ্রহন করা সম্পূর্ণরূপে ঐচ্ছিক। আমি যে কোনো সময়, বিনা কোনো কারণ দেখিয়ে, এই অধ্যয়ন থেকে নিজের নাম ফেরত নিতে পারি। এমন স্থিতিতে আমার চিকিৎসা বা আইনগত অধিকার ব্যাহত হবে না।

৩. আমি বুঝেছি যে এই অধ্যয়ন বা এই বিষয় সম্বন্ধিত অন্য অধ্যয়নে বেবহারের জন্য, আমার স্বাস্থ্য রেকর্ড পরীক্ষা করতে অধ্যয়ন কার্যকর্তা এবং নীতি সমিতি কে আমার অনুমতি নেওয়ার প্রয়োজন হবে না। আমার বিশ্বাস যে কোনো তৃতীয় ব্যক্তি বা প্রকাশনের কাছে আমার পরিচয় গোপন রাখা হবে।

৪. বৈজ্ঞানিক কার্যের জন্য এই অধ্যয়নের ডাটা এবং ফলাফল প্রয়োগের সময় আমি কোনো বাধা দেব না। ইহাতে আমার সহমতি আছে।

৫. আমি এই অধ্যয়নে অংশ নেওয়ার জন্য স্বীকৃতি দিচ্ছি।

অনশগ্রাহকের হস্তাক্ষর: _____

তদন্তকারীর হস্তাক্ষর: _____

দিনাক: _____

দিনাক: _____

ANNEXURE 3C. CONSENT FORM – HINDI

सूचित सहमति प्रपत्र

अध्ययन शीर्षक: सौम्य एवं घातक लसिकापर्व (लिम्फ नोड) के अंतर में आफ्री (ARFI) अल्ट्रासाउंड की भूमिका

अध्ययन संख्या: _____

प्रतिभागी का नाम: _____

पिता/स्वामी का नाम: _____

उम्र: _____ लिंग: महिला / पुरुष

हॉस्पिटल न: _____

मैं घोषणा करता / करती हूँ कि: (निम्नलिखित अंकों पर सही [✓] का चिह्न लगाएं)

१. दिए गए रोगी जानकारी पत्र को मैंने पढ़कर समझ लिया है। अध्ययन से सम्बंधित जिज्ञासा करने का अवसर भी प्रदान किया गया है।

२. मैं समझता / समझती हूँ कि इस अध्ययन में भाग लेना पूर्णतः स्वेच्छिक है। मैं किसी भी समय, बिना कोई कारण दिए, अपना नाम इस अध्ययन से वापस लेने की स्वतंत्रता रखता हूँ। ऐसा करने की स्थिति में, मेरी चिकित्सा एवं कानूनी अधिकारों पर कोई प्रभाव नहीं पड़ेगा।

३. मैं समझता / समझती हूँ कि इस अध्ययन के, या इस विषय से सम्बंधित किसी अन्य अध्ययन के सन्दर्भ में, मेरे स्वास्थ्य रिकॉर्ड की जांच करने के लिए, अध्ययन कार्यकर्ता एवं नीति समिति को किसी अनुमति की आवश्यकता नहीं होगी। हालाँकि, मैं समझता / समझती हूँ कि किसी तीसरे व्यक्ति अथवा प्रकाशन से मेरे परिचय को गुप्त रखा जायेगा।

४. वैज्ञानिक कार्यों के लिए इस अध्ययन के आकड़ों एवं नतीजों के प्रयोग पर मैं कोई प्रतिबन्ध नहीं लगाऊँगा / लगाउंगी।

५. मैं इस अध्ययन में भाग लेने की स्वीकृति प्रदान करता / करती हूँ।

प्रतिभागी के हस्ताक्षर: _____

जांचकर्ता के हस्ताक्षर: _____

दिनांक: _____/_____/_____

दिनांक: _____/_____/_____

ANNEXURE 3D. CONSENT FORM – TAMIL

ஆய்வினை கைநது விசாரணை அளிக்கும் ஒப்புதல் வரவுமொன்று

ஆய்வு தலைப்பு: Acoustic Radiation Force Impulse (ARFI)
 எண்ணம் கருவியின் மூலம் நெடுநிலைகளை
 புற்றுநோய் கட்டிவெண்ப்பு மற்றும் புற்றுநோய் அல்லாத
 கட்டிவெண்ப்பு எவ்வாறு உண்கையபடுத்துவது என்பதை
 பற்றிய ஒரு ஆய்வு

ஆய்வு எண்:

பங்கேற்பவரின் பெயர்:

உயது:

திரு / திருமதி _____ எண்பவரின் மகன்/மகள் சிவ
 நாயன் _____

(கீழ்க்கண்ட கட்டத்தில் குறிக்கவும்)

(i) தகவலளித்த ஒப்புதல் தகவல் தரண்பட்டதும், அதை உயிரங்களை
 கெடும் யரிந்து கெண்டிடன் ()

(ii) திருது ஆய்வின் கைநது கெண்டண்ப்பு எண்ண்ப்பு மூலம்
 கட்டிவெண்ப்பு மூலம் திருது ஆய்விலிருந்து எந்திரமும்
 கெண்டண்ப்பு விவரிப்பது கெண்டண்ப்பு அனுமதிபுள்ளது. அப்படி விவரிப்பது
 உத்தரவு எண்ண்ப்பு மருத்துவம் மருத்துவ கட்ட உரிமைகளை
 மருத்துவ மருத்துவ எண்ண்ப்பு அளிந்து கெண்டிடன் ()

(iii) திருது ஆய்வின் உயிரியர்கள்/ உண்கையபடுத்துகிற சிவ
 மருத்துவ உயிரங்களை எண் அனுமதிபுள்ளி உபயோகிக்க

ஒப்பு காரணிகளேன். கிரேப்பியை என்னது துணிப்படை
அடைபாணம்/தகவல், மருந்துகளை/மருத்துவ கிதழினால்
ஒரளவியைப் பட்டாது எண்பதையும் தெரிந்து காண்க().

(iv) கித்த ஆய்வின் முடிவு/தகவலை அறிவிக்க தோக்கத்திற்கு
மட்டுமே பயன்படுத்த நான் சம்மதிக்கிறேன்.

(v), கித்த ஆய்வை பதிக்க நான் முழுமனதுடன் சம்மதிக்கிறேன்

பதிக்கப்படும் காரணியை/காரணிகளை:

தேதி:

பெயர்:

ஆய்வாளரின் கையொப்பம்/-

தேதி:

பெயர்:

ANNEXURE 4. STUDY DATA

id	age	sex	prior	palp	site	otrst	side	sad	lad	ls	shp	otrshp	mrgn	otmr	echo	hilum	necr	qnecr	calc	clpr	vasc
1	53	2	2	2	4		1	22.8	44.4	1.95	1		1		3	1	1		1		3
2	30	2	2	2	3		1	12.5	19.3	1.56	1		1		3	2	1		1		2
3	53	1	2	1	1		1	15	26	1.73	1		1		3	1	1		2	4	3
5	39	2	1	2	2		1	95	31.4	0.3	1		1		3	1	1		1		3
6	68	2	2	2	2		1	8	10.8	1.35	4		3		3	2	1		1		2
7	51	1	2	2	4		2	11.3	27.2	2.41	1		1		3	1	1		1		1
8	55	2	2	2	1		1	12.2	20.3	1.66	1		1		3	1	1		1		3
9	63	2	2	1	2		1	11.7	16.1	1.38	2		1		3	2	1		1		1
10	27	2	2	2	1		1	87	19.6	2.25	1		1		3	1	2	1	1		2
11	23	1	2	2	3		1	7	20	2.86	1		1		3	1	1		1		3
12	52	1	2	2	1		2	97	16	1.65	1		1		3	2	2	1	1		2
13	23	2	2	2	1		1	11.7	17	1.13	1		1		1	1	1		1		1
14	60	1	2	2	3		1	82	31.6	3.85	1		1		3	1	1		1		1
16	40	2	2	2	1		1	8	19.7	2.46	1		1		3	1	1		1		1
17	31	1	2	2	4		2	29.8	44.7	1.5	1		1		3	1	1		1		3
18	49	2	2	2	1		2	11.6	18.6	1.6	2		1		3	2	1		1		3
19	19	1	2	2	1		1	98	15.5	1.58	2		1		3	2	1		1		2
20	22	2	2	3	3		1	11.4	26.1	2.46	1		1		3	1	1		1		1
21	25	1	2	2	3		2	93	25	2.69	1		1		1	1	1		1		2
22	22	1	1	3	1		1	7	14	2	1		1		3	1	1		1		3
23	30	2	2	2	1		1	16.3	17.6	0.93	4		4		3	2	1		1		2
24	33	1	1	3	3		1	6	20	3.33	1		1		3	1	1		1		1
25	37	1	2	2	1		2	21	35	1.67	1		1		3	2	1		1		3
27	75	1	2	2	2		2	7	16	2.29	2		1		3	2	1		1		3
28	26	2	2	2	2		2	25	40	1.6	1		1		3	1	1		1		1
29	44	2	2	2	1		2	5	15	3.33	1		1		3	1	1		1		1
30	17	2	2	2	2		2	9	21	2.33	1		1		3	1	1		1		1
31	48	2	2	2	1		2	9.9	18.5	1.87	1		1		3	1	1		1		3
33	45	1	2	1	1		1	18	34.7	1.93	2		1		1	2	1		1		3
34	37	2	2	2	3		1	8.9	13.3	1.49	1		1		3	1	1		1		1
35	24	1	2	2	2		1	9	17.8	1.98	1		1		3	2	1		2	3	1
36	58	2	2	2	3		1	7.3	11.4	1.56	2		1		3	2	1		1		2
37	48	2	2	2	3		1	6.1	16.8	2.75	1		1		3	1	1		1		1
38	48	2	2	2	3		2	6	12.9	2.15	1		1		3	1	1		1		1
40	42	1	2	2	3		1	12.5	26	2.08	4		1		3	2	2	1	1		2
41	41	2	2	2	2		1	9.9	14.9	1.51	1		1		3	1	2	1	1		1
42	60	2	2	1	3		2	21.4	36.1	1.69	1		1		3	1	1		1		3
43	66	1	2	2	2		2	6.1	13.9	2.28	2		1		3	2	1		1		3
44	55	1	2	2	1		2	11.3	12.7	1.12	2		1		3	2	2	1	1		3

id	ver	gar	ar	brt	swmeas	notmeas	l1	l2	l3	l4	l5	mlies	s1	s2	s3	s4	s5	mnsur	swrmeas	swr	avall	ifavl	ifben	ifmal	ifnl	omal
1	7.2	6.6	1.09	5	1		2.34	2.3	2.4	2.13	2.09	2.25	0.77	0.77	0.77	0.77	0.77	0.77	1	2.92	1	2		1		
2	2.4	2.1	1.14	5	1		3.98	4.66	5	5.19	4.29	4.62	3.38	3.38	3.38	3.38	3.38	3.38	1	1.37	1	2		2	3	BREAST
3	3.4	2.4	1.42	5	1		2.49	2.29	1.52	2.08	1.91	2.05	1.16	1.36				1.26	1	1.63	1	2		1		
5	3.2	2.7	1.19	1	1		2.04	2.05	1.92	2.05	2.09	2.03	1.28	1.51	1.36	1.23	1.12	1.3	1	1.56	1	2		1		
6	0.69	0.53	1.3	1	1		1.9	1.9	1.9	1.9	1.9	1.9	1.28	1.23	1.32	0	0	1.28	1	1.49	1	2		2	2	
7	3.2	2.9	1.1	2	1		3.83	3.47	3.72	3.97	3.14	3.63	0.72	0.83	0.96	0.76	0.95	0.84	1	4.3	1	2		1		
8	2.5	1.8	1.39	2	1		2.51	2.5	2.59	2.49	2.59	2.54	1.61	1.58	1.59	1.67	1.46	1.58	1	1.61	1	2		1		
9	1.8	1.8	1	1	1		2.13	2.12	1.94	2.02	2.09	2.06	1.4	1.61	1.63	1.68	1.5	1.52	1	1.35	1	2		1		
10	1.3	1.6	0.81	2	1		3.38	5.07	5.75	3.65	3.07	4.18	2.03	2.1	2.18	1.86	1.5	1.93	1	2.16	1	1		3		
11	1.4	1.2	1.17	4	1		4.14	4.55	4.45	4.12	3.79	4.21	2.47	2.31	2.22	2.13	2.21	2.27	1	1.85	1	1		4		
12	1.1	0.78	1.41	5	1		1	1.05	1.4	1.33	1.5	1.26	1.72	1.66	1.79	1.75	1.63	1.71	1	0.73	1	2		1		
13	1.2	1.6	0.75	4	1		2.22	2.11	2.59	2.34		2.32	0.87	0.85	0.88	0.83	0.88	0.86	1	2.69	1	1		3		
14	1.2	2	0.6	3	1		4.74	4.81	4.82	4.69	4.38	4.69	3.02	3.02	3	2.92	2.73	2.94	1	1.6	1	1		2		
16	0.56	1.1	0.51	3	1		2.49	2.36	2.23	2.17		2.31	1.77	1.33	1.44	1.53	1.48	1.51	1	1.53	1	2		1		
17	3	2.7	1.11	1	1		2.67	4.15	2.28	2.02	2	2.62	2.64	2.64	2.08			2.47	1	1.06	1	2		1		
18	2.4	1.7	1.41	1	1		4.72	4.69	5.75	5.01	5.28	5.09	2.15	2.12	2	2.26	2.66	2.24	1	2.27	1	2		2	1	
19	1.1	1.3	0.85	4	1		2.44	2.52	2.02	2.31	2.38	2.33	2.46	2.14	2.39	2.47	2.32	2.36	1	0.99	1	1		3		
20	2.3	2.7	0.85	4	1		3.36	3.09	3.47	3.37	2.81	3.22	1.52	1.76	1.54	1.39	1.46	1.53	1	2.1	1	1		1		
21	0.37	0.38	0.97	5	1		1.25	0.79	0.99	0.2	1.11	1.07	1.87	1.68	1.94	2	2.14	1.93	1	0.55	1	1		2		
22	1	1.6	0.63	3	1		1.93	1.78	1.85	1.55		1.75	0.86	0.91	0.85	0.9	0.89	0.88	1	2.02	1	1		3		
23	2.6	2.1	1.24	1	1		1.06	1.04	1	1.12	1.06	1.06	1.9	1.65	1.74	1.86	1.62	1.75	1	0.61	1	1		3		
24	0.48	0.57	0.84	4	1		1.92	2.09	1.94	2.25	2.04	2.05	2.02	2.06	1.36	1.99	2.03	1.89	1	1.08	1	1		2		
25	4.2	3.7	1.14	2	1		2.54	2.41	2.37	2.48	2.15	2.39	0.69	0.83	0.75	0.81	0.73	0.76	1	3.13	1	2		1		
27	1	0.8	1.25	1	1		3.01	3.04	3.03	3.65	3.42	3.23	1.29	1.57	1.17	1.74	1.38	1.43	1	2.26	1	2		1		
28	5.4	5.5	0.98	4	1		1.59	1.61				1.6	5.76	5.93	4.01	4.97	4.63	5.06	1	0.32	1	1		3		
29	0.44	0.56	0.75	4	1		3.13	3	3.22	3.5	2.85	3.14	2.33	2.63	2.98	2.59	2.54	2.61	1	1.2	1	1		2		
30	1	1.3	0.77	4	1		3.44	3.49	1.9	3.52	3.22	3.11	1.59	1.98	1.81	1.64	1.9	1.78	1	1.75	1	1		3		
31	1.4	1.2	1.17	4	1		3.17	3.05	3.28	3.64	3.37	3.3	3.95	3.63	3.97	4.01	3.81	3.87	1	0.85	1	2		1		
33	4	4	1	2	1		4.98	3.34	4.64	2.96	2.79	3.74	1.44	1.09	1.53	1.39	1.24	1.34	1	2.8	1	2		2	3	PAPILLARY
34	0.66	0.88	0.75	4	1		2.77	3.37	3.05	3.16	2.85	3.04	1.47	1.58	1.54	1.6	1.58	1.55	1	1.96	1	1		2		
35	0.86	1.2	0.72	3	1		0.99	0.93	0.65	0.76	0.64	0.79	1.55	1.75	1.53	1.74	1.72	1.66	1	0.48	1	1		3		
36	0.74	0.63	1.17	2	1		3.02	3.3	3.43	3.47	3.54	3.35	2.64	2.26	2.17	2.28	2.3	2.33	1	1.44	1	1		3		
37	0.39	0.52	0.75	5	1		1.68	1.51	1.52	1.34	1.66	1.54	1.98	2	2.1	1.84	1.83	1.95	1	0.75	1	1		2		
38	0.56	0.81	0.69	4	1		2.36	2.47	2.26	2.28	2.29	2.33	3.23	2.8	2.3	2.32	2.39	2.61	1	0.89	1	1		2		
40	2.1	3	0.7	4	1		0.59					0.59	2.24	2.49	2.21	2.32	2.32	2.32	1	0.25	1	1		3		
41	0.72	1.2	0.6	2	1		2.1	2.2	2.46	2.27	2.71	2.35	1.66	1.46	1.52	1.71	1.49	1.57	1	1.5	1	1		2		
42	4.7	3.6	1.31	2	1		4.38	4.58	4.32	4.9	4.44	4.52	1.93	2.08	2.02	1.94	2.05	2	1	2.26	1	2		2	2	
43	1.8	1.5	1.2	2	1		1.62	1.68	1.8	1.73	1.97	1.76	1.43	1.25	1.37	1.31	1.45	1.36	1	1.29	1	2		1		
44	1.1	1.2	0.92	3	1		1.96	2.46				2.21	4.09	3.86	4.27	4.2	4.27	4.14	1	0.53	1	1		4		

id	age	sex	prior	palp	site	otrst	side	sad	lad	ls	shp	otrshp	mgn	otmr	echo	hilum	necr	qnecr	calc	clpr	vasc
45	56	1	2	2	2		1	10.8	23.9	2.21	1		1		3	2	1		1		2
46	44	1	2	2	4		2	7	20	2.86	1		1		3	1	1		1		1
47	24	2	1	1	1		1	30.3	20.2	4.61	1		3		2	1	1		2	3	3
50	24	2	2	1	1		2	10.4	20.6	1.98	1		1		3	1	1		1		1
51	72	1	2	1	2		1	7.5	11.5	1.53	2		1		1	2	1		1		2
52	72	1	2	3	3		2	11	15.9	1.45	1		1		3	1	1		1		3
53	61	1	2	1	2		2	15.6	23.1	1.48	1		1		3	1	1		1		3
54	17	2	1	3	1		1	8.2	15.3	1.87	1		1		3	2	1		2	3	2
55	23	1	2	3	2		2	6.4	18	2.81	1		1		3	2	2	1	1		2
56	53	2	2	2	2		1	11.1	17.6	1.59	2		1		3	2	1		1		2
57	75	2	2	1	4		1	25.8	37.3	1.45	2		1		3	1	1		1		3
58	44	1	2	1	4		2	26.5	45	1.7	1		1		3	1	1		1		1
59	53	2	2	2	3		1	17.1	29.3	1.71	1		1		3	1	1		1		1
60	32	1	2	2	3		2	15	25	1.67	1		1		3	2	1		1		3
61	50	2	2	2	1		1	9.6	16.7	1.74	1		4		3	2	2	1	2	1	2
62	28	2	2	2	1		2	6	18.2	3.03	1		1		3	1	1		1		3
63	36	2	2	3	2		1	19	24	1.26	3		4		4	2	1		2	1	1
64	35	2	2	2	3		1	16	25.2	1.58	3		1		4	2	1		1		2
65	55	1	2	1	1		1	10.8	20	1.85	2		1		3	2	1		1		2
66	45	2	2	2	3		2	19	24.5	1.29	1		1		3	1	1		1		3
67	22	2	1	1	1		1	9.1	11.8	1.3	2		1		3	2	1		1		3
68	21	2	2	2	1		2	9.7	14.7	1.52	2		1		3	2	1		1		3
69	16	2	2	2	3		2	8	19	2.38	1		1		3	1	1		1		3
71	44	2	1	2	2		2	17.3	41.7	2.41	1		1		3	2	1		1		3
72	50	2	2	1	1		2	11.8	24.1	2.04	2		1		3	1	1		1		3
73	52	2	2	2	2		2	13.2	14.1	1.07	2		4		3	2	1		1		1
74	37	1	2	2	1		1	9	35.7	3.97	1		1		3	2	1		1		1
75	16	2	2	1	1		2	13.3	32.1	2.41	1		1		3	2	1		1		3
76	41	2	2	1	2		1	7.4	15.9	2.15	4		3		3	2	1		1		2
77	40	1	2	1	4		1	10	35.7	3.57	1		1		3	2	1		1		3
78	55	2	2	2	1		2	10.8	23.3	2.16	1		1		3	1	1		1		3
79	35	1	2	2	2		2	17.7	31.4	1.77	1		1		3	1	1		1		3
80	56	1	2	2	1		2	6.8	12.9	1.9	2		4		3	2	1		1		1
81	26	2	2	2	1		1	8	13.3	1.66	2		1		4	2	1		2	3	3
82	26	1	2	3	3		2	6	13.6	2.27	1		1		3	1	1		1		1
83	62	1	2	1	1		1	9.1	17.3	1.9	2		1		3	1	1		1		3
84	30	2	2	1	3		1	9	12	1.33	4		3		3	2	1		1		3
85	30	2	2	1	3		2	6.8	13.3	1.96	2		4		3	2	1		1		2
86	55	2	2	2	3		2	9.8	17.6	1.8	4		3		3	2	1		1		2

id	var	gar	ar	brt	swmeas	notmeas	l1	l2	l3	l4	l5	miles	s1	s2	s3	s4	s5	mnstur	swrmeas	swvr	avall	ifawl	ifben	ifmal	ifnl	omal
45	2.8	2.1	1.33	1	2	1							3.65	3.41	3.88	3.25	4.15	3.67	2		1	2		2		
46	1.5	1.3	1.13	2	1		5.14	5	4.41	3.93	3.79	4.45	1.17	1.71	1.56	1.68	1.49	1.52	1	2.93	1	2		1		
47	3	2.6	1.15	5	1		0.75	0.62	0.9	0.65	1.03	0.79	2.4	2.37	2.25	2.68	2.25	2.39	1	0.33	1	1	3			
50	1.4	1.7	0.82	3	1		1.05	1	1.81	1.55	1.8	1.44	3.04	2.97	2.67	2.82	2.66	2.83	1	0.51	1	1	2			
51	0.66	0.58	1.14	5	1		4.58	5.54	5.9	4.28	3.56	4.77	1.58	1.78	1.9	1.99	1.82	1.82	1	2.63	1	2		2	1	
52	1.6	1.3	1.23	3	1		2.65	2.57	2.44	2.63	2.47	2.55	1.79	1.76	1.71	1.46	1.55	1.65	1	1.54	1	1	4			
53	1.6	1.5	1.07	1	2	1						0.89	1.38	1.45	1.27	1.47	1.29	2			1	2		2		
54	0.58	1.1	0.53	3	1		2.18	2.5	2.11	2.51	2.07	2.27	2.68	2.32	2.32	2.75	2.47	2.51	1	0.91	1	1	3			
55	0.55	0.85	0.65	1	1		0.58	0.5	1.17	0.56	0	0.7	2.04	2.07	1.92	1.66	2.09	1.96	1	0.36	1	1	3			
56	2.1	1.6	1.31	5	1		1	1.88	1.27	1.53	1.36	1.41	2.55	2.37	2.87	2.23	2.74	2.55	1	0.55	1	1	3			
57	7.2	7.8	0.92	2	1		1.92	1.36	1.4	1.51	1.44	1.53	2.66	2.44	2.82			2.64	1	0.58	1	2		1		
58	2.1	1.5	1.4	1	2	1						1.37	0.96	1.03	0.95			1.08	2		1	2		2	3	ROTHELIA
59	4.3	4.2	1.02	2	2	1						1.75	2.15	2.56	2.65	2.55	2.33	2			1	2		2		BREAST
60	2.7	2.8	0.96	2	1		2.28	2.32	2.27	2.3	2.11	2.26	1.05	0.92	1.12	0.85	0.93	0.97	1	2.32	1	1	4			
61	1	1.2	0.83	5	2	2						1.66	1.48	1.73	1.79	1.85	1.7	2			1	1	3			
62	0.61	0.7	0.87	4	1		3.16	3.3	3.36	3.13	3.4	3.27	3.47	3.43	3.69	3.65	3.61	3.57	1	0.92	1	1	2			
63	3.6	4.3	0.84	4	1		1.87	1.89	1.93	1.19	1.91	1.76	1.39	1.47	1.27	1.52	1.34	1.4	1	1.26	1	1	4			
64	3	3.1	0.97	3	1		0.65	1.57				1.11	2.3	1.98	2.05	2.18	2.11	2.12	1	0.52	1	1	3			
65	1.6	2	0.8	4	1		2.93	2.55	2.9	2.73	2.69	2.76	2.3	3.2	2.45	2.78	3.01	2.75	1	1	1	1	4			
66	3.2	3.2	1.21	2	1		2.17	2.31	2.03	2.17	2.39	2.21	2.29	2.33	2.03	1.97	2.01	2.13	1	1.04	1	1	4			
67	0.81	0.81	1	5	1		0.82	0.66	0.69	0.81	0.81	0.76	3.99	4.21	3.98	3.87	4.12	4.03	1	0.19	1	2		2	3	EWING
68	1.1	1.1	1	5	1		2.02	3.07	2.95	2.68	2.88	2.72	1.71	1.87	1.82	1.88	1.94	1.84	1	1.48	1	1	3			
69	1.5	1.2	1.25	5	1		3.35	3.06	2.8	3.47	3.04	3.14	2.05	1.23	1.63	1.27	1.02	1.44	1	2.18	1	2		1		
71	5	5	1	3	1		1.81	1.59	1.66	1.41	1.61	1.62	1.75	1.6	1.63	1.75	1.65	1.68	1	0.97	1	2		1		
72	2.2	1.8	1.22	2	1		2.92	4.93	2.87	2.82	2.79	3.27	0.92	1.83	2.13	1.92	1.8	1.72	1	1.9	1	2		1		
73	1.7	1.4	1.21	4	1		0.69	0.72	0.82	0.71	0.69	0.73	1.38	1.29	1.25	1.42	1.66	1.4	1	0.52	1	1	3			
74	2.7	2.4	1.13	1	1		1.81	1.79	1.83	2.06	2.1	1.92	2.1	1.87	2.06	1.93	2.09	2.01	1	0.95	1	1	4			
75	2.5	2.7	0.93	3	1		1.26	1.68	1.05	1.67	1.06	1.34	2.91	3.2	2.95	2.88	3.42	3.07	1	0.44	1	1	4			
76	0.89	0.86	1.03	2	1		3.61	4.49	4.64	3.71	4.75	4.24	0.85	0.75	0.98	1.02	0.58	0.84	1	5.07	1	2		2		PAPILLARY
77	3.6	3.2	1.13	2	1		2.85	2.63	2.59	2.81	2.65	2.71	1.55	1.79	1.9	2.02	1.32	1.72	1	1.58	1	2		1		
78	1.8	2.2	0.82	2	1		1.95	1.75	1.68	1.53	1.66	1.71	2.14	2.26	2	2.26	2.25	2.18	1	0.79	1	1	3			
79	5.3	4.3	1.23	1	1		2.19	2.17	2.22	2.46	2.59	2.33	2.15	2.32	2.2	2.02	2.13	2.16	1	1.07	1	2		1		
80	0.65	0.78	0.83	3	1		1.11	1.02	1.74	1.95	1.72	1.52	2.47	2.01	2.28	2.26	2.04	2.21	1	0.68	1	1	4			
81	0.73	0.85	0.86	1	1		1.71	1.71	1.62	1.43	1.47	1.59	0.76	0.88	0.74	0.68	0.61	0.73	1	2.16	1	1	4			
82	0.37	0.38	0.97	5	1		1.65	1.5	1.57	1.76	1.98	1.69	1.96	1.18	1.24	1.27	1.69	1.47	1	1.15	1	1	2			
83	1.7	1.6	1.06	1	1		2.77	2.53	2.44	2.09	2.24	2.41	1.51	1.37	1.39	1.16	1.04	1.29	1	1.87	1	2		2	3	PAPILLARY
84	0.86	0.78	1.1	2	1		4.38	4.74	5.28	5.79	5.17	5.07	1.43	1.47	1.5	1.57	1.63	1.52	1	3.34	1	2		2	3	BREAST
85	0.64	0.57	1.12	2	1		2.73	3.28	3.47	3.4	3.17	3.21	1.89	1.7	1.68	1.73	1.69	1.74	1	1.85	1	2		2	3	BREAST
86	1.9	1.6	1.19	1	2	1						1.53	1.71	1.63	1.51	1.54	1.58	2			1	2		2		BREAST